TECHNICKÁ UNIVERZITA V LIBERCI

FAKULTA TEXTILNÍ

DISERTAČNÍ PRÁCE

Ing. Abdul Malik Rehan Abbasi

In-situ Polymerization of Pyrrole on Textile Substrates and Characterization of Their Applications

Liberec **2013**

Název disertační práce:	In-situ polymerization of pyrrole on textile substrates and characterization of their applications.
Autor:	Ing. Abdul Malik Rehan Abbasi
Obor doktorského studia:	Textilní materiálové inženýrství
Forma studia:	Prezenční
Školící pracoviště:	Katedra materiálového inženýrství
Školitel:	Prof. Ing. Jiří Militký, CSc.
Počet stránek textu:	111
Počet obrázků:	58
Počet tabulek:	10

Prohlášení:

Prohlašuji, že předkládanou disertační práci jsem vypracoval samostatně pod vedením školitele Prof. Ing. Jiřiho Militkého, CSc. A s použitím uvedené literatury.

Declaration:

The contents of the thesis are experimental results obtained by the author on the basis of literature and under the supervision of Prof. Ing. Jiri Militky, CSc.

Dedicated to my late parents, wife and teachers

Anotace

Kovy jsou běžně používané pro stínění elektromagnetické interference (EMI) a pro materiály generující teplo pro jejich vysokou vodivost a dielektrické konstanty. Nicméně kovy mají také nevýhody jako je jejich hmotnost, korozní vlastnosti a špatné zpracovatelské vlastnosti. Aby se zabránilo těmto nevýhodám kovů, mohou být použity elektricky vodivé polymery, např. Polypyrrol (PPy) jako materiály EMI stínění. Jedním ze způsobů, jak předejít špatným mechanickým vlastnostem vodivých polymerů, je připravit elektricky vodivý kompozit pro jeho textilní flexibilitu a mechanické vlastnosti.

V této práci byly analyzována účinnost stínění (EMSE) pro přenos a odraz za použití E-skelných tkanin různé hustoty potažených polypyrrolem. Dle mého názoru, toto je ve své podstatě nový výzkum pro použití tohoto produktu jako průmyslové textilie pro stínění místností, komor, elektronických zařízení atd. Bylo zjištěno, pokud uvažujeme dvě skelné tkaniny s různou hustotou, že EMSE skelné tkaniny s vysokou hustotou (900g.m^{-2}) potažené polypyrrolem sleduje geometrickou funkci povrchového odporu a že EMSE skelné tkaniny s nízkou hustotou (410 g.m^{-2}) potažené polypyrrolem sleduje lineární funkci povrchového odporu.

Rozsáhlé pokusy prokázaly exponenciální závislost teploty zvyšované stejnosměrným napětím dodávaným skelné tkanině potažené polypyrrolem, zatímco tepelný výkon generovaný uvnitř tkaniny vykazuje lineární trend vůči přivedenému napětí. Co se vlivu teploty na skelnou tkaninu potaženou polypyrrolem týká, zde poprvé je monitorováno chování odporu vzorku pod a nad teplotou Tg polypyrrolu. Z těchto údajů se předpokládá, že při teplotách pod Tg je menší interakce mezi nosiči náboje a ionizovanými nečistotami, a pohyblivost nosičů vykazuje obecné chování polovodičů, zatímco při teplotách blízkých a nad Tg začínají vibrace síťové struktury, které snižují pohyblivost náboje uvnitř, a proto se odpor zvyšuje.

V rámci disertační práce byl za velmi nízkou cenu vyvinut senzor deformace nanášením různých koncentrací PPy na pružnou přízi latex/PA6 a citlivost $^{dR}/_{d\varepsilon}$ byla analyzována za použití malé deformace (2%). Bylo vyhodnoceno, že vzorek, který má vysoký odpor, vykazuje vyšší úroveň citlivosti, jakož i lepší rovnoměrnost ve

srovnání se vzorky, které mají nízký odpor. Kromě toho některé experimenty také ukázaly, že vzorky s vysokým odporem vykazují zlepšenou stabilitu při skladování v místech s rozdílnou vlhkostí a pracovní teplotou.

Annotation

Typically, metals have been used for electromagnetic interference (EMI) shielding and heat generating materials, as they have a high conductivity and dielectric constants. However, metals have disadvantages, such as their weight, corrosion properties, and poor processibility. Electrically conductive polymers such as polypyrrole (PPy) can be used as EMI shielding materials to avoid the disadvantages seen in metals. To avoid the problems of poor mechanical properties of conducting polymers, one way is to prepare an electrically conductive textile composite, since these have the resiliency of a textile and excellent mechanical strength and flexibility

In this work, PPy coated on E-glass fabric of different densities and EMSE for transmission and reflection was analysed. To the best of my knowledge this is a novel work in its nature for the application of the product as an industrial textile for the shielding of rooms, chambers and electronic devices etc. By taking two fabric densities of glass fabric into account, it was found that EMSE follows power function of surface resistivity of PPy coated highly dense glass fabric (900 $g.m^{-2}$) and linear function of surface resistivity in case of comparatively low density fabric (410 $g.m^{-2}$).

Extensive experiments demonstrated exponential dependence of temperature being raised by DC voltage supplied to PPy coated fabric whereas thermal power generated in the fabric follows linear trend against voltage applied. As far as effect of temperature on PPy coated glass fabric is concerned, for the first time the behaviour of the resistance of specimen was monitored below and above Tg of PPy. From the data it was supposed that at temperatures below Tg there is less interaction between charge carriers and ionized impurities and mobility of carrier follows general behaviour of semiconductors while at temperatures near and above Tg vibrations in lattice structure of PPy starts which decreases the charge mobility in it, hence resistance increases.

Within the dissertation, strain sensor was developed at very low cost by PPy deposition on latex coated PA6 stretchable yarn with different concentrations and therefore sensitivity $dR/d\varepsilon$ was analysed at small deformation (2%). It was evaluated that high resistive specimen gives higher level of sensitivity as well as better

uniformity compared to samples which have low resistivity. In addition to this some experiments also proved that high resistive sample shows improved stability against storage under different humidity and working temperature levels.

Acknowledgement

At the outset, I would like to thank my supervisor Prof. Jiří Militký CSc. for his continuous support and direction during the entire period of this dissertation project. During our association, Prof. Militky has helped me build critical thinking and problem solving abilities. I have benefited greatly from his advice on effective communication, scientific presentation and writing. His influence on me goes beyond scientific research into my day-to-day life.

Prof. Militky's and his department colleagues also played an important role during my pursuit of scientific development. Dr. Maršalkova taught me many skills in the development and characterization of nanoparticles. Because of these works, I was able to carry out studies on production of nanoparticles of polypyrrole by high energy ball milling, characterization of size and electrical properties. She also taught me many techniques to study thermal analysis of polypyrrole such as Dynamic Mechanical Analysis, Thermo Gravimetric Analysis and most importantly Differential Scanning Calorimetry. We had many inspirational discussions about wide range of subjects from detailed experimental techniques to data analysis and fundamental physics too. I had a great time working with her. Mrs. Grabmullerova contributed immensely to my work. She trained me on micrographing from Scanning Electron Microscope. I also would like to thank Mrs. Novakova for investigation of thickness of polypyrrole deposited on glass fibre through Confocal Laser Microscope and for sharing her knowledge about microscopy of film thickness at micro scale. I would like to thank Ing. Veronika Safařova for helping me conduct experiments and sharing with me much of her understandings of physics of EMI shielding effectiveness while I was struggling with all the jargons and concepts in the literature. My heartfelt thanks to Prof. Jakub Wiener, who collaborated with me in interpreting electrical measurements presented in chapter VII, which made it possible to publish articles in journals. I had many scientific interactions with Prof. Lukas regarding manufacturing of nanofibres and characterization of viscosity of nanofluids. I would like to thank Jan Gregr who is an excellent chemist and public educator who always finds a way to explain chemistry in a clear and enjoyable way. His explanations are so interesting that it made me think that I missed a lot of fun because I didn't get trained

in chemistry. I would like to express my deep sense of gratitude to all the staff members, teaching staff and research scholars of the Faculty of Textile Engineering for their assistance in completion of my work. I would also like to thank Prof. Lubos Hes, Dr. Havelka and Dean Jana Drasarova for many discussions. I am thankful to Mrs. Mohanapriya Venkataraman for the careful review of the drafts of my dissertation. Her helpful suggestions and feedbacks were useful. I express my sincere thanks to Dr. Gabriela Krupincova and Ms. Kateřina Semerakova for helping me to go through all official documentation necessary to complete my work in time.

Special thanks must be given to my employer, the worthy Vice chancellor and other administrative authority of Balochistan University of Information Technology, Engineering and Management Sciences situated in Quetta, Pakistan who supported me to accomplish this study.

Last but not the least, I would like to thank to my departed parents and my beloved wife because I believe that behind every successful man, there is always a woman smiling with one great reason. No degree of thanks can express my gratitude to my daughter Narmeen for allowing me to be away for so long in pursuit of the doctoral I am about to gain.

List of publications in international journals

[1] Abbasi, A. M. Rehan, Militky, J. and Gregr, J. Heat generation by polypyrrole coated glass fabric, *Journal of Textiles*, (Accepted).

[2] Abbasi, A. M. Rehan, Ramadan, M. A., Wiener, J., Baheti, V. and Militky, J. Electrothermal feedback in polypyrrole coated cotton fabric, *Journal of Textile Engineering*, (Accepted).

[3] Abbasi, A. M. Rehan, Wiener, J. and Militky, J. Cotton fabric coated by polypyrrole: effect of temperature on conductivity, *Melliand International,* **19,** 2013, pp. 21.

[4] Abbasi, A. M. Rehan, and Militky, J. EMI Shielding Effectiveness of polypyrrole coated glass fabric, *Journal of Chemistry and Chemical Engineering,* **7,** 2013, pp. 256-259.

[5] Abbasi, A. M. Rehan, Marsalkova, M.and Militky, J. Conductometry and Size Characterization of Polypyrrole Nanoparticles Produced by Ball Milling, *Journal of Nanoparticles*, **2013**, 2013, (published online).

[6] Abbasi, A. M. Rehan, Mangat, M. M., Baheti, V. and Militky, J. Thermal properties of cotton fabric coated with polypyrrole, *Journal of Fiber Bioengineering and Informatics*, **5,** 2012, pp. 163-168.

[7] Ramadan, M. A., Abbasi, A. M. Rehan, Wiener, J., Baheti, V. and Militky J. Polypyrrole coated cotton fabric: The thermal influence on conductivity, *Vlakna a Textil*, **19**(3)**,** 2012, pp. 41-49.

[8] Abbasi, A. M. Rehan, Mangat, M. M., Baheti, V. K. and Militky J. Electrical and thermal properties of polypyrrole coated cotton fabric, *Vlakna a Textil*, **19**(1)**,** 2012, pp. 48-52.

[9] Abbasi, A. M. Rehan, Marsalkova, M., Baheti, V. K.and Militky. J. Polypyrrole nanoparticles prepared by planetary ball milling and its conductivity, *Journal of Nanocomposites and Nanoceramics* **2,** 2011, pp. 1-4.

List of contributions in international conferences

[1] Abbasi, A. M. Rehan, Militky, J. Joule heating in polypyrrole coated glass fabric, *8th International Conference – TEXSCI*, Liberec, 23-25 Sep 2013.

[2] Abbasi, A. M. Rehan, Militky, J. and Mazari, A. Heat generation by polypyrrole coated glass fabric, *21st ICCE Proceedings*, Tenerife, Spain, 21-27 July 2013

[3] Abbasi, A. M. Rehan, Gregr, J., Baheti, V. and Militky, J. Heat generation by polypyrrole coated glass fabric, *19th International Conference STRUTEX Proceedings,* Liberec: Livox s.r.o Liberec, 2012.

[4] Abbasi, A. M. Rehan, and Militky, J. EMI shielding effectiveness of polypyrrole coated glass fabric, *International Technical Textile Conference,* Izmir: Meta Basim Press, 2012, pp. 29-30.

[5] Abbasi, A. M. Rehan, Mangat, M. M.and Militky, J. Thermal properties of cotton fabric coated with polypyrrole, *5th Textile Bioengineering and Informatics Symposium Proceedings,* Ueda: TBIS, Hong Kong China, 2012, pp. 757-761.

[6] Abbasi, A. M. Rehan, Ramadan, M. A. and Militky, J. The influence of temperature on polypyrrole coated cotton fabric, *41st Textile Research Symposium Proceedings,* Guimaraes, Portugal: Universidade Minho, 2012, pp. 280-285.

[7] Abbasi, A.M. Rehan, Marsalkova, M., Baheti, V. K. and Militky J. Development of polypyrrole coated glass fabric composite as EMI shield, *12th AUTEX World Textile Conference,* Zadar: University of Zegreb, Croatia, 2012, pp. 1529-1532.

[8] Abbasi, A. M. Rehan, Baheti, V. K. and Militky J. Production of nanoparticles of polypyrrole by ball milling, *2nd Nanomaterials and Nanotechnology Meeting Proceedings,* Ostrava: Repronis, 2011, pp. 93-94.

[9] Abbasi, A. M. Rehan, Marsalkova, M., Baheti, V. K.and Militky. J. Optimization of milling conditions for the production of polypyrrole nanoparticles, *18th international conference STRUTEX,* Liberec: Livox s.r.o., 2011, pp. 237-241.

[10] Abbasi, A. M. Rehan, Marsalkova, M.and Militky, J. Rheological and electrical properties of polypyrrole nanocomposites, *18th international conference STRUTEX,* Liberec: Livox s.r.o., 2011, pp. 401-404.

[11] Abbasi, A. M. Rehan, Militky, J.and Baheti. V. K. Production of nanoparticles of polypyrrole by ball milling, *40th Textile Research Symposium,* Kyoto, 2011.

List of contributions in domestic conferences

[1] Abbasi, A. R., and Militky, J. Production of PPy nanoparticles by ball milling and electrical conductivity of their composite with polyurethane. *Workshop pro doktorandy FS a FT TUL,* 2011, Svetlanka: Vysokoskolsky podnik Liberec, spol. s.r.o. pp. 8-12.

[2] Abbasi, A. M. Rehan, EMI shielding effectiveness of polypyrrole coated textile fabric, *Workshop pro doktorandy FS a FT TUL,* 2012, Svetlanka: Vysokoskolsky podnik Liberec, spol. s.r.o. pp. 8-11.

Contents

List of Figures

List of Tables

Chapter 1

General Introduction

1.1. Introduction to the topic

Rapid development in various electrical and electronic instruments has polluted the working environment by generating invisible electromagnetic radiations. This electromagnetic radiation which comes out from these instruments can easily interfere with other electrical and electronic devices and reduce their working efficiency and life. These electromagnetic radiations are not only harmful for electrical and electronic instruments; they can also affect human health [1, 2].

To protect electrical and electronic instruments and mankind from these electromagnetic radiations, metals were first preferred because of their high conductivity and dielectric constants. However, the usage of metals has been limited due to its weight, stiffness, corrosion and poor processibility and there was a growing demand for highly flexible conductive material. Textile with metal in its structure was developed to satisfy the above requirement i.e. good flexibility and high conductivity. An electrically conductive textile is a relatively new branch of technical textiles and has become popular from 1950 onwards due to industrialization. However, its usage is limited due to its corrosive nature in humid environment. This problem can be eliminated by coating conductive polymer on textiles [3].

The conducting polymers (also called synthetic metals) are polyconjugated, which possess electronic (conductive, magnetic, optical) properties of metals, while retaining the mechanical properties and processibility of conventional polymers. They acquire high conductivity due to incorporation of a small concentration of dopants into the matrix of the initial polyconjugated polymers having conductivity ranging from 10^{-10} to 10^{-5} S cm^{-1}. The resulting materials have conductivities typical of metals or semiconductors, 1 to 10^{5} S cm^{-1}.

The doping is performed by means of chemical or electrochemical oxidation (p-doping) or reduction (n-doping) of a polymer. As a result, the polymeric chains acquire positive or negative charges, respectively [4].

Coating conducting polymers on textiles has received considerable attention due to their potential applications in the areas of electromagnetic shielding [5,6], chemical sensors [7,8] and heating fabrics [9]. Polyester is one of the most commonly used substrate [5, 10-14]. Other textiles such as nylon [10, 15-17], polyethyleneterephthalate [18], cotton [19], glass wool [20] and wool [19-21] have also been used as substrates for conducting polymers. The coating technique is often based on *in-situ* chemical polymerisation of monomers such as pyrrole and aniline in the presence of textiles. It was reported that the *in-situ* polymerisation process consists of two competitive processes at the initial stage of the polymerisation reaction; physical adsorption of oligomers and polymers onto the textile fibre and polymerisation in solution [15]. The formation of the conductive polymer coating on the textile substrate starts from deposited oligomers, which form islands in the initial stage and finally grow and cover the surface of the substrate completely.

Electromagnetic shielding is one of the most important means of suppression electromagnetic compatibility. Materials used for the production of electromagnetic shielding are characterized by high electrical conductivity and high permeability. Electrical conductivity is one of the crucial parameters for improving immunity to electromagnetic smog, reducing the tendency to build up static electricity and construction of intelligent fabrics containing conductive tracks. Electrically conductive fabric is often used in special clothing and technical textiles, where the purpose is to replace traditional metals with other materials using flexible (textile) structures. Regarding the harmful effects of radiation in workplaces with high intensity or long exposure time (workers substation high voltage, line installers, computer operators, etc.) it is thus essential to limit the direct exposure of workers by wrapping sheets for devices, curtains or screens, etc. For this purpose, appropriate use of fabrics with increased resistance to electrical radiation with enough tensile strength that also meet the requirement of maintaining circulation of air in the workplace is mandatory.

One of the aims of the dissertation is to develop EMI shield with the help of polypyrrole (PPy) coated E-glass fibre fabric through improved resistance to electromagnetic radiations while maintaining the essential characteristics imposed on textiles used in the textile industry at very low cost. In the rest of this dissertation E-glass fibre fabric is written as glass fabric only. In order to investigate the relation

between electrical conductivity and electromagnetic shielding effectiveness, sets of glass fabric samples having different densities and porosity were coated with different concentrations of PPy.

A large part of the dissertation is devoted to investigate Joule heating effect and electrothermal effect in PPy coated glass fabric. For the deep understanding of electrothermal phenomenon and theory, PPy films were prepared in the same manner and characterized by DSC.

A part of thesis includes the characterization of PPy coated Latex/PA6 stretchable yarn as a sensor for monitoring breathing rate and body movement at much reduced cost. In order to study the uniformity of the sensing behaviour multiple samples were developed by varying PPy concentration and their response on cyclic loading at different time intervals was analysed.

1.2. Research objectives

The present investigation encompasses studies on (i) *in-situ* polymerization of pyrrole on glass fabric and PA6 wrapped Latex yarn and (ii) characterization of properties of these materials under different conditions. Sub objectives of the dissertation are divided in several areas as follows;

- Development and characterization of electrical conductivity, weight gain, mechanical properties etc. of PPy coated glass fabric.
- Study the dependence of electromagnetic shielding effectiveness on the concentration of oxidizing agent and on the density of the fabric as well.
- Study the Joule heating and electrothermal effect in PPy coated glass fabric at different levels of voltage and temperature respectively.
- Development and characterization of inexpensive strain sensor based on Latex/PA6 yarn coated by PPy.
- Evaluating the dependence of resistance of PPy coated Latex/PA6 yarn, on the length.
- Determination of dependence of sensitivity of PPy coated Latex/PA6 yarn against small deformation.
- Study the dependence of resistivity of PPy coated Latex/PA6 yarn on standard washing cycles, storage time, temperature and relative humidity.

1.3. Dissertation outlines

The dissertation is separated into nine chapters.

Chapter 2 is a brief literature survey on the subject. This literature survey provides guidance for the entire study.

Chapter 3 describes the materials i.e. textile materials under study, monomer, doping agent and oxidizing agent used for developing specimens for this research work. The process parameters for the preparation of specimens such as concentration of oxidizing agent and doping agent as well as different techniques for the characterization of properties of specimen are discussed in this chapter as well.

Chapter 4 discusses the influence of concentration of oxidizing agent on weight gain and tensile properties of the glass fabric specimen. The surface morphology and characterization of thickness of PPy coating on glass fibres are also included here.

The characterization of electrical resistivity and its effect on EMI shielding effectiveness is discussed in chapter 5. The effect of different densities of glass fabric on electromagnetic shielding effectiveness is also discoursed in this chapter.

Chapter 6 analyses the Joule heating of polypyrrole coated glass fabric specimen under different electrical fields as well as heat transfer to air by convection is also covered in it.

Chapter 7 discusses about the electrothermal effect in PPy coated glass fabric substrate under different temperatures near the glass transition temperature of PPy.

Chapter 8 discourses about the response of resistance of PPy coated Latex/PA6 yarn against cyclic stress loading in order to find its suitability as body movement sensor. Beside strain sensing of specimen, the influence of standard washing cycles, relative humidity and environment temperature on electrical resistance are also studied.

Finally, the summary of the entire study, the numerous conclusions drawn from the conducted studies and future plan of work are presented in chapter 9.

Chapter 2

Literature Review

2.1. Introduction

From the time of invention till the advent of industrial revolution, the primary function of textile materials is to cover a body as a social and religious norm as well as protect us from natural variations in climatic conditions. But the innovations in the field of science and technology have created situations in which the traditional textile materials were not able to give the required amount of protection to the wearer. To protect and improve the quality of human life a new area of textile materials has been developed which is classified as 'technical textile'. In recent literature electrically conductive textile materials are also classified under technical textiles.

The extensive usage of electrical and electronic instruments has improved the quality of human life. At the same time, developments in the various electrical and electronic industries bring a lot of inevitable problems in the various working environments. One of the serious problems is electromagnetic interference (EMI). Whenever a current passes through a conductor it produces an electromagnetic field around the conductor. These electromagnetic fields can easily interfere with other electrical devices and reduce the efficiency of that instrument. The electromagnetic fields or radiations are not only harmful for electronic devices; it can also affect human health like crystalline lens in the eye ball, the nerve systems and the function of heart vessel [2].

Typically, metals have been used for EMI shielding and heat generating [22, 23] materials, as they have a high conductivity and dielectric constants. However, metals have disadvantages, such as their weight, corrosion properties, and poor processibility [24]. Electrically conductive polymers can be used as EMI shielding materials to avoid the disadvantages seen in metals [25,26]. However, conductive polymers are insoluble and infusible, which restricts its fabrication, and it has poor mechanical properties [27]. One of the ways to avoid these problems is to prepare an electrically conductive textile composite, since these have the resiliency of a textile and excellent

mechanical strength and flexibility, but also retain the electrical properties of the conductive polymer [28-31].

To prepare conductive composite fabrics, many researchers have focused on chemical oxidative polymerization and electrochemical polymerization of pyrrole in the presence of a nonconductive matrix, such as PA6 fabric,[29-32] nonwoven fabric,[33] and acryl fabric[34]. Also, using the microwave absorbance characteristics of conductive polymers, Contex®, (a chemically synthesized conductive polymer on PET fabric), has been used as camouflage netting by the Milliken Co.[35]. However, its application to industrial scale is limited, since the substrates or matrices used have inadequate tensile strength and stability to environmental factors.

This research focused on a new PPy–fabric composite with a high electrical conductivity and a high EMI shielding efficiency (EMSE). This work also investigated the thermal stability and the temperature dependence of the conductivity as well as heat generation by applying electrical field to the composite fabrics which were fabricated.

Electrically conducting polymer films can only withstand limited strain before breaking and cannot perform well in evaluating large strains [36]. To overcome this problem, substrates were employed to provide the necessary support and the surface for conducting polymer film deposition. Generally, fabricating a strain sensor using this approach means that the mechanical properties are highly attributed to the substrate while the conducting polymer introduces the electrical conductivity. This practice is commonly found in the research field of smart textiles which are conductive fabrics produced by coating conducting polymers onto commercial fabrics such as nylon, polyester and Lycra [37-40]. Although excellent results have been demonstrated with smart textiles using conducting polymers, the intended applications are mainly aimed at enhancing the usability of fabric beyond its current use as a protective layer. As a general purpose strain sensor, the substrate requires having some degree of rigidity and fabrics are not an ideal material due to its soft structure. Furthermore, repetitive strain can cause permanent elongation on individual fibres where the strain may not be distributed equally. This can lead to individual fibres having different mechanical properties that will affect the strain sensing performance. The proposed solution is to replace fabric with Latex/PA6 stretchable yarn, which has

good combination of rigidity and elasticity. One of the studies has succeeded in fabricating a strain sensor using PPy and natural rubber substrate where PPy powder is embedded into the structure of the rubber directly [41]. Compared to the coating methods, that approach requires knowledge of rubber manufacture as well as an access to the equipment to produce rubber with consistent mechanical properties.

This work is aimed at developing a low cost, small to large strain sensor using PPy and Latex/PA6. This stretchable yarn was chosen as the substrate due to its excellent resilience and elasticity. Commercial Latex/PA6 strip was purchased and used to produce the strain sensor. PPy as thin film was coated onto this substrate by means of vapour phase polymerisation technique that provides a good adhesion between the two components of the strain sensing element.

2.2. Intrinsically conducting polymers

Electrically conductive organic polymers are a novel class of polymers that combine the chemical and mechanical properties of polymer with the electronic properties of metals [42,43]. The conductive polymer polyacetylene was discovered by Hideki Shirakawa, Alan G. MacDiarmid and Alan J. Heeger in the year 1977 [44-47]. In recognition of their work on conducting polymers in the year 2000, Nobel Prize in chemistry was awarded to Hideki Shirakawa, Alan G. MacDiarmid and Alan J. Heeger. Following their discovery there has been an explosion of activity about the characterization, synthesis and use of conductive polymers in a wide range of fields from electronic to medicine. As a result, an entire class of polymeric conductors was developed. Typical representatives of this class are poly(p-phenylene) [48], polypyrrole [49] polythiophene[50] and its 3-methoxy- derivative,[51] polyaniline [52]. The common feature of the structure of conducting polymers is polyconjugation in the p-bonding system of their backbone (for polyaniline, this holds only in the case of doped polymer).

The conducting polymers (also called synthetic metals) are polyconjugated, which possess electronic (conductive, magnetic, optical) properties of metals, while retaining the mechanical properties and processibility of conventional polymers. They acquire high conductivity due to incorporation of a small concentration of dopants into the matrix of the initial polyconjugated polymers having conductivity ranging from 10^{-10}

to 10^{-5} S cm^{-1}. The resulting materials have conductivities typical of metals or semiconductors, 1 to 10^4 S cm^{-1}, few examples have been presented in Table 1.

Table 1: Conductivities of different conducting polymers with selected doping agents [53]

Polymer	**Doping materials**	**Conductivity [S/cm]**
polyacetylene	I_2, Br_2Li, Na, AsF_5	10^4
poly(3-alkylthiophene)	BF_4^-, ClO_4, $FeCl_4^-$	10^3-10^4
polyphenylene-vinylene	AsF_5	10^4
polypyrrole	BF_4^-, ClO_4, tosylate	500-7500
polythienylene-vinylene	AsF_5	$2.7 \cdot 10^3$
polythiophene	BF_4^-, ClO_4, tosylate, $FeCl_4^-$	10^3
polyphenylene	AsF_5Li, K	10^3
polyphenylenesulphide	AsF_5	500
polyaniline	HCl	200
polyfuran	BF_4^-, ClO_4	100
polyisothianaphthene	BF_4^-, ClO_4	50
polyazulene	BF_4^-, ClO_4	1

The linear-backbone "polymer blacks" (polyacetylene, polypyrrole, and polyaniline) and their copolymers are the main class of conductive polymers. Poly(p-phenylene vinylene) (PPV) and its soluble derivatives have emerged as the prototypical electroluminescent semiconducting polymers. Today, poly(3-alkylthiophenes) are the archetypical materials for solar cells and transistors.[54]

The Table 2 presents some organic conductive polymers according to their composition. The well-studied classes are written in bold and the less well studied ones are in italic.

Table 2: Different classes of conducting polymers according to their molecular structure

The main chain contains	**Heteroatoms present**		
	No heteroatom	**Nitrogen-containing**	**Sulfur-containing**
Aromatic cycles	*Poly(fluorene)s* *polypyrenes* *polyazulenes* *polynaphthalenes*	The N is in the aromatic cycle: **poly(pyrrole)s (PPy)** *polycarbazoles* *polyindoles* *polyazepines* The N is outside the aromatic cycle: **polyanilines (PANi)**	The S is in the aromatic cycle: **poly(thiophene)s (PT)** **poly(3,4-ethylenedioxythiophene) (PEDOT)** The S is outside the aromatic cycle: **poly(p-phenylene sulfide) (PPS)**
Double bonds	**Poly(acetylene)s (PAC)**		
Aromatic cycles and double bonds	**Poly(p-phenylene vinylene) (PPV)**		*Poly(p-phenylene sulfide)* *Poly(isothianaphthene)*

2.2.1. Synthesis

Conducting polymers except ionomeric polymers may be produced using typical methods of polymerization [55-57] including Witting, Horner and Grignard reactions, polycondensation processes and metal catalyzed polymerization techniques. Oxidative coupling with oxidizing Lewis acid catalysts generally leads to polymers with aromatic or heterocyclic building blocks.

Conductive polymers may be synthesized by either one or more of the following techniques:

- Electrochemical polymerization
- Chemical polymerization
- Concentrated emulsion polymerization

- Photochemical polymerization
- Metathesis polymerization
- Soluble precursor polymer preparation
- Solid-state polymerization
- Inclusion polymerization
- Plasma polymerization
- Pyrolysis

Among all the above categories, chemical polymerization [58-61] is the most useful method for preparing large amounts of conducting polymers, since it is performed without electrodes [62]. Chemical polymerization is followed by the oxidation of monomers to a cation radical and their coupling to form dication and the repetition of this process generates a polymer. The mechanism of this reaction has been discussed in the section 2.2.3.1.

Electrochemical polymerization [45-48] can be carried out potentiometrically by using a suitable power supply (potentiogalvanostat). Generally, galvanostatic conditions are recommended to obtain thick films while potentiostatic conditions are recommended to obtain thin film. The electrochemical technique has received wider attention both because of the simplicity and the added advantage of obtaining a conductive polymer being simultaneously doped. Moreover, a wider choice of cations and anions for use as "dopant ions" is available in the electrochemical polymerization technique.

Photochemical polymerization [63] takes place in the presence of sunlight. This technique utilizes photons to initiate a polymerization reaction in the presence of photosensitisers. Pyrrole can be photopolymerised using a ruthenium (II) complex as photosensitizer. Under photoirradiation, Ru(II) is oxidized to Ru(III) and the polymerization is initiated by a one-electron transfer oxidation process. PPy films may be obtained by photosensitized polymerization of pyrrole using a copper complex as the photosensitizer.

Plasma polymerization [64] is a technique for preparation very thin uniform layers (50-100Å) that strongly adhere to a suitable substrate. Electric glow discharge is used

to create low-temperature plasma. The advantage of this technique is that it eliminates various steps needed for the conventional coating process.

Metathesis polymerization is unique, differing from all other polymerization in that all the double bonds in the monomer remain in the polymer. It was a natural development of Ziegler-Natta polymerization in that the catalysts used are similar, and often identical, i.e. a transition metal compound plus generally an organometallic alkylating agent [65].

Pyrolysis is probably one of the oldest approaches utilized to synthesis conducting polymers by eliminating heteroatoms from the polymer by heating it to form extended aromatic structures. The product of polymer hydrolysis can be film, powder or a fibre depending on the form and the nature of the standing polymer including the pyrolysis condition Weiss and co-workers described the pyrolysis of tetraiodopyrrole to produce highly conductive PPy [66].

Nevertheless, conducting polymers have also been synthesized by other techniques such as chain polymerization, step-growth polymerization, chemical vapour deposition, solid-state polymerization soluble precursor polymer preparation, concentrated emulsion polymerization etc. However, most of these techniques are time-consuming and involve the use of costly chemicals and apparatuses.

2.2.2. Doping

Moreover, the conductivity of a polymer can be increased several-fold by doping it with an oxidative/reductive substitution or by donor/acceptor radicals. Shirakawa and Ikeda [67] discovered that doping of polyacetylene with metallic regimes increases its conductivity by 9-13 orders of magnitude. Doping is accomplished by chemical methods of direct exposure of the conjugated polymer to a charge transfer agent (dopant) in the gas or solution phase, or by electrochemical oxidation or reduction.

The doping is usually quantitative and the carrier concentration is somehow proportional to the dopant concentration. Doping of conducting polymers involves random dispersion or aggregation of dopants in the disordered structure of entangled chain and fibrils. Polymer doping leads to the formation of conjugational defects such as solitons, polarons or bipolarons in the polymer chain. An x-ray diffraction study on

iodine-doped polyacetylene shows that the C-C bond length of the chain increases with donor doping but decreases on acceptor doping.

The presence of localized electronic states of energies less than band-gap arising from changes in local bond order, including the formation of solitons, polarons and bipolarons have led to the possibility of new types of charge conduction present in these polymer systems.

Polymers may be doped by the following techniques:

- Gaseous doping
- Electrochemical doping
- Solution doping
- Self-doping
- Radiation-induced doping
- Ion-exchange doping

Of these, the first three techniques are widely used because of convenience and low cost. In the gaseous doping process, polymers are exposed to the vapours of the dopant under vacuum. Solution doping involves the use of a solvent in which all the products of doping are soluble. Effective doping of polymer anions during chemical polymerization of pyrrole using Fe^{+3} based oxidants and electrolytes increases the conductivity several-fold [68]. Researchers have demonstrated [62] that certain dopants could give rise to magnetic ordering in these polymers along with the electron acceptor (e.g. iodine, $FeCl_3$, AsF_5, etc.) or electron donor (e.g. Na, Li, etc.) to the polymer which is considered to generate positive carrier (holes) or negative carriers (electrons) in the π-conjugated system.

2.2.3. Polypyrrole

Polypyrrole first synthesized in 1916 [69] is a conjugated polymer that displays particular electronic properties including conductivity. PPy is generally synthesized by chemical or electrochemical means. Chemical synthesis is used when large quantities of material are required and involves mixing a strong oxidizing agent (typically $FeCl_3$) with a monomer solution [70,71]. Electrochemical synthesis is preferred for research purposes due to the simplicity of the technique, control over

material thickness, the facility for doping during synthesis, the wide choice of available dopant ions and the generation of good quality films [72,73]. It leads to the development of adherent surface conformal deposits i.e. thin solid films, from the bulk solution phase of monomer units. The electrodeposition on the positively polarized working electrode proceeds via a condensation reaction between the monomer units of the five-membered heterocyclic pyrrole. Alongside, negatively charged counter ions must be present in solution to maintain charge balance within the polymer since positive charges are developed along the PPy backbone.

2.2.3.1. The mechanism of electrochemical synthesis of polypyrrole

Basically the oxidation of pyrrole to produce PPy is irreversible. The mechanism of this reaction was widely studied, [74-83] yet, the problem still remains not fully determined. Among the mechanisms anticipated, two have gained the greatest attention. One of those is the oxidative coupling of monomer molecules (Scheme 1) as shown in Figure 1 [74]. The first stage of the reaction is the electrode oxidation of monomer molecules yielding radical cations with the radical state delocalised over the pyrrole ring (B). The maximum spin density is at the α-position; [77] hence, of the three possible resonance states, C, D and E, the latter is the most stable. The radical cations dimerise, that is the rate-controlling stage of the reaction [74, 76] and expel two protons. The dimers, owing to stronger conjugation, are more readily oxidised under the given reaction conditions than the monomer. The chain growth proceeds by addition of a newly formed radical cation to an oligomeric one. Some authors deny the possibility of dimerization of radical cations because the latter experience strong Coulombic repulsion [75].

The alternative mechanism proposed for polymerisation of pyrrole is the free radical reaction (Scheme 2) as shown in Figure 3 [75]. This scheme implies that formation of a radical cation on the anode is followed by the loss of a proton and attack of the radical on a neutral monomer. After reoxidation of the dimeric radical and proton loss, the dimeric molecule can experience subsequent oxidation, which results in chain growth. The release of protons in the course of oxidation of pyrrole was observed experimentally [80].

Kinetic studies using isotopically labelled reactants and experiments with radical traps [78] showed that Scheme 1 is more probable. According to Scheme 2, any free-radical initiator would trigger the polymerisation of pyrrole, which is not the fact.

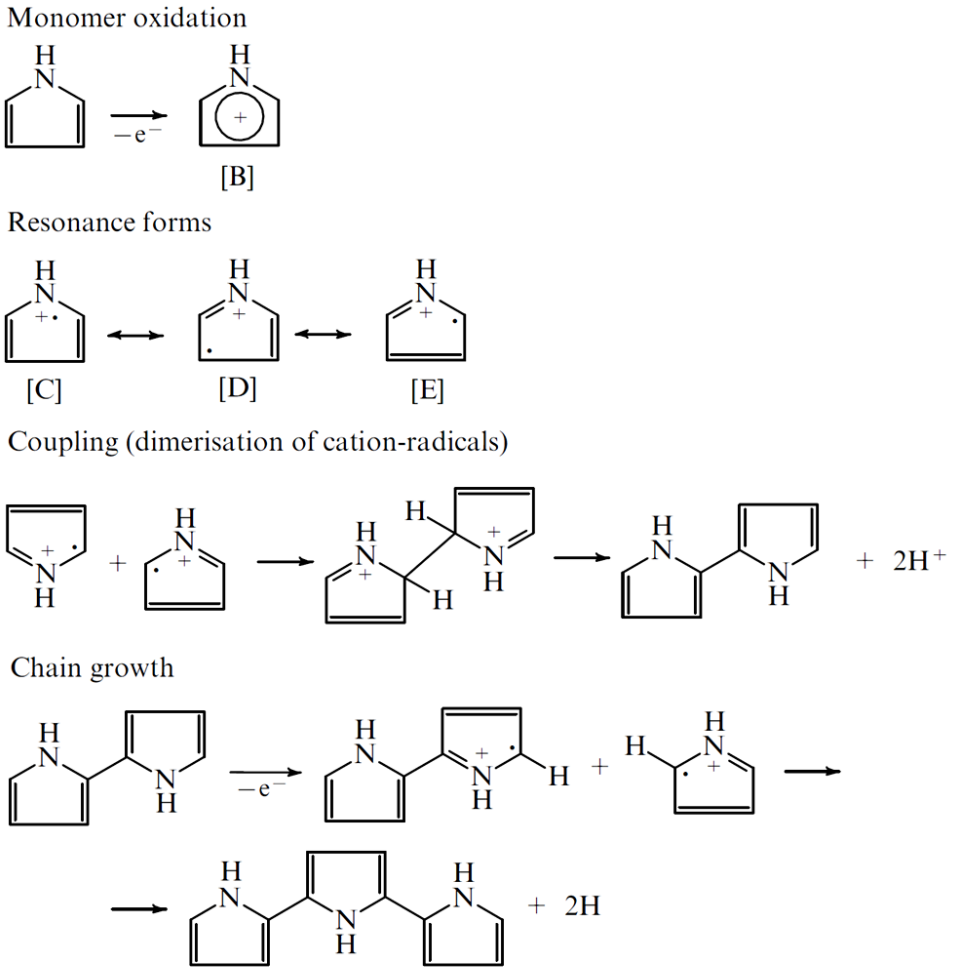

Figure 1: Scheme I of mechanism of oxidation of pyrrole

In addition to that, Scheme 2 cannot account for the experimentally observed fact that polymerisation proceeds only when monomer oxidation occurs in parallel with the oxidation of the polymer (the oxidation potentials for the dimer and oligomers of pyrrole are lower than that for the monomer). The pyrrole dimers were detected in the electrolyte [79, 80].

Electropolymerization of pyrrole, in the presence of water, in addition to the above-described dimerisation of the pyrrole cation radicals (see Scheme 1), can involve the side reaction of the cation radicals with water yielding undesirable electrochemically inert products (Figure 2) [84].

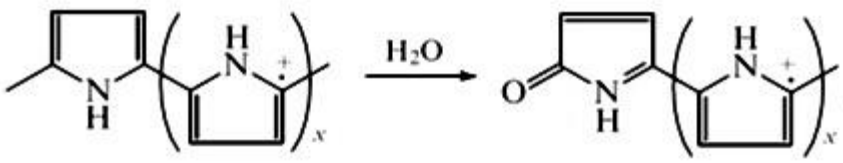

Figure 2: Side reaction of cation radical with water

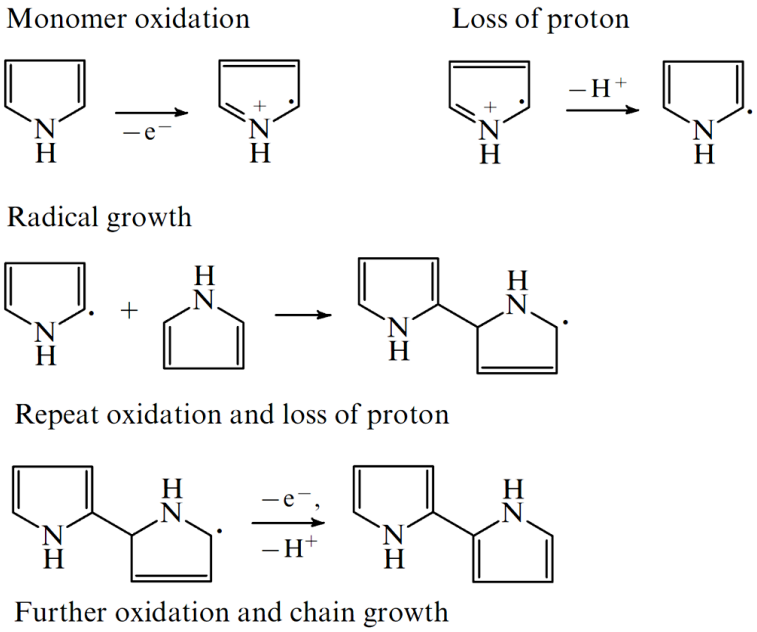

Figure 3: Scheme 2 of mechanism of oxidation of pyrrole

This polymer formed thus has shorter chains and, hence, poorer mechanical and electronic properties compared with PPy prepared from acetonitrile solution.

2.2.3.2. Chemical polymerization of pyrrole

Chemical synthesis of polypyrrole proceeds via the oxidation of pyrrole with an oxidant such as $FeCl_3$. The mechanism is similar to that for electropolymerization of pyrrole and conductivities are comparable. The resulting polymer in its oxidized form is conducting with charge compensation afforded by $FeCl_4^-$. The conductivity of polypyrroles formed from different ferric salts (effect of dopant ion) has been related to the Fe^{2+}/Fe^{3+} redox potential with strong acid anions providing the most oxidizing ferric species. Weaker acid anions typically coordinate Fe^{3+} ions more strongly, reducing its oxidizing potential [85]. An investigation into the ferric ion equilibrium in aqueous solutions showed that above a concentration of 0.5 M $HClO_4$ there was no change in the amount of available $Fe(H_2O)_6^{3+}$ [86].

The solvent in which the reaction occurs also changes the redox potential. For example the Fe^{2+}/Fe^{3+} redox potential is lower in water than acetonitrile. If the redox potential is too high, an irreversible dissolution of PPy can occur, as for ferric perchlorate in acetonitrile [87]. Methanol has been found to produce the best conducting polymer based on conductivity and morphology [88,89]. The conductivity was related to the redox potential of the Fe^{2+}/Fe^{3+} system and could be varied by adding $FeCl_2$. The optimum redox potential in methanol was +0.5 V vs saturated calomel electrode (SCE). The solvent also has an influence on the dopant ion that remains in the PPy film. In ether using $FeCl_3$ as oxidant leaves $FeCl_4^-$ as the dopant ion, while in methanol, the dopant is mainly Cl^- with some $FeCl_4^-$ [85]. Water was found to be trapped in the PPy with formation of pyrrolidinone rings at chain terminations similar to electrochemically produced films [85].

Other counter ions to the ferric ion will also be incorporated into the PPy film [85] as will ions present in solution. Dopants whose bonds are labile such as Cl-O, B-F, P-F, should be avoided for sake of polymer stability [90]. Polymerisation of pyrrole in the presence of surfactants such as dodecylbenzyl sulphonic acid or a salt like sodium dodecyl sulphate, leads to an increase in mass yield due to incorporation of the salt/surfactant into the polymer [91]. Cationic surfactants were found to inhibit the polymerization of pyrrole. Polymerisation of pyrrole in the presence of polystyrene sulphonate (PSS) produced particles (non-colloidal) with the size being inversely proportional to the concentration of ferric chloride oxidant [92]. The size effect is due to the affinity of pyrrole and the ferric ion to PSS. The acid concentration affects the polymerisation process. The conductivity of PPy increases as the synthesis temperature is reduced. This is thought to be due to a reduction in the number of side reactions.

Polypyrrole derivatives have been prepared and their properties studied. By blocking the 3,4- positions on the pyrrole ring, unwanted side reactions at these sites are eliminated. This has been noted to yield higher conductivity in the case of poly 3,4-dimethoxypyrrole [93,94]. Many alkylene oxypyrroles have been synthesised and studied including a series of soluble species [93,95,96]. N-substituted pyrroles tend to induce twisting relative to adjacent pyrrole rings, thus limiting the conjugation length and conductivity. Elevated temperatures in air reduce the quinoid content and oxidise the 3,4-positions. Dodecyl sulphate is less stable than p-toluene sulphonate at elevated

temperatures. Under argon the dodecyl sulphate doped film become brittle indicating cross linking at elevated temperatures [97]. The polymer produced by electrochemical or chemical synthesis is generally an inflexible solid or powder.

2.2.3.3. The nature of electronic conduction of polypyrrole

Molecules can have several molecular orbitals, generally we need to consider only the behaviour of the highest occupied molecular orbital (HOMO) and the lowest unoccupied molecular orbital (LUMO). Whether a material is a metal, a semiconductor or an insulator will depend on the band structure and the filling of the energy states within the band. For a partially filled band, either a single band or a pair of overlapping bands, the application of an electric field is in itself sufficient to promote electron from filled states to adjacent empty states within the same band, thereby allowing a net flow of charge [98].

In semiconductors promotional energy can be obtained by direct photon absorption, or by raising the temperature, when an electron may receive sufficient thermal energy from the lattice (electron-phonon collision). Intrinsic semiconductors are therefore, materials with energy gaps between valence and conduction bands that are not much larger than thermal energies whereas materials with large energy gaps are insulator [98].

The interest in the electronic properties of polyconjugated polymers was boosted by the 1964 paper by Little [99], where the possibility of superconductivity in one-dimensional structures was predicted. The neutral (undoped) PPy is a dielectric with the gap of 4 eV [100]. Upon oxidation (doping), an electron is removed from the polymer backbone by yielding a radical and a spin less positive charge. Next, the newly formed cation and the radical are coupled to each other by local resonance. The gap reduces to $\leq$2.5 eV and the polymer becomes a semiconductor. During coupling, quinoid-like consecutive rings are also formed and utilized to provide higher energy of distortion than the remaining part of the chain. The created lattice distortion is usually extended over four pyrrole rings (charged site) and when they coupled with a radical, this structure is called polaron. As a result, further oxidation of the polaron yields a new spin less defect called bipolaron [101,102] having a lower energy than two distinct polarons. At higher doping levels, polarons are eventually replaced by bipolarons. For a heavily doped PPy it is suggested that the upper and lower

bipolarons merge to the valence and conduction bands respectively to produce partially filled bands and provide metallic-like conductivity for the final polymer [103]. In chemical terms, the formation of a polaron is equivalent to formation of a radical cation as shown in Figure 4 and of a bipolaron, to dication as shown in Figure 5.

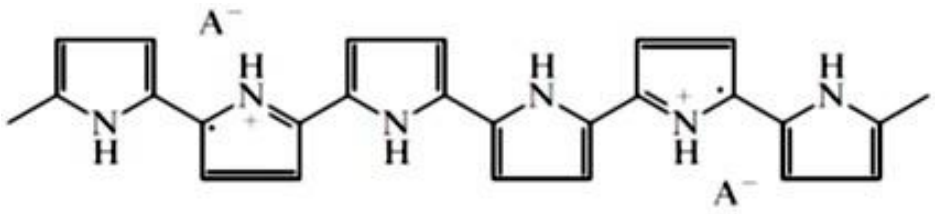

Figure 4: Formation of polaron (a radical cation)

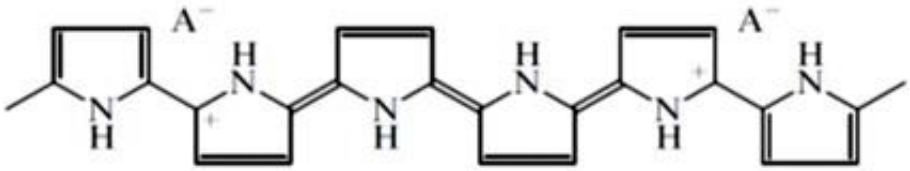

Figure 5: Formation of bipolaron (a dication)

The polaron and bipolaron in PPy are extended structures spread over three to four monomeric units of the chain [104] The separation of the positive charge on the chain in the bipolaron structure predetermines the energy of the system. The further positive charges lower the stability of the system, since it contains more rather unstable quinoid rings. The calculations of the energetics showed that formation of a bipolaron requires 0.45 eV less than formation of two polarons [101,102]. This result led to a suggestion that bipolaron is the major charge carrier in PPy [105,106].

2.2.4. Formation of conducting polymer on textile substrates

One of the earliest reports of the deposition of PPy onto fibres involved a two-step process, whereby paper was soaked in a $FeCl_3$ solution before immersion in a pyrrole solution [107]. Variations on this method include exposing the $FeCl_3$ to pyrrole monomer in the vapour phase [108,109] and soaking the substrate in monomer before polymerization in an oxidizing solution [110]. The process is also applicable to the use of various solvents [111].

The easiest method of applying conductive polymer to a textile is from a solution of the conducting polymer. The solubility of highly conducting polymers (PPy, PANI and Polythiophene) is limited to solvents that are not generally compatible with the textiles [112].

In-situ polymerization is another method for producing conductive coatings on textile substrates [113-115]. The mechanism for conducting polymer deposition proceeds through the adsorption of oligomeric species onto the textile surface, nucleation, from which subsequent polymerization occurs, growth, forming a smooth continuous film. Neither the monomer nor the oxidant is adsorbed to produce nucleation sites. In the presence of a fibrous surface, little or no polymer is found in solution. The coatings made by this method do not form significant fibre-to-fibre bonds, unlike solution and emulsion methods.

Polymer deposition is independent of surface material yielding films approx. 1 um thick and very uniform for coverage of 1-5%. Substrate material does not have a significant effect on the polymerization of pyrrole, yielding essentially the same conductivity for the same mass of textile. Factors important to determining the conductivity include surface area, hydrophobicity, surface polarity and porosity. Porous fibres (nylon and polyacrylonitrile) and materials with polar groups tend to increase adhesion and polymer deposition while non-polar fibres such as polyethylene and poly tetrafluoroethylene and dense crystalline fibres such as polyester yield poorer adhesion. The conductivity is not a linear function of the mass of PPy deposited [116]. Fabrics prepared from continuous filament yarns produce better conducting films than those prepared from spun fibre yarns [117].

Kinetics of the PPy deposition on textiles has been studied [114]. The rate of polymerization is dependent on the concentration of monomer and type of oxidizing agent. Ammonium persulfate, APS, is much faster than $FeCl_3$. Acidic $FeCl_3$ is much faster than more basic $FeCl_3$ as the acid drives the equilibrium

$$Fe(H_2O)_6^{3+} \leftrightarrow Fe(H_2O)_5\,(OH)^{2+} + H^+$$

to the left. The hydrated species is smaller and not as tightly coordinated, so the reaction is more simplistic. Highly coordinating ligands or high pH slows the reaction rate. Comparing reactions with and without the presence of fibres in the reaction

vessel, the reaction rate is faster with fibres present and second order, though first order reaction rates can be achieved if the Fe^{3+} concentration is significantly increased. Without fabric, the reaction rate is second order and slower. Pure solvents such as methanol, methylene chloride or acetonitrile permit polymerization to occur in the solution phase, so no PPy is deposited on the fabric.

Textiles may be scoured with surfactants before sale and these may have an effect on PPy formation. Surfactants that are cationic or nonionic do not promote adsorption while dodecylbenzene sulfonic acid, DBSA, marginally decreases adsorption. Hydrophobic surfactants such as alkylnaphthylsulfonate promote film formation. Other additives, such as 1,4-dihydroxybenzene, reduce adsorption while p-nitrophenol does not interfere. PPy – Fabric (Polyethyleneterphthalate and Polyethylene) samples have been chemically polymerized, using Poly (vinyl alcohol) as a surfactant to improve PPy coating on non-woven materials and NSA as a dopant with APS as oxidant [118]. Conducting fibres have also been fabricated by electropolymerising pyrrole with cotton, silk or wool fibre wrapped around the electrode [119].

2.3. Electromagnetic interference

An electromagnetic field is generated from various different components of electric field E and magnetic field H. An electric field is created due to a voltage difference across the points and magnetic field is generated by a moving charge, i.e. by a current flowing through a substance. Every current passing through an object is thus accompanied by both an electric and a magnetic field that can be shown in terms of waves as Figure 6.

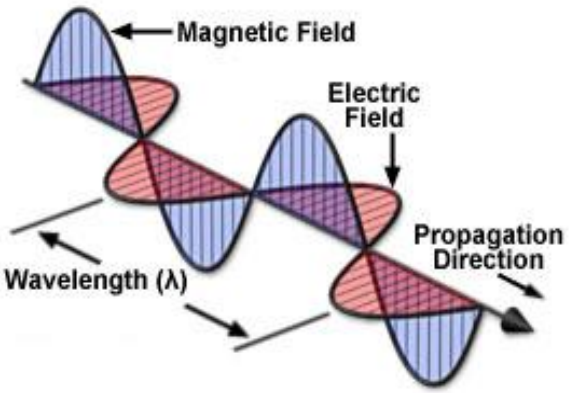

Figure 6: An electromagnetic wave

The ratio of E to H is defined as the wave impedance Z_w, [Ω] and depends on the type of source and the distance from the source. Large impedances characterize electric fields and small ones characterize magnetic fields. The near-field, far-field and the transition zone are regions of time varying electromagnetic field around any object that serves as a source for the field and these terms describe the way electromagnetic field change with distance from source object. The far field area begins when the distance to the source is large enough to form a coupled electric and magnetic field for which the field components are perpendicular to each other. Besides, this field can be considered locally to be a plane wave, so that the exposure is uniform over the body or body part. The more distant part of the electromagnetic field is the "radiative" field or far-field and it is familiar type of electromagnetic radiation seen in "free space", far from any electromagnetic field sources [120].

In the far field area the ratio between the electric field E [V m^{-1}] and the magnetic field H [A m^{-1}] remains almost constant and equal to 377Ω, i.e. the intrinsic impedance of free space. It is thus sufficient to measure only the electric field or the magnetic field to establish that the actual values are not being exceeded. In the near field area, the magnetic and electric fields are no longer coupled and the components of each field must be evaluated separately. Exposure in the near field area is no longer uniform. In the near field the exposure depends on the spatial distribution of the electric or magnetic field, the frequency used, the specific conductivity of tissue σ, the dielectric permittivity of tissue ε, the contact of the body with the ground and the machine, and the position, thus the geometry of the exposed person. The far field starts at a distance *r* from the source, for which,

$$r \geq \frac{2D^2}{\lambda}$$

In this relation *D* is the maximum dimension of the antenna and λ the wavelength, both in meters.

2.3.1. Electromagnetic interference shielding

The electromagnetic plane wave theory is generally applied for electromagnetic shielding in the region where the distance between the radiation source and the shield is larger than λ/2π (λ is the electromagnetic field wavelength) and it is the far field

shielding region. When the distance is less than $\lambda/2\pi$, it is in the near field shielding and the theory based on the contribution of electric and magnetic dipoles is used for electromagnetic shielding.

The amount of attenuation due to shield depends on the electromagnetic waves reflection from the shield surface, absorption of the waves into the shield and the multiple reflections of the waves at various surfaces or interfaces in the shield. The multiple reflections require the presence of large surface area (porous or foam) or interface area (composite material containing fillers with large surface area) in the shields. The loss in electromagnetic field intensity connected with multiple reflections that can be neglected when the distance between the reflecting surfaces or interfaces is large compared to the skin depth δ [m], defined as;

$$\delta = \frac{1}{\sqrt{\pi f \mu K}} \tag{1}$$

where f [Hz] is the frequency, μ [H.m^{-1}] is the measure of the ability of a material to support the formation of a magnetic field within itself and known as permeability and K [S.m^{-1}] is the electrical conductivity.

Efficiency of electromagnetic shields is commonly expressed by the *total shielding effectiveness* SE_T [dB] and mathematically expressed as;

$$SE_T = 10 \log_{10} \frac{P_t}{P_i} \tag{2}$$

Here, P_t = transmitted power, P_i = incident power

According to definition *of shielding effectiveness*, it is possible to express the shielding effectiveness SE_E for electric field and the shielding effectiveness SE_H for magnetic field by the following relations.

$$SE_E = 20 \log_{10} \frac{E_t}{E_i} \qquad SE_H = 20 \log_{10} \frac{H_t}{H_i}$$

where E_i [V m^{-1}] (or magnetic H_i [A m^{-1}]) is the field strength outside of shielding layer and E_t (or H_t) is the resulted field strength after passing through shielding layer. Typical behaviours of SE_E and SE_H as a function of frequency are given in Figure 7

[121]. It has been observed that below a certain frequency of electromagnetic field f_t shielding of electric and magnetic fields behave in opposite sense. At the frequency beyond f_t, shielding effectiveness for electric field surges to link the shielding effectiveness for magnetic field.

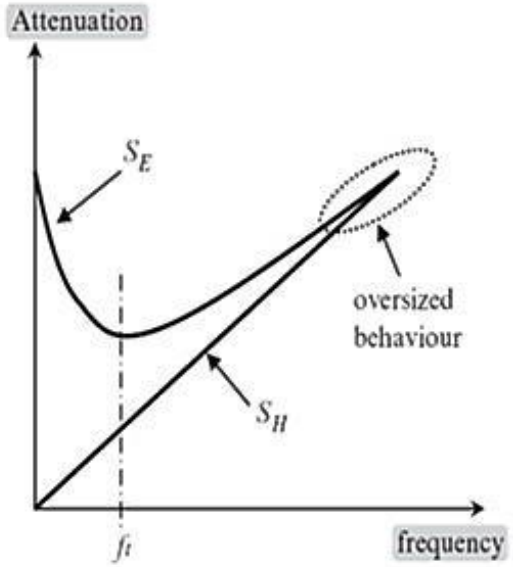

Figure 7: Dependence of electric and magnetic shielding effectiveness on frequency [10]

Shielding effectiveness of the conductive materials having thickness *t* can be expected by the following expression [122,123];

$$SE_T = 50 - 10\log_{10}\left(\frac{f}{K}\right) + 1.7t\sqrt{fK} \tag{3}$$

The practicality of this model can be established by comparison with the model of White [124], which is typically used to predict the shielding effectiveness.

$$SE_T = 168 - 10\log_{10}\left(\frac{K_c f}{K}\right) + 1.315t\sqrt{f\,\frac{K}{K_c}} \tag{4}$$

where K_c is the conductivity of Copper ($5.82\ 10^5$ S cm^{-1}). For a single layer, the theoretical value *SE* can be written as;

$$SE_T = 20\log_{10}\left(1 + \frac{K \cdot t \cdot Z_0}{2}\right) \tag{5}$$

Z_0, is the free-space wave impedance, 377Ω [125].

2.4. Heat generation

A medium through which heat is conducted may involve the conversion of mechanical, electrical, nuclear, or chemical energy into heat (or thermal energy). In heat conduction analysis, such conversion processes are characterized as heat (or thermal energy) generation. When a potential difference is applied across the ends of a conductor, the free electrons are accelerated and acquire kinetic energy. As the electrons move through, they collide with the positive ions and atoms of the conductor and transfer their kinetic energy to them. Between two collisions, the electrons again pick up kinetic energy from the electric field. As a result, the kinetic energy of vibration of these lattice ions or atoms increases. This increases the thermal energy of the lattice, which means that the temperature of the conductor increases. Since the source of electromotive force (emf) (e.g., a battery) is maintaining current in the conductor, the electrical energy supplied by the battery is converted into heat in the conductor and known as Joule heating.

Joule heating is the dominant mechanism for heat generation due to the flow of electrical current through the material. It is defined by Joule's law, which for an ohmic conductor has the form;

$$\dot{e}_{gen} = j^2 \rho \tag{6}$$

Here j is the current density vector in [A.m^{-2}], ρ is the specific electrical resistivity in [Ω.m] and $\dot{e}_{gen}$ is the generated heat per unit volume in [W.m^{-3}]. This is usually the main effect responsible for heat generation in resistively heated systems. Some devices like micro sensors and micro actuators are designed to optimize the Joule heating effect in a controlled manner in order to improve transduction efficiency.

The rate of heat generation in a medium may vary with time as well as position within the medium. When the variation of heat generation with position is known, the *total* rate of heat generation in a medium of volume v can be determined from;

$$\dot{E}_{gen} = \int_v \dot{e}_{gen} dv \tag{7}$$

In the special case of *uniform* heat generation, as in the case of electric resistance heating throughout a homogeneous material, the relation in Equation 7 reduces to $\dot{E}_{gen} = \dot{e}_{gen} v$ where $\dot{e}_{gen}$ is the constant rate of heat generation per unit volume.

2.4.1. Heat conduction: Electric field interaction

Consider heat conduction through a large plane wall such as the wall of a house, the glass of a single pane window, the metal plate at the bottom of a pressing iron, a cast-iron steam pipe, a cylindrical nuclear fuel element, an electrical resistance wire, the wall of a spherical container, or a spherical metal ball that is being quenched or tempered. Heat conduction in these and many other geometries can be approximated as being one-dimensional since heat conduction through these geometries is dominant in one direction and negligible in other directions.

Consider a thin element of thickness Δx in a large plane object. Assume the density of the object is ρ, the specific heat is c, and the area of the wall normal to the direction of heat transfer is A. An *energy balance* on this thin element during a small time interval Δt can be expressed as;

Rate of heat conduction at x	−	Rate of heat conduction at x+Δx	+	Rate of heat generation inside the element	=	Rate of change of energy content of the element

$$\dot{Q}_x - \dot{Q}_{x+\Delta x} + \dot{E}_{gen,element} = \frac{\Delta E_{element}}{\Delta t} \tag{8}$$

But the change in the energy content of the element and the rate of heat generation within the element can be expressed as;

$$E_{element} = E_{t+\Delta t} - E_t = mc\left(T_{t+\Delta t} - T_t\right) = \rho c A \Delta x \left(T_{t+\Delta t} - T_t\right) \tag{9}$$

and

$$\dot{E}_{gen} = \dot{e}_{gen} v_{element} = \dot{e}_{gen} A \Delta x \tag{10}$$

Substituting into Equation 8 and dividing by $A\Delta x$ gives,

$$-\frac{1}{A}\frac{\dot{Q}_{x+\Delta x} - \dot{Q}_x}{\Delta x} + \dot{e}_{gen} = \rho c \frac{\left(T_{t+\Delta t} - T_t\right)}{\Delta t} \tag{11}$$

Taking the limits as $\Delta x \rightarrow 0$ and $\Delta t \rightarrow 0$ yields

$$\frac{1}{A}\frac{\partial}{\partial x}\left(kA\frac{\partial T}{\partial x}\right)+\dot{e}_{gen}=\rho c\frac{\partial T}{\partial t} \tag{12}$$

Since, from the definition of the derivative and Fourier's law of heat conduction,

$$\lim_{\Delta x\to 0}\frac{\dot{Q}_{x+\Delta x}-\dot{Q}_x}{\Delta x}=\frac{\partial \dot{Q}}{\partial x}=\frac{\partial}{\partial x}\left(kA\frac{\partial T}{\partial x}\right) \tag{13}$$

Noting that the area A is constant for a plane object, the one-dimensional transient heat conduction equation in a plane object becomes;

Variable conductivity:
$$\frac{\partial}{\partial x}\left(kA\frac{\partial T}{\partial x}\right)+\dot{e}_{gen}=\rho c\frac{\partial T}{\partial t} \tag{14}$$

The thermal conductivity k of a material, in general, depends on the temperature T (and therefore x), and thus it cannot be taken out of the derivative. However, the *thermal conductivity* in most practical applications can be assumed to remain *constant* at some average value. The Equation 14 in that case reduces to;

Constant conductivity:
$$\frac{\partial T}{\partial x}+\frac{\dot{e}_{gen}}{k}=\frac{1}{\alpha}\frac{\partial T}{\partial t} \tag{15}$$

where, the property $\alpha=k/\rho c$ is the *thermal diffusivity* of the material and represents how fast heat propagates through a material.

2.5. Thermal influence on resistance

In metals, where the valence bands are only partially filled even in the ground state, the effective concentration of carriers is barely affected by temperature. Actually, the conductivity decreases slightly with increasing temperature, because at higher temperatures the lattice vibrations scatter electrons and their mobility goes down. For the same reason mobility also decreases with temperature in the case of semiconductors, but the conductivity still increase with temperature, because the steep rise of carrier concentration suppresses the more gradual decline in mobility [98].

Doping agent and lattice defects also affects the mobility by acting as scattering centres for electrons and holes. In high purity materials scattering by lattice vibrations (carrier-phonon interactions) is the principal scattering mechanism at room

temperature, but scattering by impurities becomes dominant at low temperature as the lattice vibrations are frozen out.

Conducting polymers are amorphous with short conjugation lengths. Therefore, it has been suggested that electrical conduction takes place by charge hopping between polymeric chains. A model used to describe the conduction process is the one originally developed for amorphous silicon by Mott and Davis [126]. When applied to conducting polymers, it assumes that electron transport originates from localized or fixed states within the polymer chain. The charge transfer between the chains takes place by hopping, referred to as phonon assisted hopping, between two localized states. Lattice vibrations enhance this process of tunnelling from one localized state to another.

Most conducting polymers showed a temperature dependence of DC conductivity consistent with the Variable Range Hopping Conduction process, obeying the following relationship:

$$\sigma = \sigma_0 \exp\left[-\left(\frac{T_0}{T}\right)^{1/4}\right] \tag{16}$$

where Mott's parameters are listed as follows;

$$\sigma_0 = e^2 R^2 \upsilon_{ph} N(E_F)$$

$$T_0 = \frac{\lambda \alpha^3}{kN(E_F)}$$

$$R = \left[\frac{9}{8\pi\alpha kTN(E_F)}\right]^{1/4}$$

$$W = \frac{3}{4\pi R^3 N(E_F)}$$

Here,

σ = conductivity of sample at temperature T [S.cm^{-1}]

σ_0 = pre-exponential factor [S.cm^{-1}]

T_0 = characteristic temperature [K]

e = electronic charge (1.602×10^{-19}C)

k = Boltzmann's constant (8.616×10^{-5}eV.K^{-1})

R = average hopping distance [cm]

υ_{ph} = phonon frequency ($\approx 10^{13}$Hz))

$N(E_F)$ = density of localized states at the Fermi level (cm^3.eV^{-1})

λ = dimensional constant (≈ 18.1)

α = coefficient of exponential decay of the localized states [cm^{-1}]

W = hopping activation energy [eV]

Taking the natural logs of both sides of Equation 16, the following relationship is obtained:

$$\ln \sigma = \ln \sigma_0 - (T_0)^{1/4} (T)^{-1/4}$$

By assuming the localization length of localized electrons as 3 Å, which is approximately equal to the length of the pyrrole monomer, Kaynak [127] observed that nature of the $ln\sigma$ vs $T^{-1/4}$ plots justifies the validity of Equation 16 for PPy film at very low temperatures however this relation has not been studied at the temperatures around Tg of PPy.

Chapter 3

Materials and Methods

This chapter mainly deals with the materials chosen for experiments and method of coating of PPy on selected textile substrates. This chapter also contains the testing procedures to characterize the PPy coated substrate such as electrical resistivity, percentage weight gain, tensile properties, Scanning Electron Microscopy, Laser Scanning Confocal microscopy, Fourier's Transform Infrared spectroscopy and Differential Scanning Calorimetry.

3.1. Materials

3.1.1. Glass fabric samples

Two structures of glass fabric have been chosen with the intension of investigating electromagnetic shielding effectiveness of PPy coating of the same in this dissertation. One structure was designated as suffix "T" for PPy coated samples whereas second structure was designated as suffix "D". The specifications of selected fabric structures are tabulated in Table 3.

Table 3: The particulars of the glass fabric structures selected for experiments

Properties		**Structure 1**	**Structure 2**
Weave		3/1 4-ends Broken Twill	Plain
Fineness [tex]	**Warp**	125	1250
	Weft	135	1250
Warp/cm		22	3.67
Weft/cm		10	3.5
Cover factor (SI) [%]	**Warp**	24	13
	Weft	11.6	12.4
Areal density [g.m^{-2}]		410	900
Thickness [mm]		0.54	1.1
Fabric porosity *(ϕ)*		0.701	0.678

Fabric porosity has been calculated by following formula [128];

$$\phi = 1 - \frac{\rho_{fa}}{\rho_f}$$

Here, ρ_{fa} is the density of fabric that can be evaluated through dividing areal density by the thickness whereas ρ_f is the known density of fibre.

The microscopic images of the structures with their corresponding weave pattern are illustrated in Figure 8 and Figure 9.

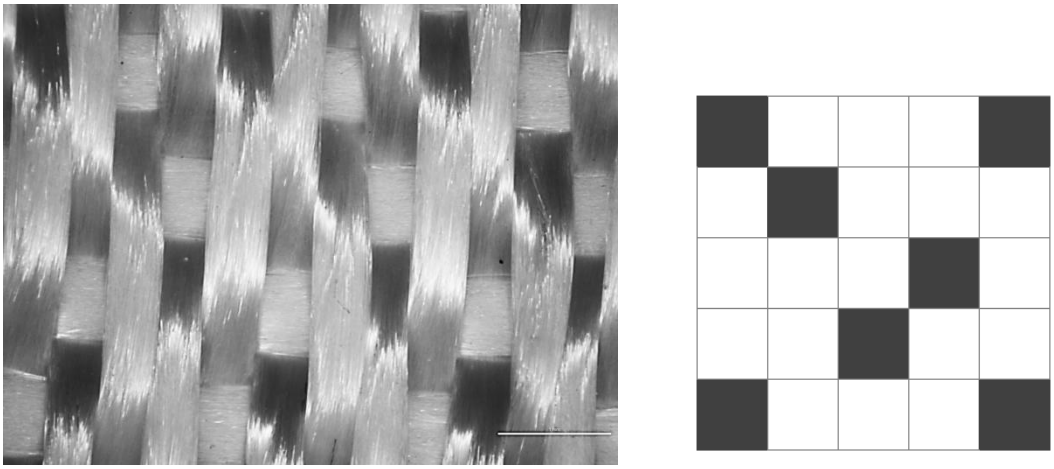

(a) (b)

Figure 8: Structure 1 (a) microscopic image (b) weave pattern

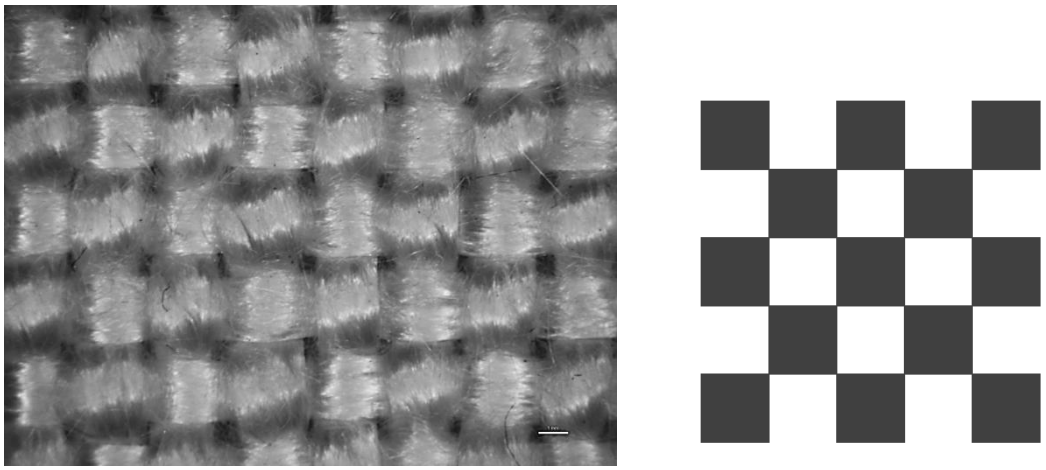

(a) (b)

Figure 9: Structure 2 (a) microscopic image (b) weave pattern

3.1.2. Latex/Polyamide-6

For developing the strain sensor, PA6 wrapped Latex yarn produced by PEGA® Czech Republic, has been selected as a substrate for the deposition of PPy. The microscopic images are shown in Figure 10 and the specifications of this yarn are described in Table 4.

Table 4: The particulars of PA6 wrapped latex yarn

Properties		**Index**
Diameter of Latex [mm]		0.6
***Effective diameter of whole thread [mm]**		0.68
Linear density of Latex [tex]		36.8
Fineness of PA6 [tex]		22x3
No. of turns of PA6 around Latex [cm^{-1}]		12
Composition [%]	**PA6**	42
	Elastodiene	58

*Yarn packing density was assumed as $\mu = 0.525$ [128]

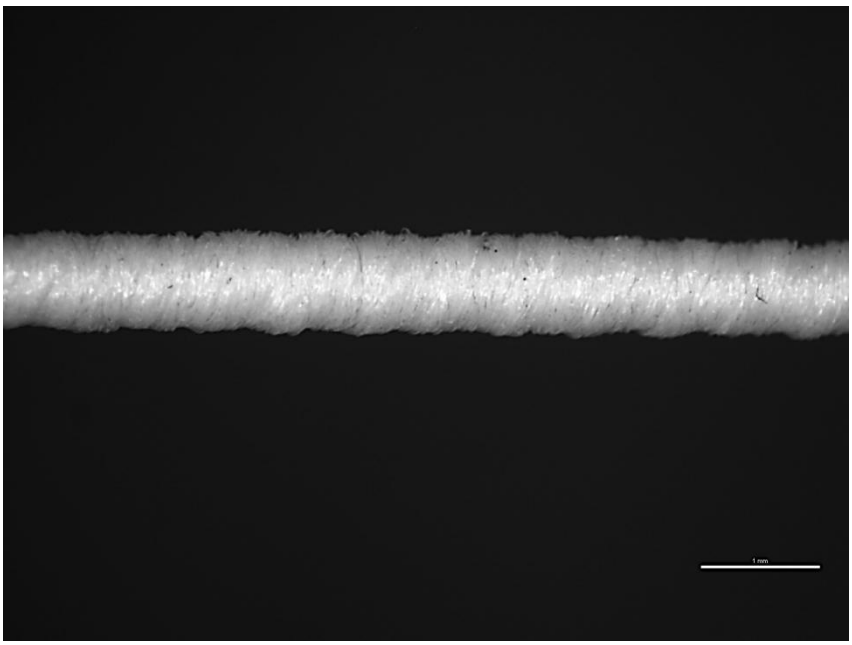

(a)

(b)

Figure 10: Latex/PA6 yarn microscopic images (a) longitudinal view (b) end view

3.1.3. Chemicals

3.1.3.1. Pyrrole (monomer)

Pyrrole is available in the market with different synonyms such as 1H-Pyrrole, Divinylenimine, Imidole, Azole, Monopyrrole, 1-Aza-2,4-cyclopentadiene. For this dissertation Pyrrole 98% was received from Alfa Aesar® and was used after distillation to remove colouring impurities.

Due to participation of lone pair of Nitrogen in aromaticity, pyrrole has exceptionally strong acidic properties. It can react with strong bases or Grignard reagent or potassium metal in inert solvents and with sodium amide in liquid ammonia, to give salt-like compounds which can be used to alkylate or acylate the nitrogen atom [129].

If PPy is released to air, a vapour pressure of 8.35 mm Hg at 25 °C indicates pyrrole exists solely as a vapour in the ambient atmosphere. Vapour-phase pyrrole is degraded in the atmosphere by reaction with photochemically-produced hydroxyl radicals; the half-life for this reaction in air is estimated to be 4 days. Pyrrole does not absorb light in the environmental UV spectrum, and is not expected to directly photolyze. Pyrrole does not readily undergo biodegradation in water unless bacteria exists there that have had previous exposure to pyrrole. Given this need for acclimation, the decomposition of pyrrole may be very slow. Hydrolysis is not

expected to occur due to lack of hydrolyzable functional groups. Occupational exposure to pyrrole may occur through inhalation and dermal contact with this compound at workplaces where pyrrole is produced or used [130].

3.1.3.2. Oxidizing agent: Iron(III) Chloride

Anhydrous Iron(III) Chloride 97% was ordered from Sigma-Aldrich® and was used as received. It has molar mass 162.2 $g.mol^{-1}$ and density of 2.898 $g.cm^{-3}$.

Anhydrous Iron(III) chloride is a fairly strong Lewis acid, and it is used as a catalyst in organic synthesis. It serves as catalyst in various chemical reactions. Just like aluminum chloride, Iron(III) chloride is a low Lewis acid. When dissolved in water, Iron(III) chloride undergoes hydrolysis and gives off heat in an exothermic reaction. The resulting brown, acidic, and corrosive solution is used as a flocculants in sewage treatment and drinking water production, and as an etchant for copper-based metals in printed circuit boards.

Iron(II) ions are easily oxidised to Iron(III) ions, and iron(III) ions are fairly easily reduced to Iron(II) ions. The redox potential of the reaction is E°=+0.77V [131] and the equilibrium of the reaction would be:

$$Fe^{+3}_{(aq)} + e^{-} \rightleftharpoons Fe^{+2}_{(aq)}$$

During the reduction of $FeCl_3$, one chloride Cl^- gets free which stabilizes the cation of the monomer [132]. In any case if chlorine molecule is being generated during the reaction, it is again well known oxidising agent. Notice that the equilibrium is still written with the electrons on the left-hand side of the equation. That's why the chlorine gas has to appear on the left-hand side rather than on the right and redox potential of the reaction is E°=+1.36V [132].

$$Cl_{2(g)} + 2\ e^{-} \rightleftharpoons 2\ Cl^{-}$$

Notice that the E° value is much positive than the Ferric one. The position of the Iron(III) / Iron(II) equilibrium is not as far to the right as the chlorine equilibrium. That means that Fe^{3+} ions do not pick up electrons as easily as chlorine does. Chlorine is a stronger oxidising agent than Fe^{3+} ions.

3.1.3.3. Doping agent: Tetraethylammonium p-toluenesulfonate

Tetraethylammonium p-toluenesulfonate also called tosylate (TsO^-) was obtained from Aldrich and was used as received.

Many researchers [133,134] have studied the effect of the counterion on the electropolymerization process. The high concentration of counterion employed means that it can have a dramatic effect on the polymerization process. The electrolyte will influence the conductivity of the solution, the polymer properties, and hence the rate of polymerization. The "magical" counterions in terms of conductivity and mechanical properties appear to be sulfonated aromatics, [135,136] in particular, p-toluene sulfonate (TsO^-). It has been shown that the benzene sulfonates induce a degree of crystallinity [137,138], which results in higher conductivity that, in turn, enables the polymerization process to proceed efficiently. It has also been suggested that the sulfonated aromatics exhibit surfactant-like behaviour in that the radicals are stabilized and presumably protected from unwanted side reactions with the solvent, oxygen or other nucleophiles

3.2. Method for the sample preparation

3.2.1. Optimizing oxidant and dopant molar ratio

Series of experiments were conducted in order to optimize the molar ratio of $FeCl_3$ and TsO^- before preparing the final recipe for the deposition of PPy on textile substrates. For this purpose four aqueous baths of $FeCl_3$ and TsO^- with different molar ratio were prepared and glass fabric samples of structure 1 were treated with it as described in the following section. Different molar ratios of $FeCl_3$ and TsO^- were prepared as shown in Table 5.

Table 5 Selected molar ratios of $FeCl_3$ and TsO^- for optimization of recipe

	1	**2**	**3**	**4**
Molar ratio $FeCl_3$: TsO^-	2 : 0.5	2 : 1	2 : 1.5	2 : 2

The influence of this variable of synthesis on the resistivity of the vapour deposited PPy on glass fabric is presented in Figure 11.

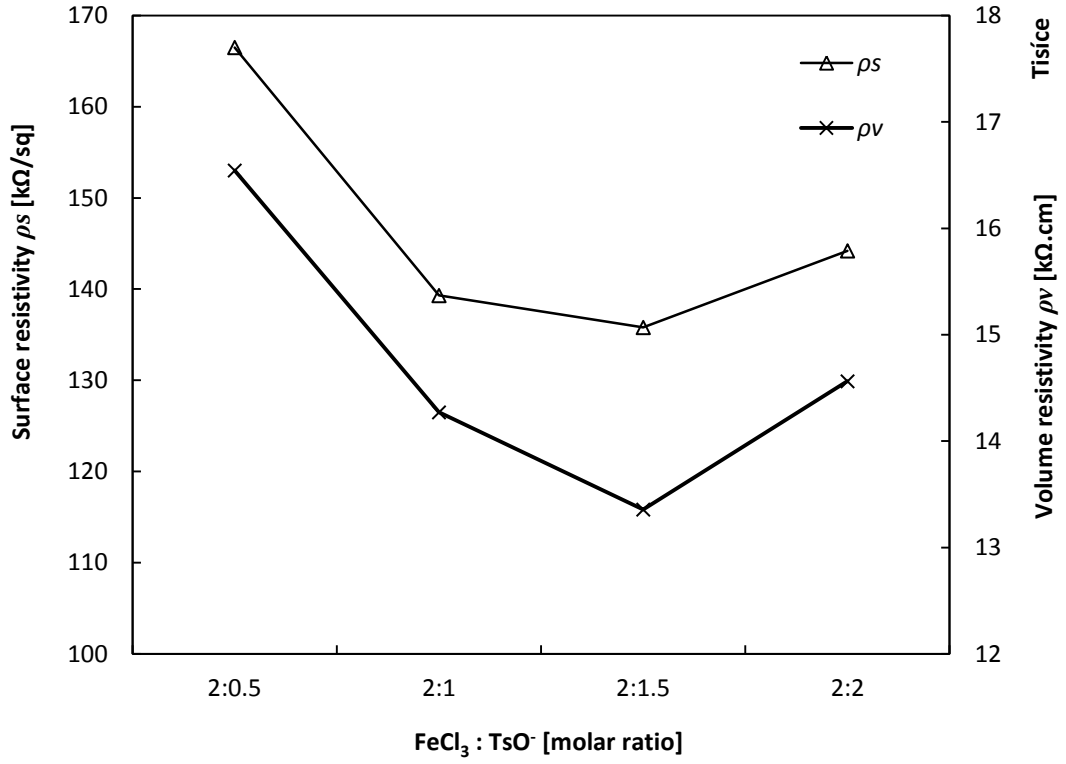

Figure 11: Effect of molar ratio of $FeCl_3$ and TsO^- on surface and volume resistivity of PPy coated glass fabric

Conductive glass fabric was obtained by keeping concentration of $FeCl_3$ constant and concentration of TsO^- was varied. As it can be observed from the Figure 11, the increase of the electrolyte concentration from 0.5 to 1 M gives fabric with decreased resistivity. The radical cations can be stabilized at increasing electrolyte concentrations. If the electrolyte concentration is lower, the radical cations have higher reactivity and, consequently, the obtained polymer should have many defects and a short conjugated structure, with a lower conductivity. This explanation is supported by the strong basicity of TsO^- anions (pK_a=-1.34), which promotes a high interaction with monomeric radical cations.

Higher concentrations than 1 M seems to affect the resistivity of the obtained fabric sample very little but increase the cost of synthesis only therefore considered as optimized concentration of doping agent. This behaviour can be explained from the polymerization mechanism as discussed in section 2.2.3.1, in terms of the stability of the intermediate radical cations generated by pyrrole oxidation [74]. Thus, the

electrolyte concentration reflects the strength of the interaction between the electrolyte and the radical cation.

3.2.2. Glass fabric samples' preparation

The glass fabric samples used in this dissertation were washed thoroughly with acetone to remove impurities such as, dust, dirt and spin finish present in the fabric. The washed samples were dried at room temperature 20±2°C.

3.2.2.1. Coating of sample by polypyrrole

An aqueous liquor bath was prepared using 2:1 molar ratio of $FeCl_3$ and TsO^-. This molar ratio between oxidant and dopant was optimized by the series of experiments as discussed earlier. As $FeCl_3$ follows exothermic reaction when comes in contact with water, ice was used to reduce the temperature of the solution around 20°C. The fabric sample was immersed in bath for 1 min followed by squeezing at 70% pickup (maximum pickup by glass fabric) with the help of pneumatic squeezing rollers. Sample was then placed with the help of holders in a glass desiccator filled with pyrrole vapours immediately after padding and squeezing. The temperature of desiccator was kept at 20±2°C and sample was remained into it for 6 h under ambient atmospheric pressure. Sample was then taken out and washed with ethanol in order to stop polymerization and subsequently with plenty of distilled water for several times to remove bi-products and unreacted chemicals. Finally sample was dried in air at 20±2°C for 24 h. Four different samples of each structure of glass fabric were prepared in exactly the same way by varying the concentration of $FeCl_3$ and TsO^- as mentioned in the Table 6.

Table 6: Recipes for the preparation of PPy coated glass fabric samples

Sample label Structure 1	Sample label Structure 2	Iron(III) Chloride ($FeCl_3$) [mol/L]	Tosylate (TsO^-) [mol/L]
T1	D1	0.3	0.15
T2	D2	0.4	0.2
T3	D3	0.5	0.25
T4	D4	0.6	0.3

3.2.3. Latex/PA6 samples' preparation

3.2.3.1. Coating of sample by polypyrrole

Latex/PA6 yarn was used as it was received. The method for coating PPy on Latex/PA6 samples was the same as discussed above. Three different samples of Latex/PA6 were prepared in exactly the same way by varying the concentration of $FeCl_3$ and TsO^- as mentioned in the Table 7.

Table 7: Recipes for the preparation of PPy coated Latex/PA6 yarn samples.

Sample label Latex/PA6	Iron(III) Chloride ($FeCl_3$) [mol/L]	Tosylate (TsO^-) [mol/L]
SY1	2.0	1.0
SY2	0.6	0.3
SY3	0.1	0.05

3.3. Characterization of samples

3.3.1. Measurement of electrical resistivity of PPy coated glass fabric

All the fabric samples were conditioned at standard atmospheric conditions of (20 ± 2)°C *temperature* and (40 ± 2)% *relative humidity* before measurements conforming to ČSN 80 0059.

For evaluation of electrical properties of fabrics, two parameters were selected, namely the surface and volume resistivity. These parameters can be calculated from the information of surface and bulk resistivity, the dimensions of the electrodes, and/or the thickness of the sample. For this purpose, concentric electrode system was used conforming to DIN EN 1149-1, EN 100 015, EN 61340-5-1 together with Agilent 53131A digital multimeter. Measurements of electrical resistance were also performed in the climatic conditions, in accordance with the standard ČSN 80 0059.

The relationship between surface resistivity and the surface resistance for concentric ring probe geometry can be found by defining a surface current density in the area

between rings. Knowing the surface current density, it is possible to find electric field intensity between the electrode rings as shown in Figure 12. Hence the surface resistivity ρ_s can be calculated which is related to the surface resistance R_s by a constant that depends on the geometry of the electrodes as follows;

$$\rho_s = R_s \frac{2\pi}{\ln r_2 / r_1} \tag{17}$$

Where, r_1= outer radius of inner or centre electrode and r_2= inner radius of outer ring electrode

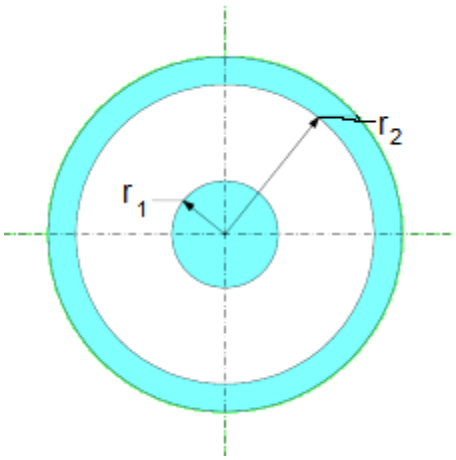

Figure 12: Surface resistance measurement configuration for concentric ring electrodes

Similarly, volume resistivity ρ_v can be determined by using two centre electrodes facing each other keeping the fabric substrate sandwich between them. In this case it will be;

$$\rho_v = R_v \frac{2\pi r_1}{d} \tag{18}$$

Here, d is the thickness of the fabric substrate measured with the help of thickness gauge tester according to IS: 7702:1975 and R_v is the resistance measured through the electrodes.

3.3.2. Measurement of electrical resistivity of PPy coated Latex/PA6 yarn samples

With the intention of measuring electrical resistance *R* of PPy coated Latex/PA6 samples, stainless steel clamps were used to hold the sample together with connecting wires and a digital multimeter as shown in the Figure 13. The electrical resistivity ρ of the yarn sample was calculated from the Equation 19, by knowing average cross-sectional area of the yarn sample "*a"* and the length of the sample "*L"* between two measuring electrodes A and B.

$$\rho = R\frac{a}{L} \tag{19}$$

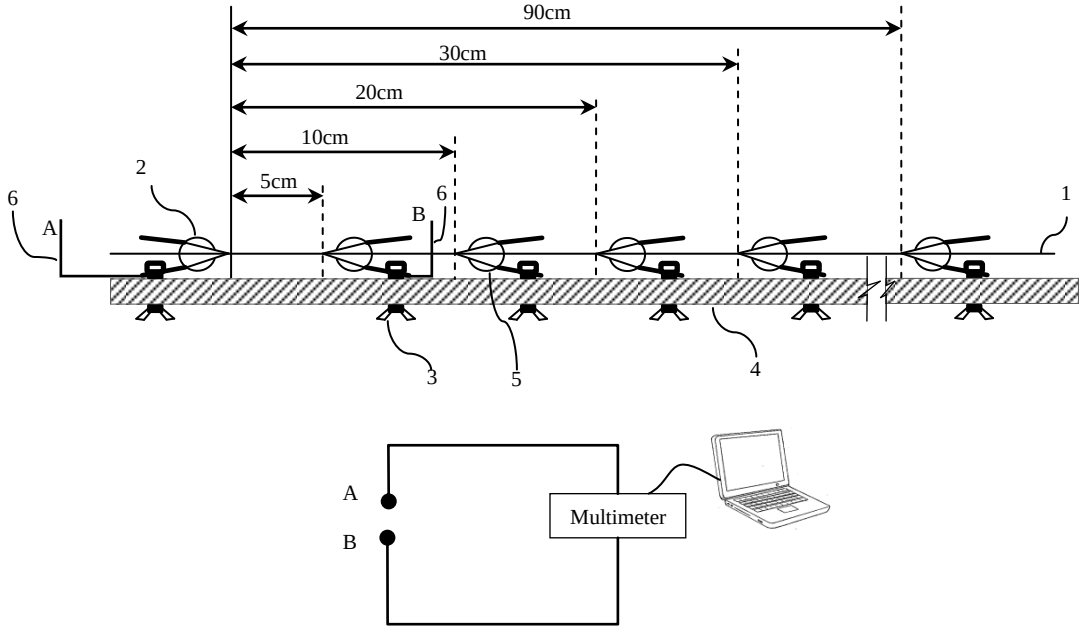

Figure 13: Schematic diagram of experimental setup for the measurement of electrical resistance of yarn (1) the sample (2) stainless steel clamp type electrode to hold sample (3) clamp supporting bolt and washers (4) supporting pad made of an electrically non-conductive material, (5) other electrode clamp with change in length of the measured section (6) wires connected to the electrodes and multimeter

With the objective of determining the dependence of electrical resistance on length of a sample, the resistance was measured by varying the distance from 5cm to 90cm between measuring electrodes.

3.3.3. Estimation of mass gain

The influence of concentration of $FeCl_3$ and TsO^- on the total mass gain of the glass fabric was studied. By keeping the molar ratio of $FeCl_3$ and TsO^- as 2:1, concentration $FeCl_3$ was varied and different samples were coated by PPy in the same way as described earlier.

The amount of PPy deposited on the substrate was calculated as per the relation given below;

$$\text{Mass gain [\%]} = \frac{(\text{Mass of the sample after coating} - \text{Mass of sample without coating})}{\text{Mass of sample without coating}} \times 100 \quad (20)$$

Mass of the samples was measured according to IS: 1964:1970 with the help of digital weighing balance from Kern & Sohn® GmbH till four decimal places of accuracy.

3.3.4. Measurement of EMI shielding effectiveness

For measuring EMSE, specimen holder EM-2107A from Electro-metrics® USA along with ZNC3-Vector Network Analyser from Rohde & Schwarz® GmbH & Co. Germany, were used. The EM-2107A is a standard test fixture for evaluation of the electromagnetic shielding effectiveness of planar material. The fixture is an enlarged section of coaxial transmission line and complies fully with the requirements of ASTM test method D4935-1. The measured data relates to the shielding effectiveness due to a plane wave (far field EM wave).

All glass fabric samples described in Table 6 were tested for EMSE for transmission as well as for reflection in the frequency range from 300 MHz till 1.5 GHz by conforming ASTM test method D4935-1 and data were collected. The coaxial transmission line method was used to measure the SE of the specimens as shown in Figure 14.

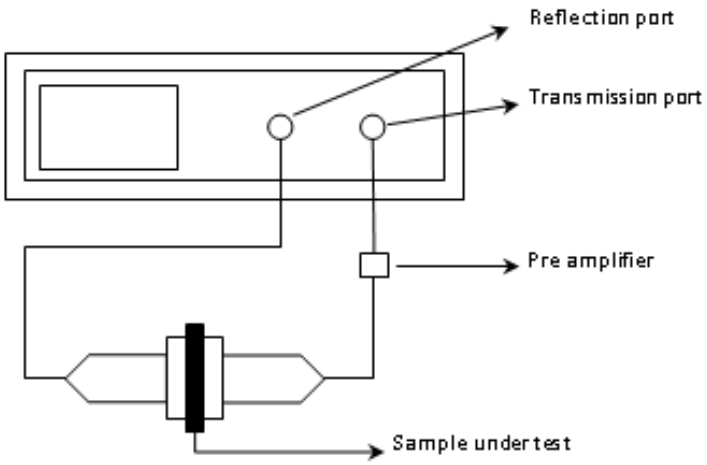

Figure 14: A typical coaxial transmitter for EMSE testing

For the purpose of summarizing the results in the dissertation, the dependence of EMSE for transmission and reflection on electrical resistivity have been plotted against the frequency of 800 MHz (commonly used for Bluetooth and GSM networks).

3.3.5. Measurement of heat generation by PPy coated glass fabric

For the purpose of evaluating heat generation by PPy coated glass fabric, a specimen of 2 cm wide and 7 cm long was cut from D4 sample however the distance between clamps was set as 6 cm. Different DC voltage i.e. 5V, 10V, 15V and 20V by the voltage supplier NZ-2229.2 from Statron® Czech Republic, were applied via stainless steel clamp type electrodes. Meanwhile DC current passing through substrate was measured by connecting Agilent 53131A digital multimeter in series. Three samples were taken for each measurement and in this way total twelve samples were tested. The experimental setup is shown in Figure 15. The rise in temperature was determined by Infra-Red thermal camera by Fluke® together with k-type thermo couples in connection with ART® data acquisition module. Infra-Red thermal camera was helpful to figure the homogeneity of the specimen out.

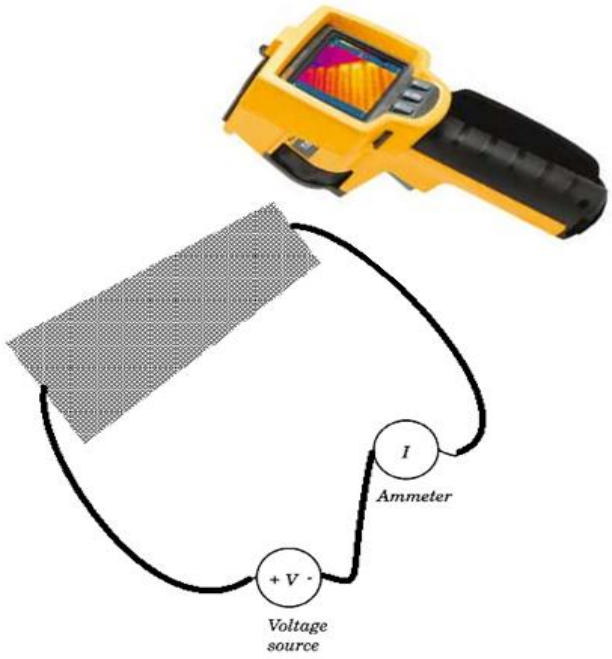

Figure 15: Experimental setup for measuring heat generation by PPy coated glass fabric samples

3.3.6. Measurement of electrothermal effect in PPy coated glass fabric

With the intention of investigating electrothermal effect in PPy coated glass fabric, specimen of 2 cm wide and 11 cm long was cut from sample T4 and placed between two stainless steel clamp type connectors by keeping the distance between clamps as 10 cm. Sample was then placed in laboratory oven from Venticell® MMM at particular temperature as shown in Table 8 for approx. 5 h and change in electrical resistance was measured through Agilent® 53131A digital multimeter each after 1s. The data was recorded in computer through the software run on LabView. Each measurement was repeated thrice with a freshly prepared sample each time and in this way 15 samples were measured in total. The experimental setup is shown in Figure 16.

Table 8: Different levels of temperature applied to analyse electrothermal effect

Factor	**Level 1**	**Level 2**	**Level 3**	**Level 4**	**Level 5**
Temperature *T* [°C]	30	60	90	120	150

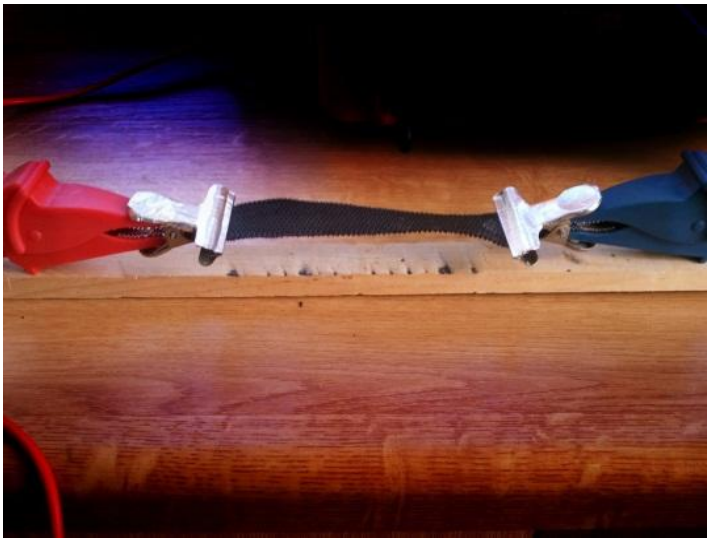

(a)

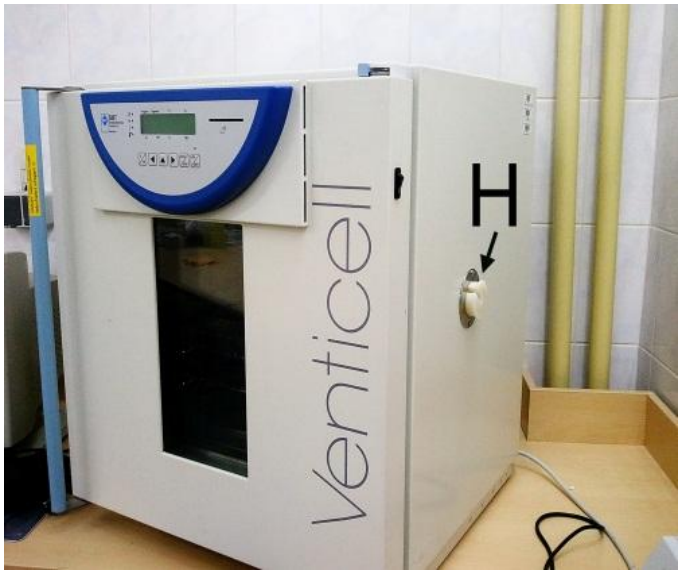

(b)

Figure 16: Experimental setup for the measurement of resistance upon heating (a) Electrodes holding fabric sample mounted on wooden stick (b) Heating oven having hole "H" in the side wall

3.3.7. Measurement of tensile properties

Specimens of 6 cm wide and 20 cm long were cut for the test, which were made 5 cm wide by removing longitudinal yarns from the sides. Two sets of three specimens each were tested, one set for the warp direction tensile strength having the long dimension parallel to the warp direction, and the other set for weft direction tensile strength having the long dimension parallel to the weft direction.

No specimen was taken nearer the selvage than 1/10th the width of the fabric. The distance between the pair of jaws on the apparatus was 10 cm at the start of the test. The rate of separation of the jaws was 100 ± 1 mm per minute. No two specimens for breakage contained the same set of yarns. The test was performed on Dynamometer TIRAtest® 2300 from Germany.

The initial modulus was calculated as first derivative of stress/strain curve near origin whereas elongation at break (Ultimate Elongation) was calculated as follows:

$$\text{Elongation at break [\%]} = \frac{X_1 - X_0}{X_0} \cdot 100$$

X_0= distance between jaws at start of rest

X_1= distance between jaws at moment of rupture

3.3.8. Surface morphological studies

Few fibres were taken out from PPy coated sample D4 and viewed under Scanning Electron Microscope (SEM) Carl Zeiss® Ultra plus and TESCAN VEGA® as well as under Laser Scanning Confocal Microscope (LSCM) Olympus® Japan. For SEM imaging, fibres were fixed at sample holder by double sided adhesive tape and then coated by gold before taking the images. For LSCM, the fibres were placed on a glass slide and images were recorded along with their corresponding reflected data.

The aim of this microscopic study was to analyse the surface morphology of the PPy coated fibres and estimation of thickness of PPy on glass fibres as well.

3.3.9. Measurement of sensitivity of PPy coated Latex/PA6 yarn

With the objective of characterizing sensitivity of PPy coated Latex/PA6 yarn samples against deformation, all the samples from Table 7 were subjected to cyclic loading by using tensile testing machine Labtest from LaborTech® Ltd Czech Republic. The arrangement of the experiment environment can be seen in Figure 17. The cycle was set for 2% strain at the jaw moving speed of 100mm/min with a rest of 1 second at relaxed or initial position to synchronize normal human breathing rhythm. One set of measurement includes 40 cycles, therefore in this way 5 sets of readings

were recorded and sensitivity $dR/d\varepsilon$ of the yarn sample was monitored. Here dR is the average change in resistance (R_1-R_o) of the specimen calculated from 5 sets of 40 cycles during extension of 2% and $d\varepsilon$ is the change in length [mm]. R_1 is the resistance of specimen at 2mm extension whereas R_o is the resistance at relaxation or initial point.

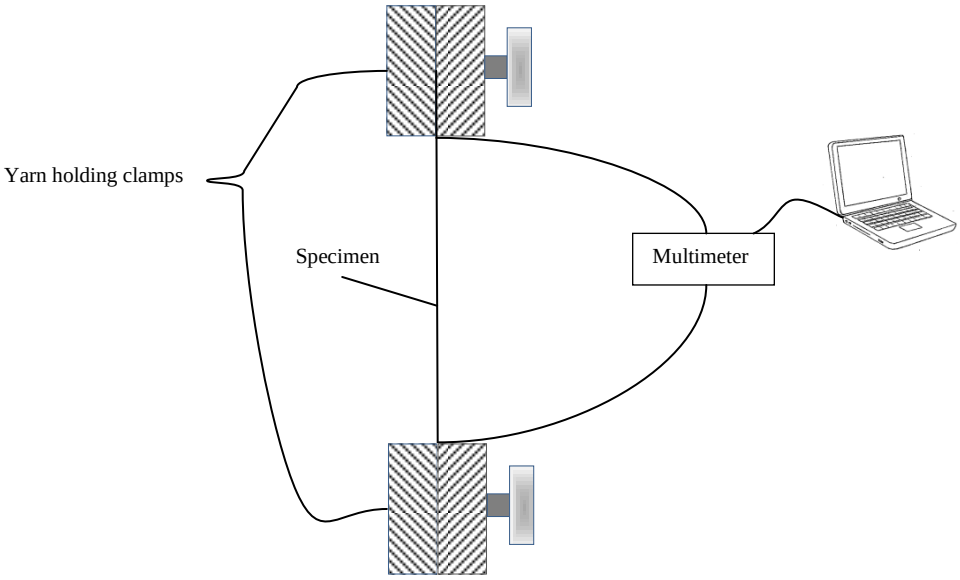

Figure 17: Experimental arrangement for measuring sensitivity at cyclic loading

3.3.10. Measurement of effect of washing on PPy coated Latex/PA6 yarn samples

As PPy coated Latex/PA6 yarn can find its practical application in the field of body movement sensor after being embedded in the garment, it is very important to analyse the change in electrical resistance after domestic or commercial laundering. Therefore, a sample of 10cm long was taken from each of PPy coated Latex/PA6 yarn sample described in Table 7 and subjected to washing fastness test conforming ISO 105-C06:2010. The said test actually specifies the method intended for determining the resistance of the colour of textiles of all kinds and in all forms to domestic or commercial laundering procedures used for normal household articles using a reference detergent. However, in this study, test was applied to estimate the change in electrical resistance of the yarn sample after laundering, therefore multi-fibre fabric was not attached with the sample during the washing procedure. The wash liquor was prepared with 4g/l of standard detergent and the test was conducted at 40°C for 30

min with 10 steel standard balls at 20 rpm in Ahiba Nuance dyeing machine. After washing cycle, sample was thoroughly washed with distilled water and dried in ambient conditions for 24 h. Total five washes were carried out in exactly the same way and electrical resistance was recorded each after single wash.

3.3.11. Measurement of decay of conductivity of PPy coated Latex/PA6 yarn

The major disadvantage of the conducting polymers is that they drop their electrical conductivity with the passage of time. Therefore, in order to utilise them in some practical application, it is very necessary to have knowledge about the decay of conductivity under working conditions. In this context 10 cm long sample from each PPy coated Latex/PA6 yarn sample was kept under (20 ± 2) °C temperature and (40 ± 2) % relative humidity for 21 weeks and electrical resistance was recorded each after 4 weeks.

3.3.12. Measurement of effect of relative humidity and temperature on resistance of PPy coated Latex/PA6 yarn

Being as chemical conductor, all the conducting polymers get affected by the relative humidity and the temperature. By taking this fact into account, a sample of 12 cm long was held between the clamp electrodes and conditioned for 24 h at different levels of relative humidity and temperature using climate test chamber by Vötsch® VC-0018. The wires from digital multimeter Agilent® 53131A were connected to the specimen through the hole located in the wall of the chamber. Different levels of temperature and humidity used in order to conduct this experiment are shown in Table 9. From these three levels of factors the factorial experiment was realized.

Table 9: Three different levels of temperature and relative humidity chosen to study their effect on resistance of PPy coated Latex/PA6 yarn samples

Factors	**Minimum level (-1)**	**Medium level (0)**	**Maximum level (+1)**
Temperature [°C]	10	30	50
Relative humidity [%]	30	50	70

Chapter 4

General Properties of PPy Coated Glass Fabric

As discussed in section 2.2.3.1 it is a well-known fact that polymer film grows on the fabric surface gradually and forms a continuous network for the transport of electric charges across the fabric structure during *in-situ* polymerization process. In this chapter, results for the characterization of PPy coated samples by SEM, LSCM, DSC, FTIR and weight gain as confirmation techniques are discussed.

4.1. SEM analysis

SEM was performed with the purpose of investigating the morphology of the surface as well as the thickness of PPy on glass fibres by vapour deposition technique. The formation of the PPy coating on the textile substrate starts from deposited oligomers, which form islands in the initial stage and finally grow and cover the surface of the substrate completely [139].

The average thickness of coating of PPy on glass fibre was measured as 1.165±0.502µm as measured from Figure 18. It can also be perceived that through vapour deposition technique PPy covers each individual fibre in the fabric very well

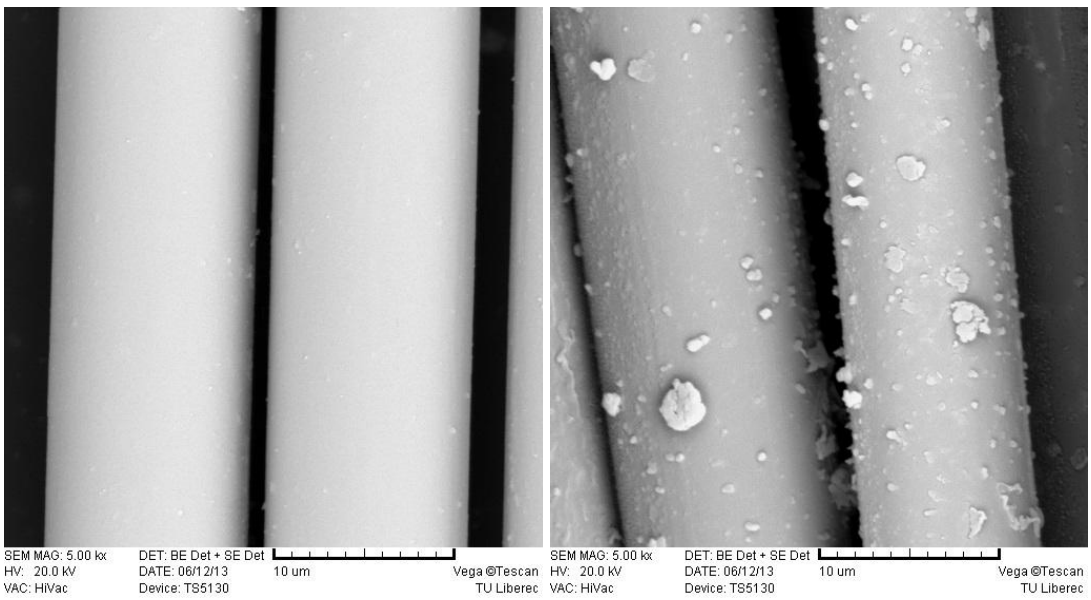

(a) (b)

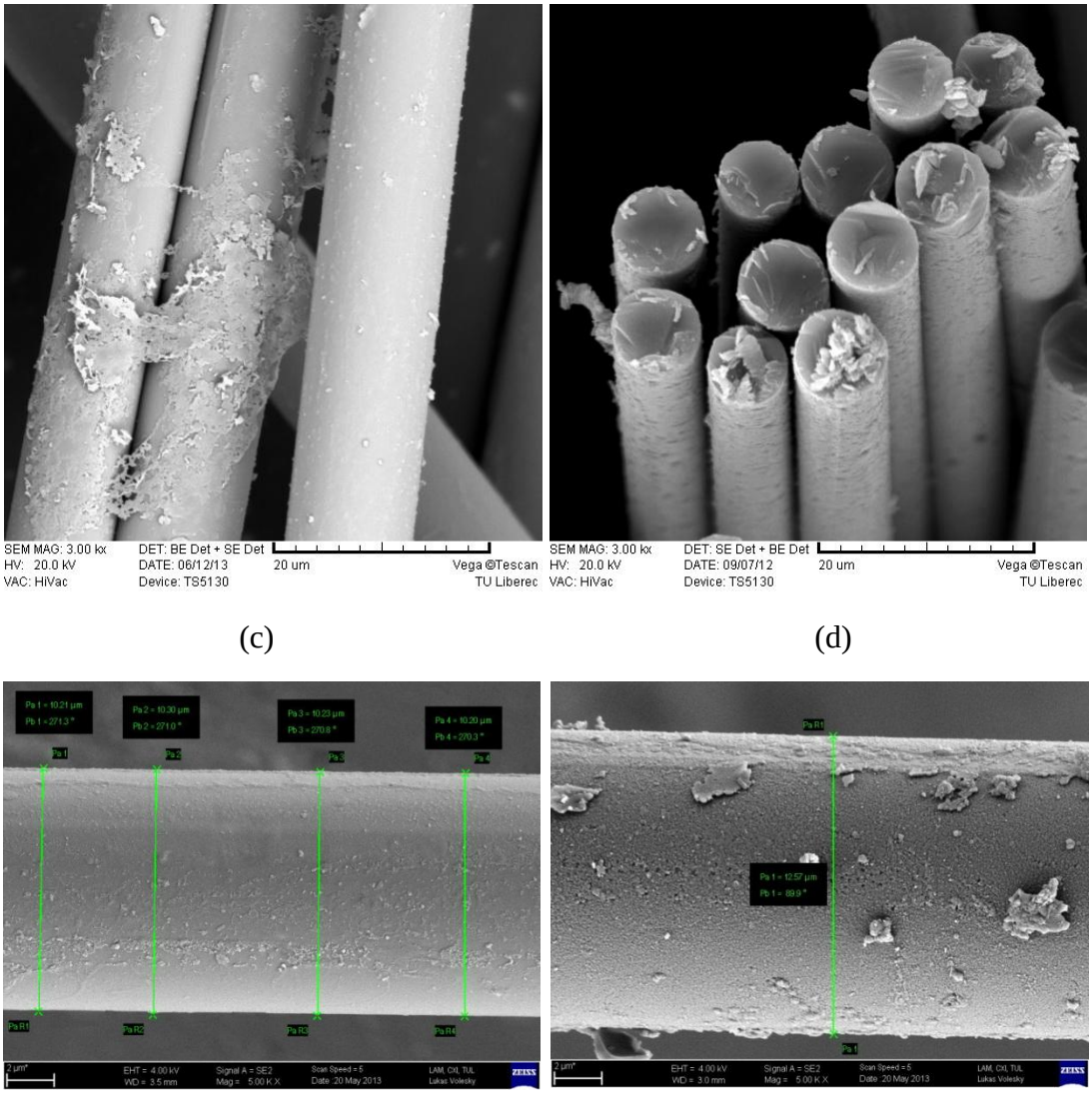

(c) (d)

(e) (f)

Figure 18: SEM micrographs, (a) and (e) are glass control (b), (c) (d) and (f) are glass fibres coated with PPy taken out from sample D4 at different view angle and magnification.

SEM analysis also shows that after covering of glass fibre, PPy starts making thin film like structure on the surface of fibre.

4.2. LSCM analysis

In order to characterize the average thickness of PPy on glass fibres, LSCM analysis was also carried out. Laser scanning process scans the three dimensional surface of an object point-by-point by means of a focused laser beam, and creates the over-all picture by electronic means similar to those used in SEM [140]. Figure 19 shows the 3 dimensional image obtained by the reflected data of control glass fibre and PPy coated glass fibre from sample D4. Figure 20 illustrates the microscopic images of

control glass fibre and PPy coated fibre and shows that after vapour phase polymerization glass fibre surface is coated by PPy completely.

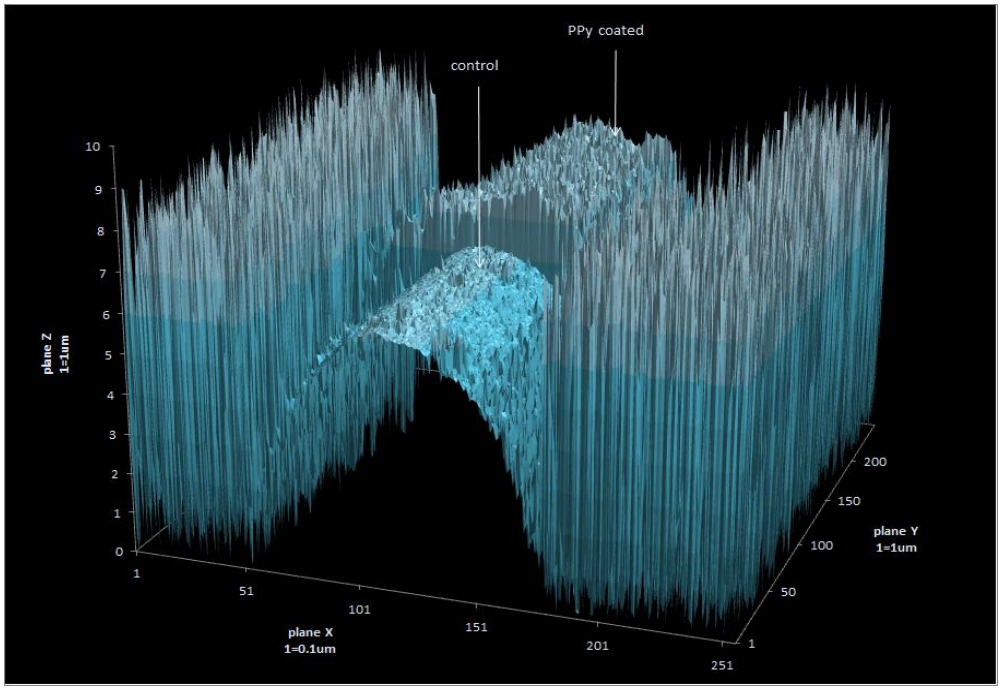

Figure 19: 3d image plotted from the data of LSCM of control and PPy coated portion from sample D4

(a)

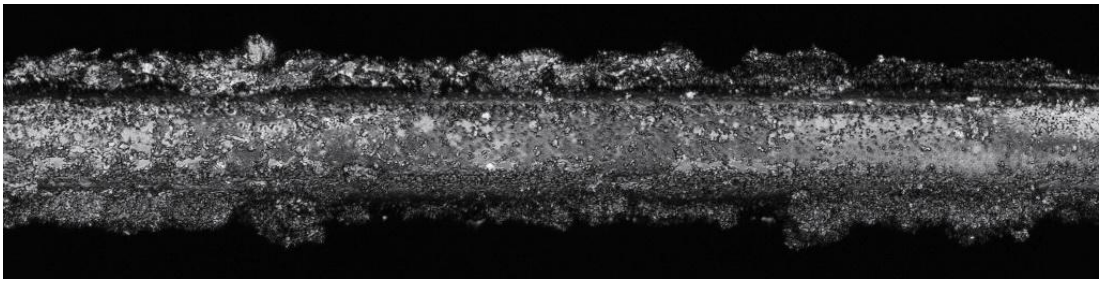

(b)

Figure 20: LSCM images of (a) glass control (b) glass coated with PPy from sample D4

The z-plane reflected data from the highest curvature point of the fibre surface was obtained both from control and coated part and compared in Figure 21.

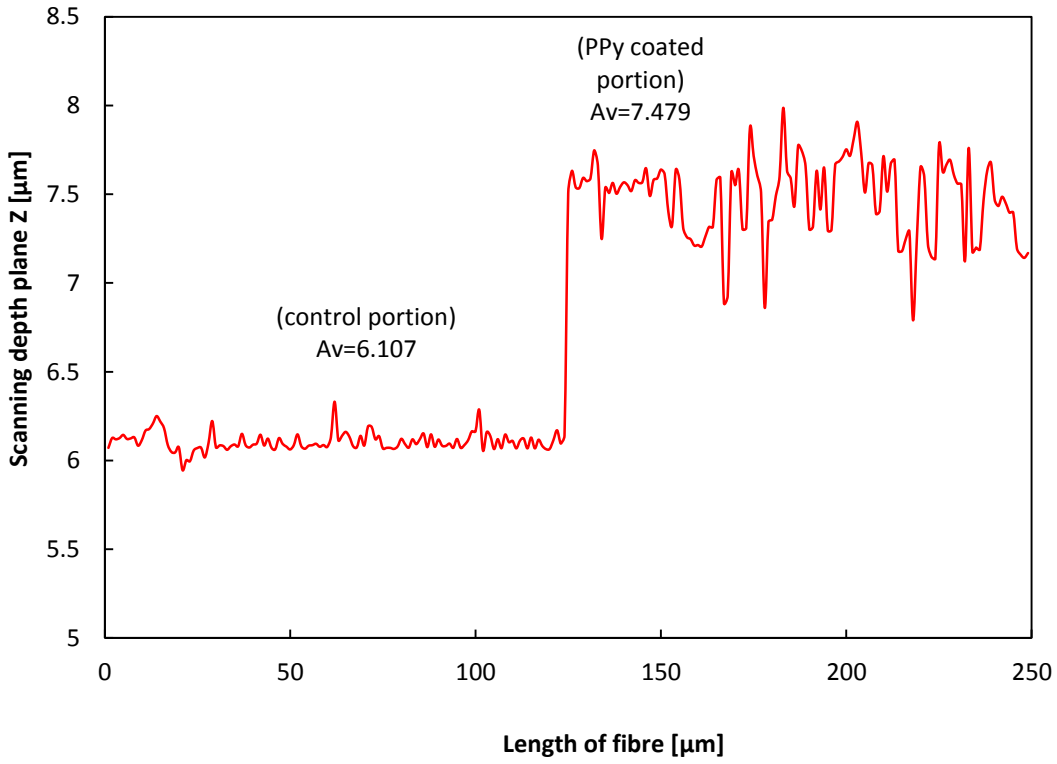

Figure 21: Characterization of thickness of PPy on glass fibre from sample D4 compared to control fibre

From this figure it can be seen that the average thickness of the PPy layer on glass fibre is 1.372µm whereas the standard deviation was calculated as 0.223µm.

4.3. FTIR analysis

The presence of PPy on the glass fabric specimen was characterized by Fourier transform infrared spectroscopy (FTIR) as shown in Figure 22.

The strong absorbance of control specimen at 958 cm^{-1} shows the occurrence of Si-O-Si and Si-OH in glass structure. The absorption at 1546 and 1452 cm^{-1} assigned to ring vibration of C=C and C=N as well as at 1168 cm^{-1} for N-C vibration confirms the presence of pyrrole ring of PPy. Absorptions at 1303 and 1035 cm^{-1} confirms in-plane vibration of =C-H whereas absorption at 788 cm^{-1} shows out plane vibration of =C-H.

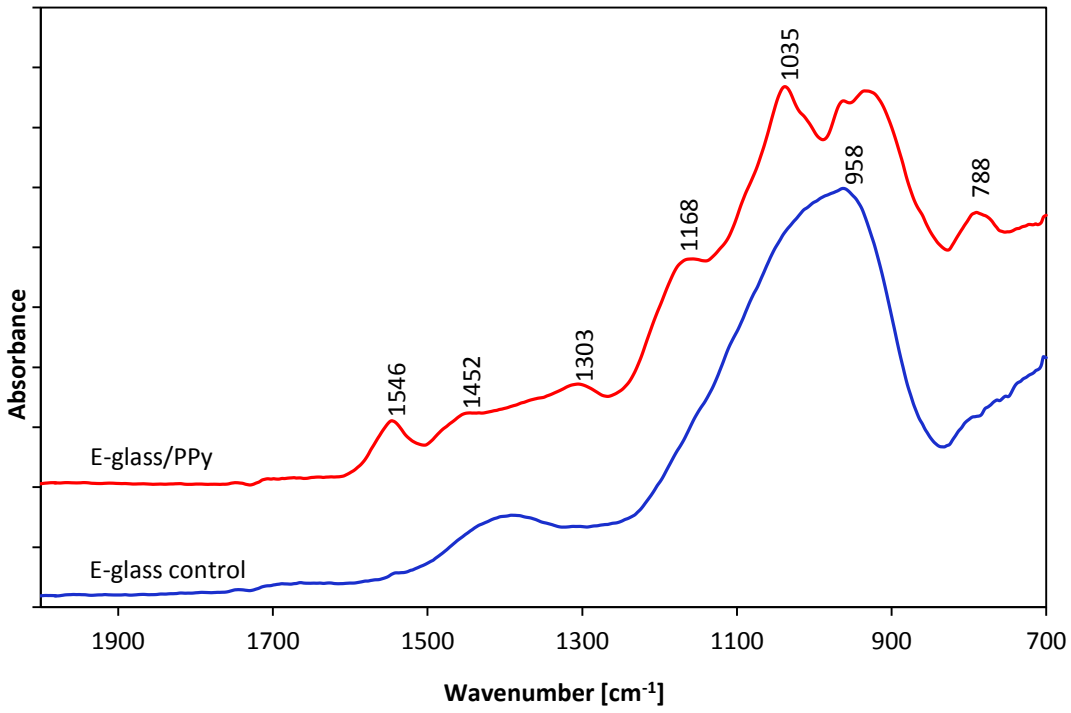

Figure 22: FTIR absorbance curves of glass control and glass coated with PPy

4.4. DSC analysis

PPy film was prepared in exactly the same way as described in section 3.2.2.1. Instead of glass fabric the film was collected from the surface of the oxidizing bath. The analysis was conducted by using DSC-6 from Perkin Elmer® along with software Pyris™. The test was carried out in Nitrogen atmosphere in two cycles. In the first cycle PPy sample was heated till 100°C with the step of 15°C/min to illuminate water from the chain structure and cooled to 25°C. In second step sample was heated in the temperature range from 25°C to 400°C with the same step.

The inflection point at 76.1°C shown in Figure 23 represents the glass transition temperature Tg of the sample which is in the close agreement to the point (71.3°C) observed by Sarbu [141] but lower than found by Guo [142] that is (120.7°C). PPy also gives peaks at 307.9°C and 359°C which might be a melting point as quoted by Kulkarni [143] or due to some decompositions of PPy sample.

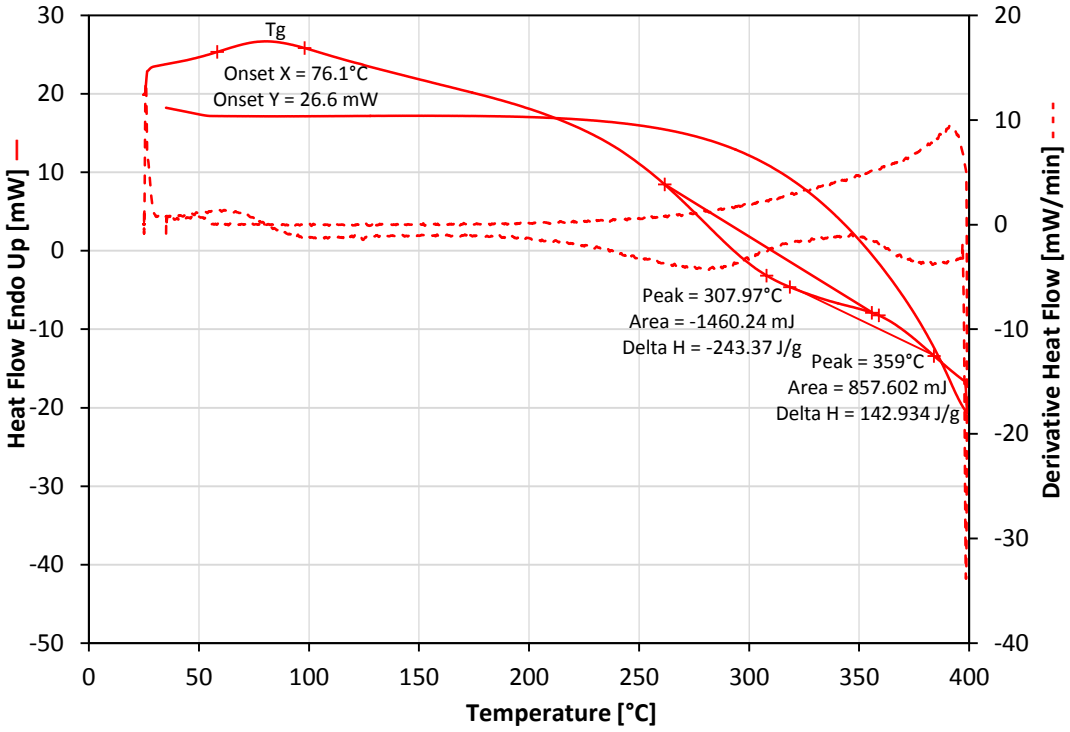

Figure 23: DSC plot of PPy film produced by vapour deposition technique. Solid line represents Endothermic heat flow [mW] whereas broken line shows derivative curve of heat flow in [mW/min] with respect to temperature

4.5. Weight gain by glass fabric after coating

The influence of concentration of $FeCl_3$ and TsO^- on the total mass of the glass fabric was studied. Figure 24 describes the dependence of mass gain on the concentration of $FeCl_3$ while the molar ratio between $FeCl_3$ and TsO^- was kept 2:1. It can be perceived from this figure that weight gain by both glass fabric structures follow a linear function to the concentration of the oxidant. This relation can be written as line passing through origin. By the least squares regression for this model the following relations were obtained;

$$W_1 = 12.017 \cdot C \tag{21}$$

$$W_2 = 9.0442 \cdot C \tag{22}$$

Here, W_1 is the weight gain by structure 1, W_2 the weight gain by structure 2 and C is the concentration of $FeCl_3$.

The coefficient of determination R^2 is calculated as 0.9682 and 0.962 respectively.

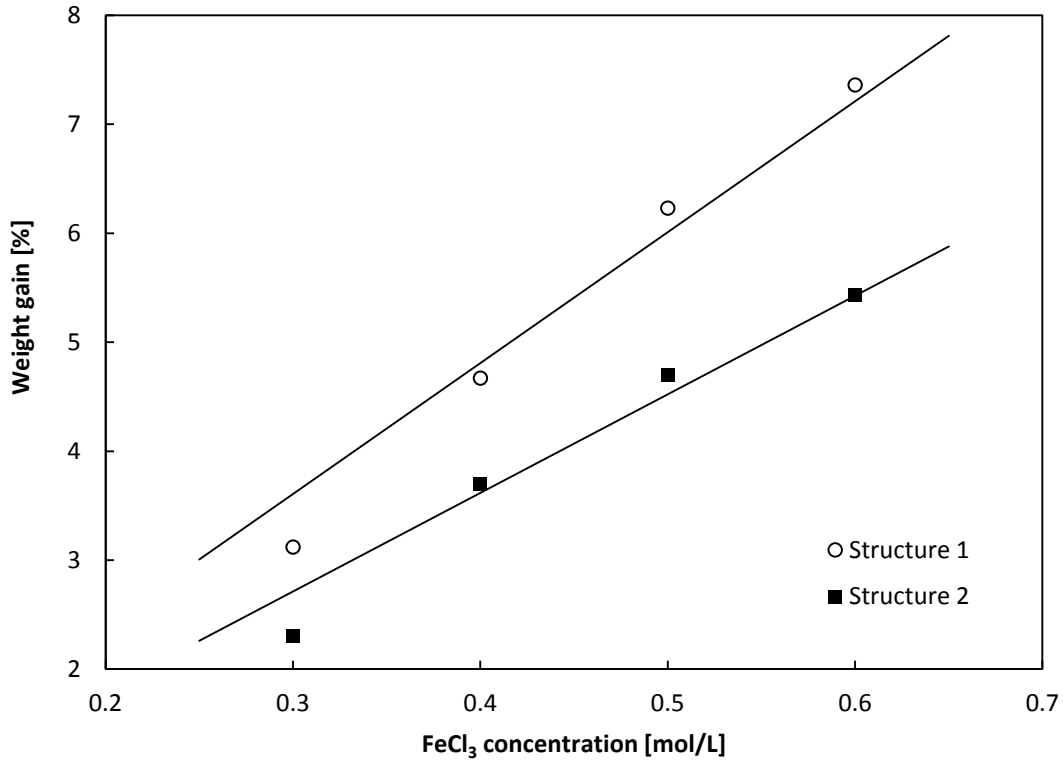

Figure 24: Dependence of weight gain by the glass fabric on the concentration of $FeCl_3$

It can also be observed here that, the structure 1 gains more weight than structure 2. The structure 2 has very dense yarns in its structure which doesn't allow PPy to be synthesised in the inner layers of the fabric and hence PPy forms at the outer layers only. This explanation is discussed more in detail in the section 5.1.

4.6. Tensile properties of PPy coated glass fabric

The influence of concentration of $FeCl_3$ used during the polymerization of PPy on the tensile properties of both structures of glass fabric has been studied in terms of tensile strength and initial modulus. The average force-elongation curves of structure 1 and structure 2 in the direction of warp and weft are shown in Figure 25 and Figure 28. The break load and break elongation are the coordinates of maximum on force elongation curves.

Glass is strong fibre with low extensibility. The extension at break of the control sample of structure 1 fabric in warp direction was recorded as 3.82% and 1.72% in weft direction. Expectedly, when the brittle conductive PPy was deposited on the glass fabric samples, elongation at break of the samples decreased by around 42- 76%

compared to that of the control sample in warp direction and 31- 70% in weft direction depending on the concentration of $FeCl_3$.

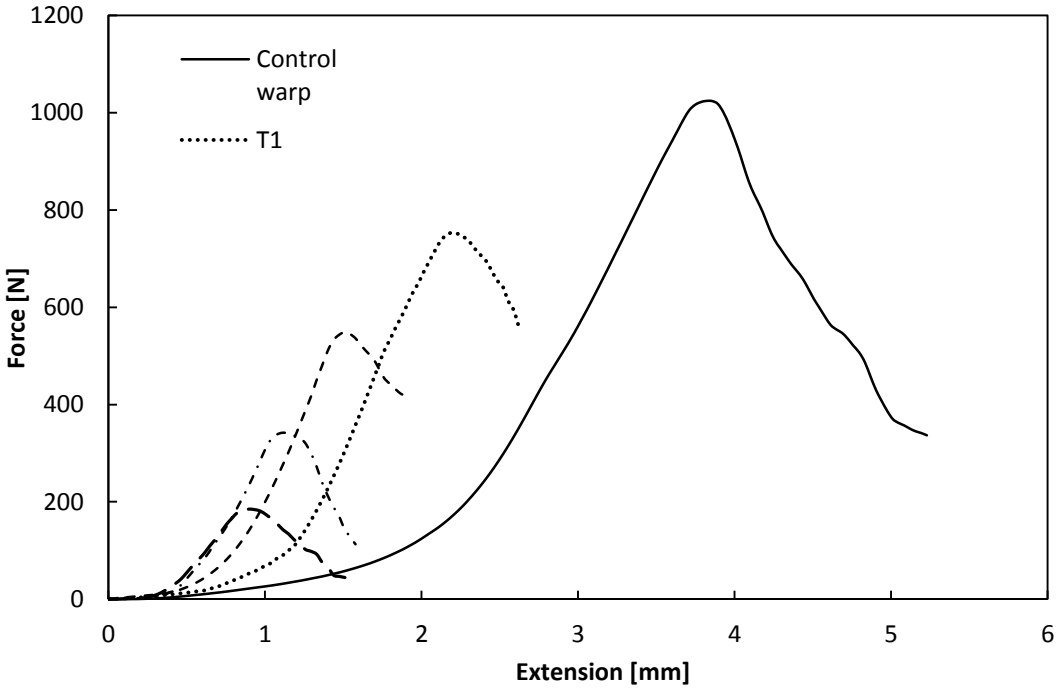

(a)

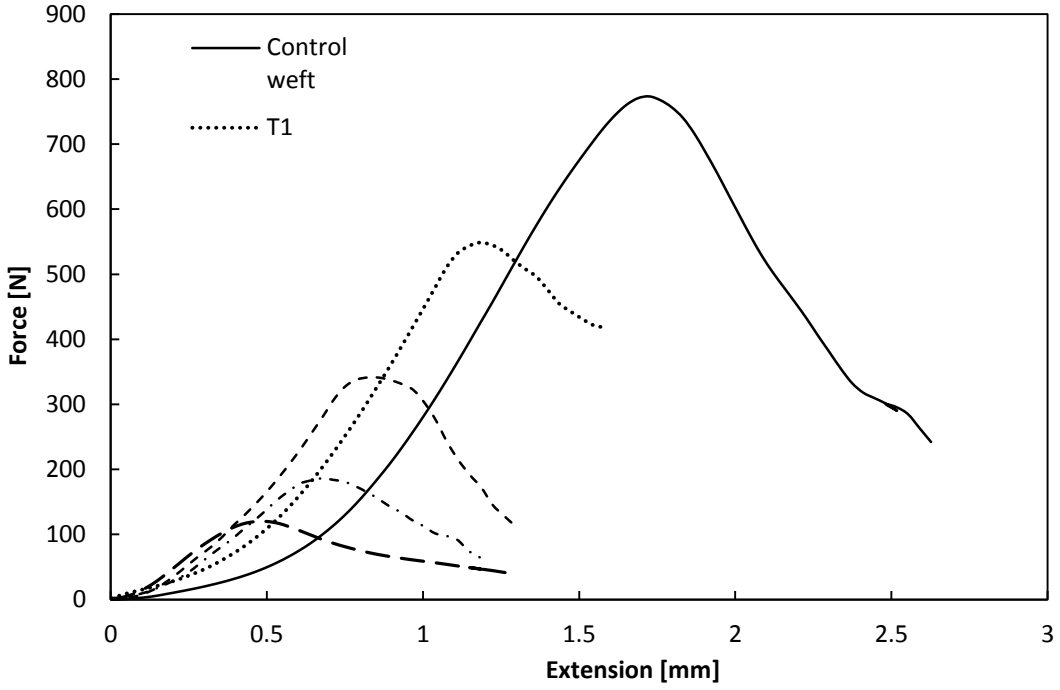

(b)

Figure 25: Average force-elongation curves of control glass fabric and PPy coated glass fabric samples of structure 1(a) warp direction (b) weft direction

In Figure 26 a significant loss in tensile strength of glass fabric samples of structure 1 on the concentration of $FeCl_3$ used for the deposition of PPy can be observed. The maximum force at break was recorded as 1024.02N and 773.57N in the direction of warp and weft respectively, which decreases 26- 81% and 29- 84% depending upon the concentration of $FeCl_3$.

The linear dependence of tensile strength on the concentration of $FeCl_3$ can be expressed as general line passing through point with zero concentration of FeCl3. By the least squares regression for this model the following relations were obtained;

$$F_{\max}(warp)[N] = -1295.3 \cdot C + 1024 \tag{23}$$

Coefficient of determination R^2=0.952

$$F_{\max}(weft)[N] = -1077 \cdot C + 773.57 \tag{24}$$

Coefficient of determination R^2=0.958

Here, C is the concentration of $FeCl_3$ in [mol/L] used for the polymerization of PPy on glass fabric samples.

As far as the dependence of initial modulus on the concentration of $FeCl_3$ is concerned, no trend was observed other than the fact that it increases slightly at 0.4mol/L in case of warp and 0.3mol/L in case of weft. Afterwards modulus decreases continuously and there is significant decrease (30-50%) can be seen in terms of 0.6mol/L $FeCl_3$ concentration as shown in Figure 27.

In terms of structure 2, the average elongation at break of the control sample in warp direction was noted as 4.97% and 4.504% in weft direction. Surprisingly, elongation at break of the samples increased by around 15- 61% compared to that of the uncoated sample in warp direction and 8- 57% in weft direction, when PPy deposited on fabric samples that can be seen in Figure 28. This change in trend might be due to high friction between fibres in thick dense structure which are kept entangled till they are broken.

Like structure 1, major loss in tensile strength of PPy coated glass fabric samples of structure 2 has been observed as shown in Figure 29. The maximum force at break

was noted as 2512.24N and 1946.85N in the direction of warp and weft respectively, which decreases 11- 64% and 22-62% depending upon the concentration of $FeCl_3$.

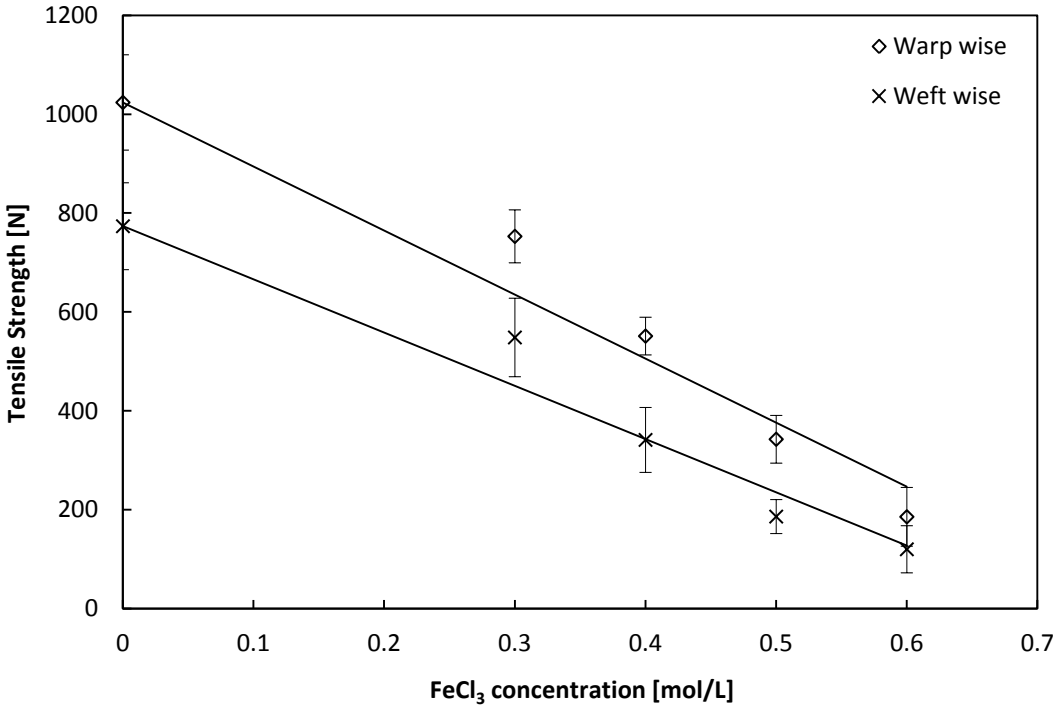

Figure 26: Dependence of tensile strength of PPy coated glass fabric samples in warp and weft directions of structure 1 on the concentration of $FeCl_3$

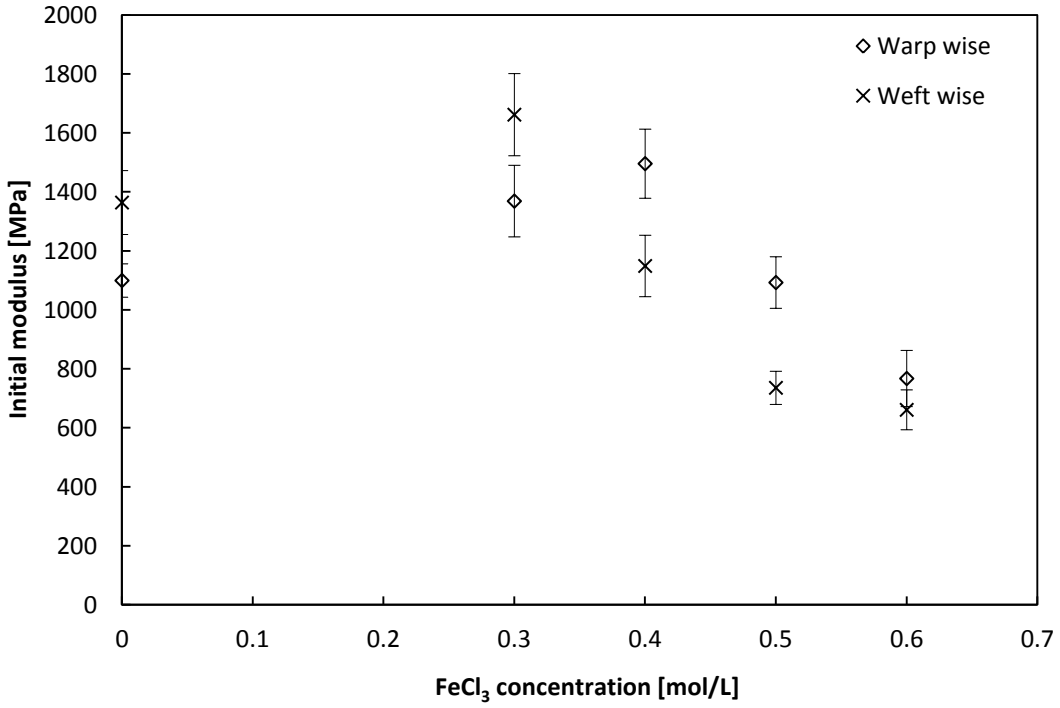

Figure 27: Dependence of initial modulus of PPy coated glass fabric samples in warp and weft directions of structure 1 on the concentration of $FeCl_3$

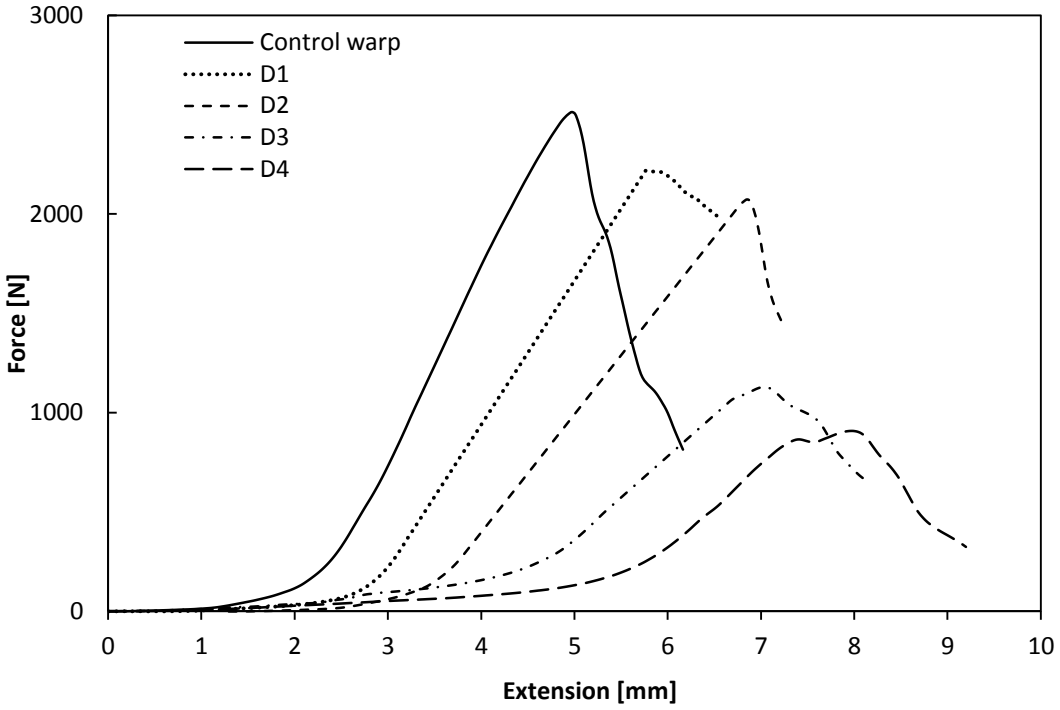

(a)

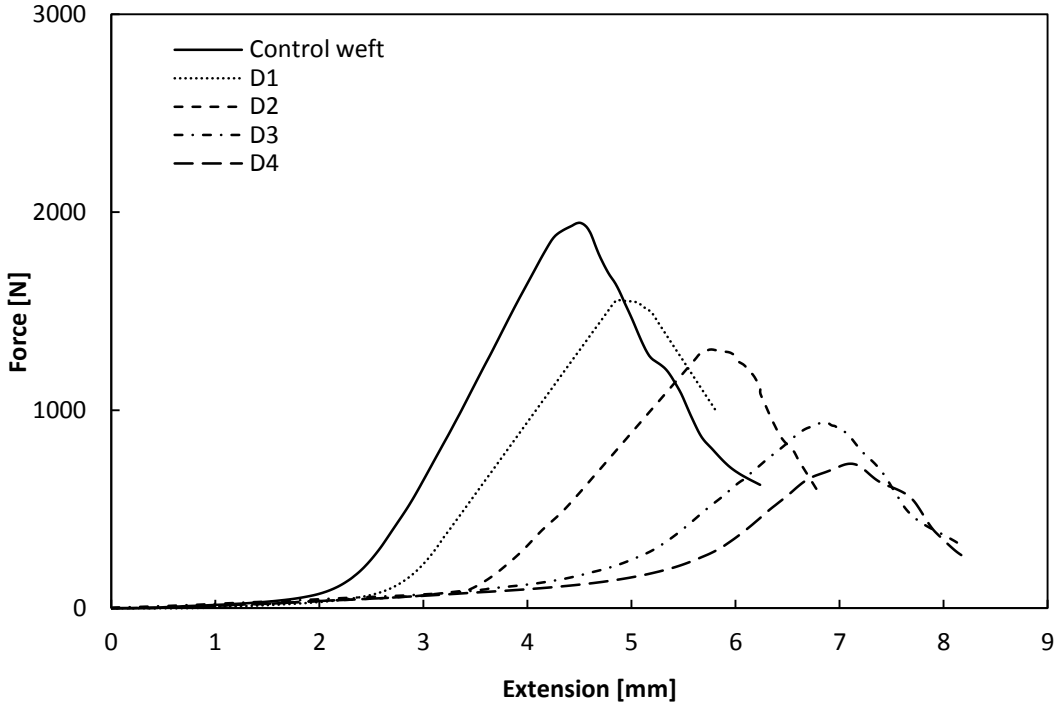

(b)

Figure 28: Average force-elongation curves of control glass fabric and PPy coated glass fabric samples of structure 2 (a) warp direction (b) weft direction

The linear dependence of tensile strength of PPy coated sample from structure 2 on the concentration of $FeCl_3$ can be expressed as general line passing through point with

zero concentration of FeCl3. By the least squares regression for this model the following relations were obtained;

$$F_{\max}(warp)[N] = -2229.3 \cdot C + 2512.2 \quad (25)$$

Coefficient of determination R^2=0.7554

$$F_{\max}(weft)[N] = -1871.4 \cdot C + 1946.9 \quad (26)$$

Coefficient of determination R^2=0.94

Here, *C* is the concentration of $FeCl_3$ in [mol/L] used for the polymerization of PPy on glass fabric samples. While the dependence of initial modulus on the concentration of $FeCl_3$ is studied, linear decreasing trend was detected as the concentration increases. The initial modulus for control sample of structure 2 was recorded as 1830.74MPa and 1640.24MPa in warp and weft direction respectively. There is significant decrease (27-60%) in warp direction and (19-55%) in weft direction depending on $FeCl_3$ concentration as shown in Figure 30.

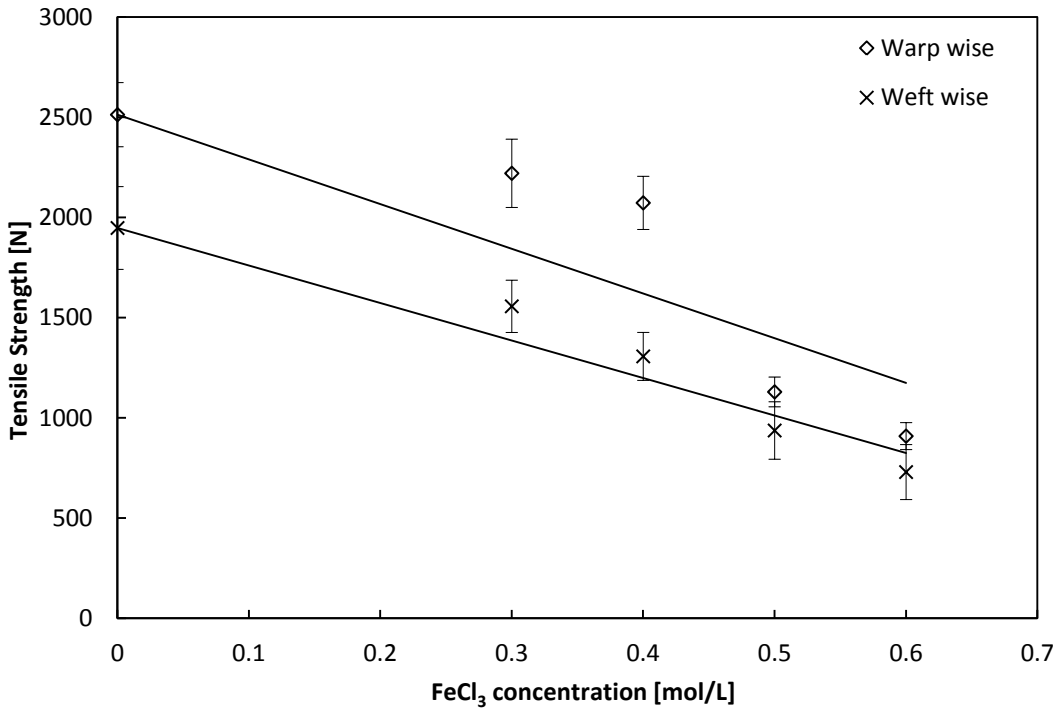

Figure 29: Dependence of tensile strength of PPy coated glass fabric samples in warp and weft directions of structure 2 on the concentration of $FeCl_3$

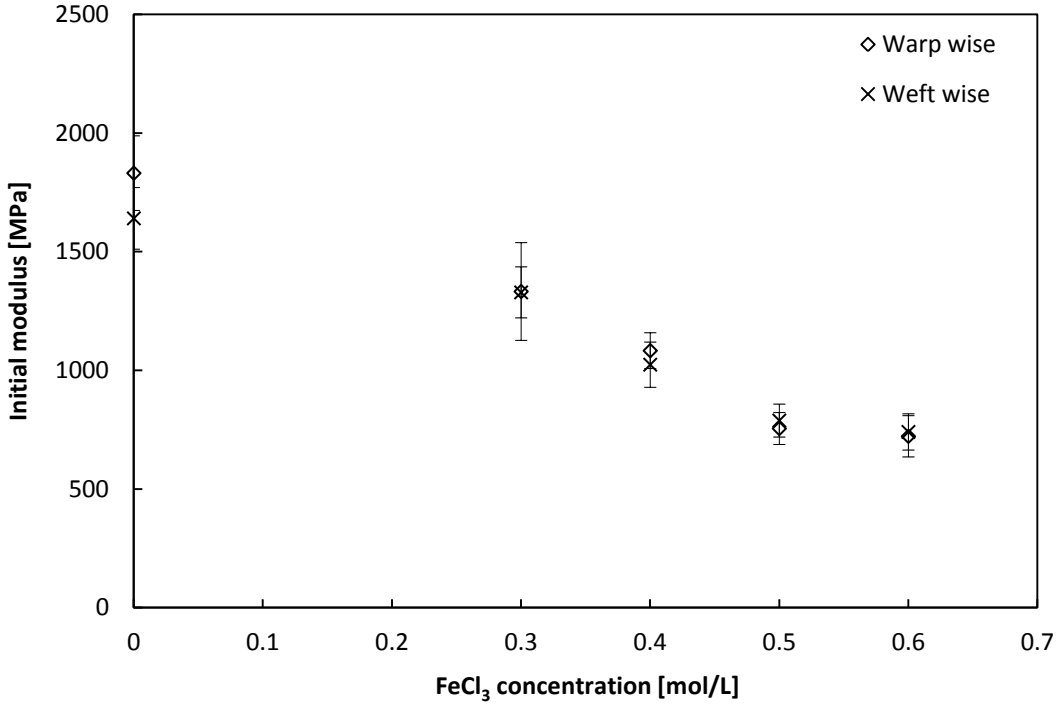

Figure 30: Dependence of initial modulus of PPy coated glass fabric samples in warp and weft directions of structure 2 on the concentration of $FeCl_3$

It is not surprising that all mechanical properties are lower in the PPy coated glass fabric samples, since the bonding of the PPy coating to the glass fibre was not optimized. Similar loss in tensile strength has also been observed by Patil [144] and Kaynak [145] after coating PPy on cotton and wool substrates respectively. Kaynak also showed that oxidant and dopant are not responsible for the loss in mechanical properties but textile substrates lose their strength when polymerization of pyrrole is completed and effect becomes more pronounced with the increase in PPy mass.

Chapter 5

Dependence of EMSE on Resistivity

Although dopant has a large influence on the conductivity of the PPy however, the concentration of $FeCl_3$ controls the yield of PPy formed in the system. This chapter mainly deals with the effect of concentration of $FeCl_3$ on the electrical resistivity of the PPy coated glass fabric samples. The amount of conducting polymer chiefly influences the fabric resistivity therefore, in the later sections EMSE for transmission and reflection as a function of electrical resistivity of said samples is discussed.

5.1. Electrical resistivity of PPy coated glass fabric

The resistivity of PPy coated samples was determined by concentric ring electrodes. The linear decrease in surface as well as volume resistivity of the specimens was observed in case of structure 1 as shown in Figure 31. The general line model of surface as well as volume resistivity on $FeCl_3$ dependence was used. By the least squares regression for this model the relations written as Equation 27 and 28 were obtained having R^2= 0.9936 and 0.9985 respectively.

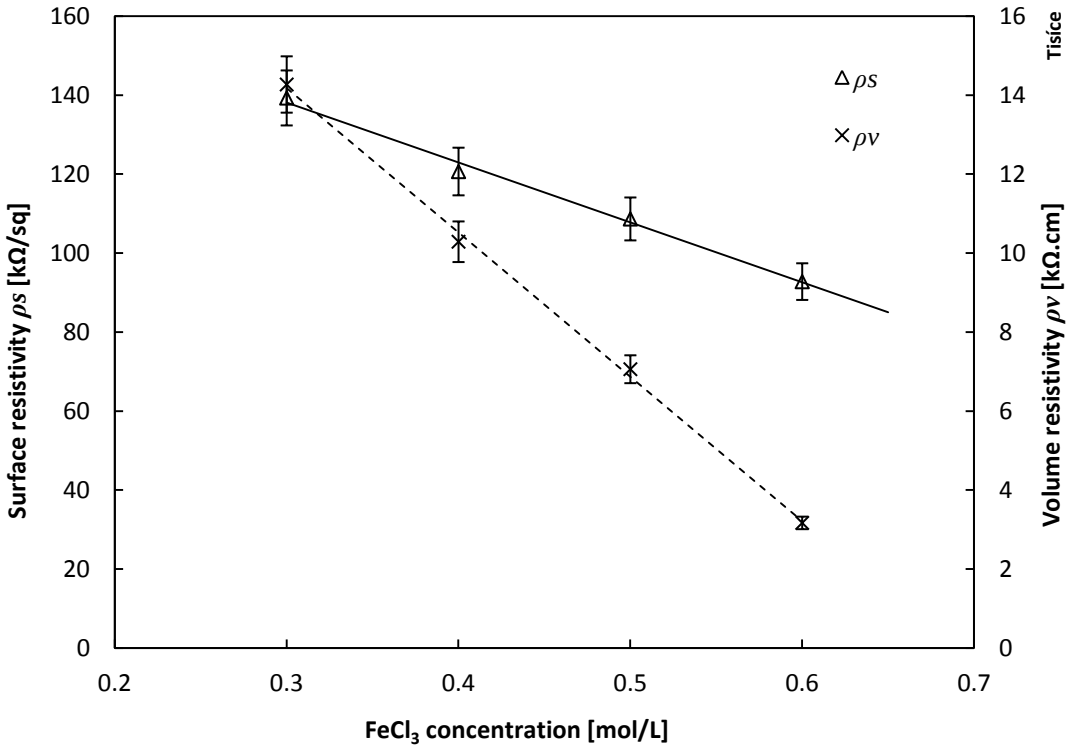

Figure 31: Dependence of resistivity of PPy coated glass fabric of structure 1 on concentration of $FeCl_3$

$$\rho_s = -151.53 \cdot C + 183.54 \tag{27}$$

$$\rho_v = -36529 \cdot C + 25136 \tag{28}$$

Here, C is the concentration of $FeCl_3$ in [mol/L].

By taking structure 2 into account the decrease in resistivity follow power function of concentration of $FeCl_3$ as presented in Figure 32. The power type model with intercept equal to infinity for surface as well as volume resistivity on $FeCl_3$ dependence was used because resistivity at zero concentration was very high. By the least squares regression for this model the relations written as Equation 29 and 30 were obtained with R^2=0.993 and 0.927 respectively;

$$\rho_s = 0.32 \cdot C^{-1.893} \tag{29}$$

$$\rho_v = 4.32 \cdot C^{-3.718} \tag{30}$$

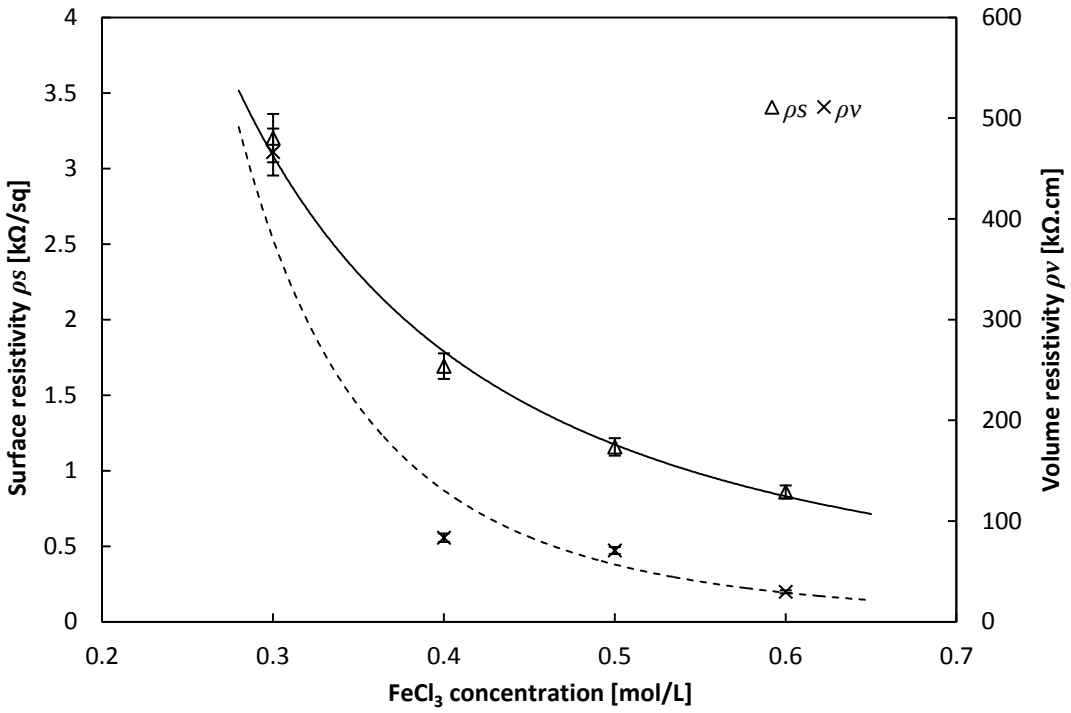

Figure 32: Dependence of resistivity of PPy coated glass fabric structure 2 on concentration of $FeCl_3$

The structure 1 is comparatively a thin structure and it allows the oxidant and dopant to adsorb thoroughly meanwhile, pyrrole vapours also penetrate in the fabric structure and ultimately each individual fibre is coated with PPy. Whereas structure 2 being as

a dense structure does not allow pyrrole vapours to adsorb in the fabric thoroughly and eventually PPy is not produced in the core of the yarns as illustrated by the Figure 33.

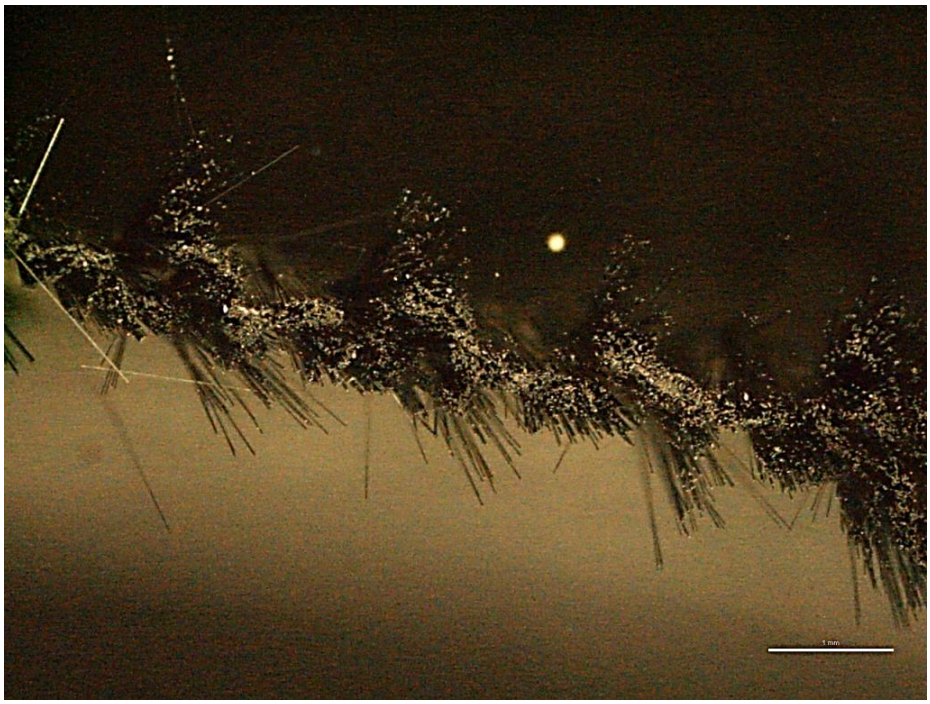

(a)

(b)

Figure 33: Cross-sectional view of PPy coated glass fabric sample (a) T4 (b) D4

5.2. EMSE of PPy coated glass fabric

All glass fabric samples from both structure 1 and 2 described in Table 6 were tested for EMSE for transmission as well as for reflection in the frequency range from 300 MHz till 1.5 GHz by conforming ASTM test method D4935-1 and data was collected. The curves of the shielding effectiveness for transmission and reflection of PPy coated glass fabric samples depending on the concentration of oxidant concentration are graphically presented in Figure 34 and Figure 35.

The higher SE for transmission in dB describes the higher efficiency of the shielding material, while lower SE for reflection in dB illustrates the better efficiency and vice versa. It can be seen from both the figures that, with the increase in concentration of oxidant and dopant, SE for transmission increases in the case of structure 1 as well as of structure 2 also. However, SE for reflection decreases with the increase in concentration of oxidant and dopant, which shows that there are less power of electromagnetic radiation being reflected by the shielding material in terms of higher concentration of oxidant and dopant.

For the purpose of summarizing the results in this dissertation, the dependence of EMSE for transmission and reflection on electrical resistivity is plotted against the frequency of 800 MHz (commonly used for Bluetooth and GSM networks) as shown in Figure 36 andFigure 37. This frequency was chosen because in daily life, this is the mostly exposed frequency especially emitting from electronic devices such as communication devices.

In glass fabric structure 1 the dependence of EMSE for both transmission and reflection is found to be a linear function of resistivity of the sample which is in the close agreement to the results found by Yildiz and co-workers in [146] as well as Kim and co-workers in [147]. As the resistivity of the PPy coated samples of structure 2 follows power function of the concentration of $FeCl_3$ shown in Figure 32 therefore, EMSE also follows power function when plotted against resistivity of the same samples that is clear from the Figure 37.

The general line model of EMSE for transmission and reflection for the PPy coated samples of structure 1 on surface resistivity was used. By the least squares regression

for this model the relations (Equation 31 and 32) were obtained with R^2= 0.97 and 0.92 respectively.

$$SE_t = -0.0971 \cdot \rho_s + 14.92 \quad (31)$$

$$SE_r = 0.23 \cdot \rho_s - 15.96 \quad (32)$$

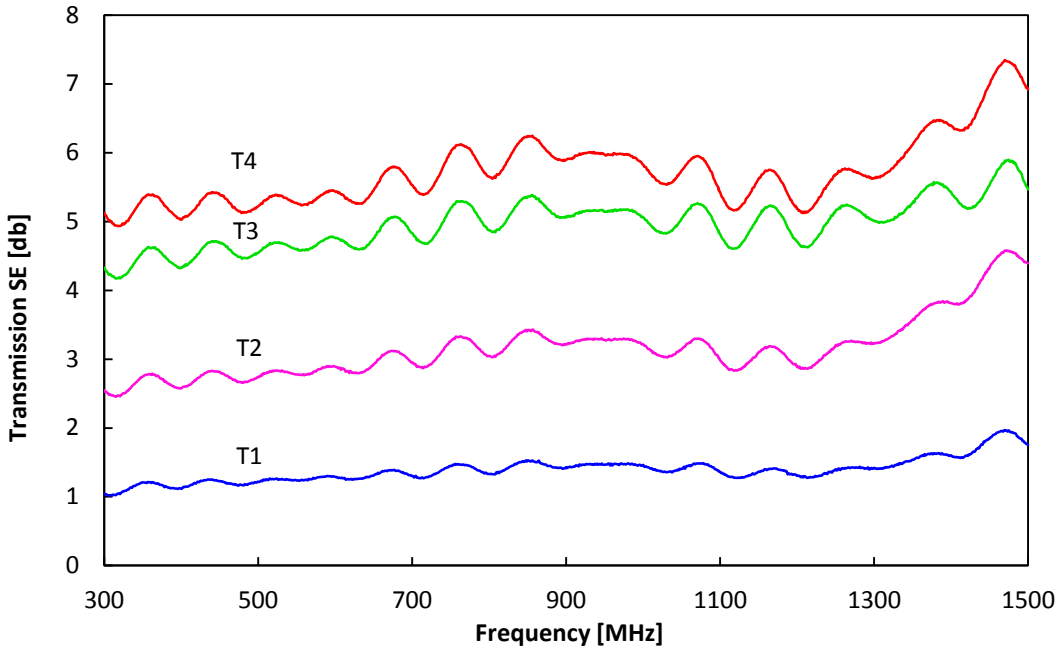

(a)

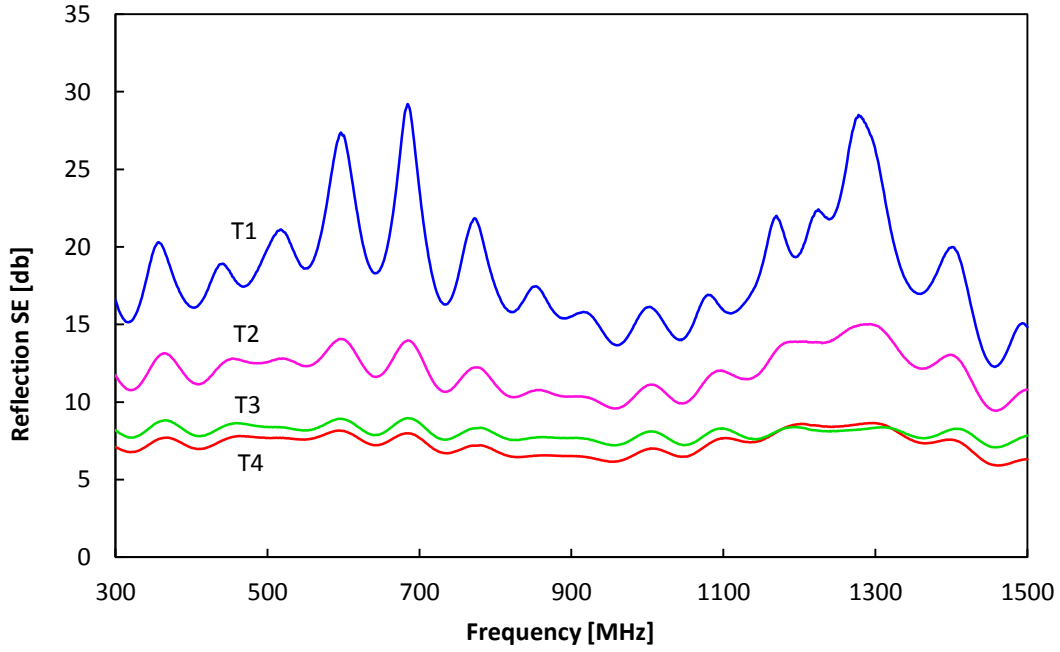

(b)

Figure 34: EMSE curves of PPy coated glass fabric structure 1 (a) SE transmission (b) SE reflection

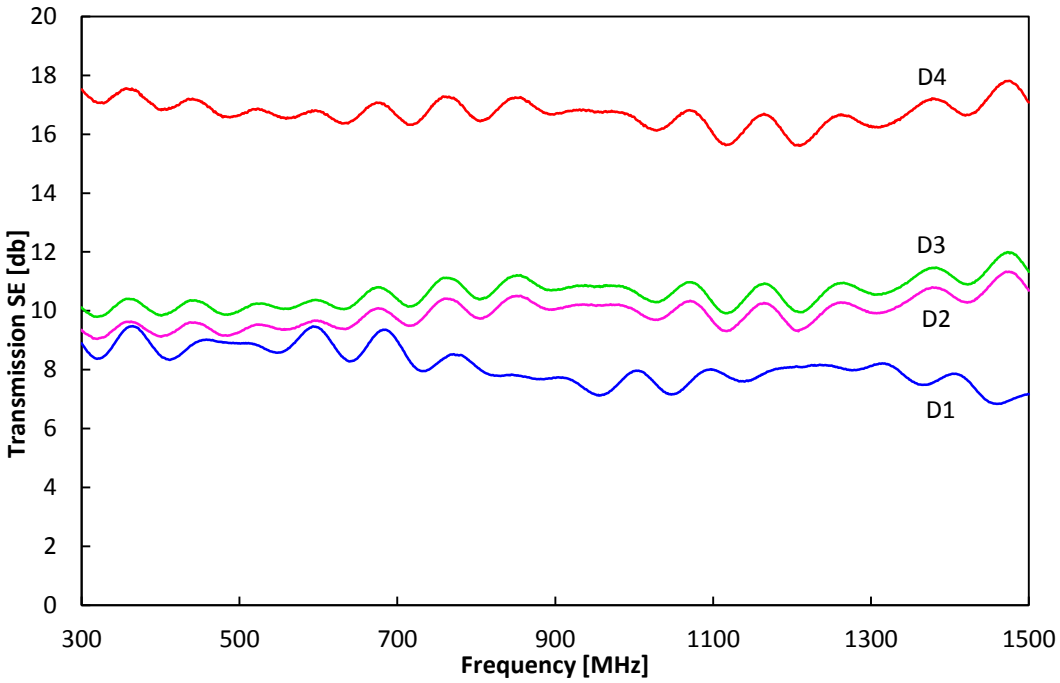

(a)

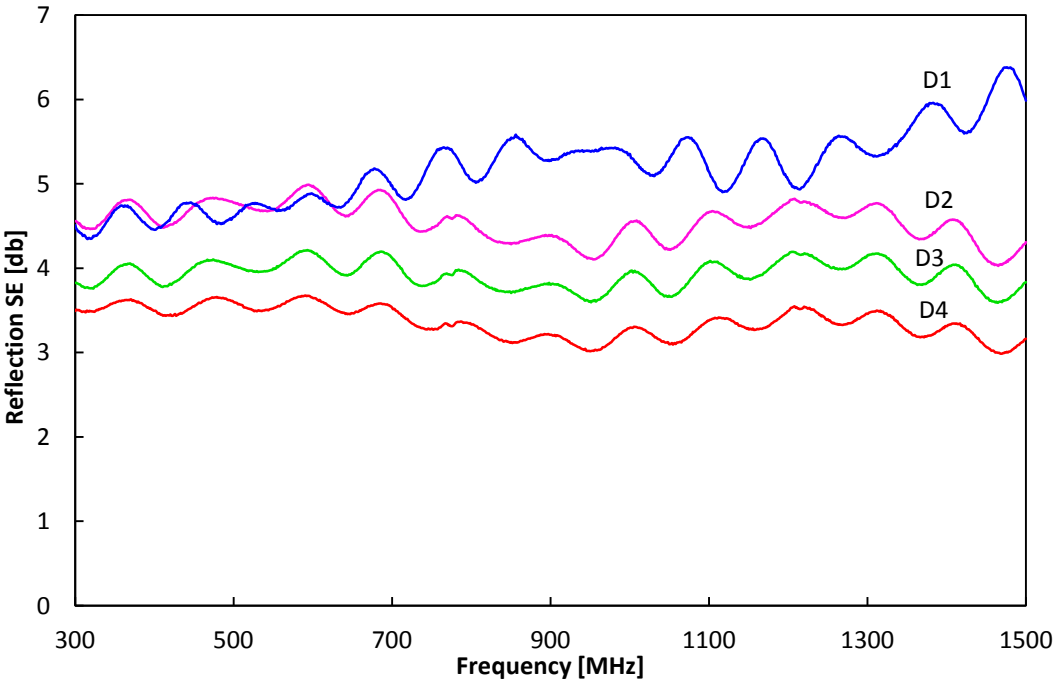

(b)

Figure 35: EMSE curves of PPy coated glass fabric structure 2 (a) SE transmission (b) SE reflection

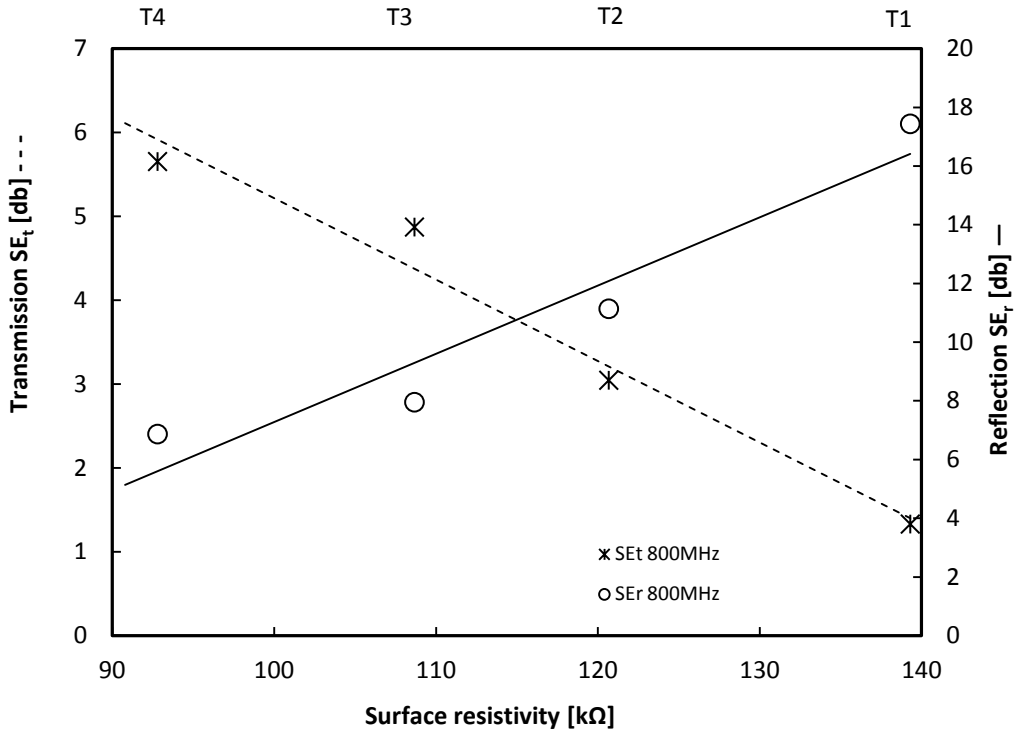

Figure 36: Dependence of SE_t and SE_r on surface resistivity of PPy coated glass fabric sample of structure 1

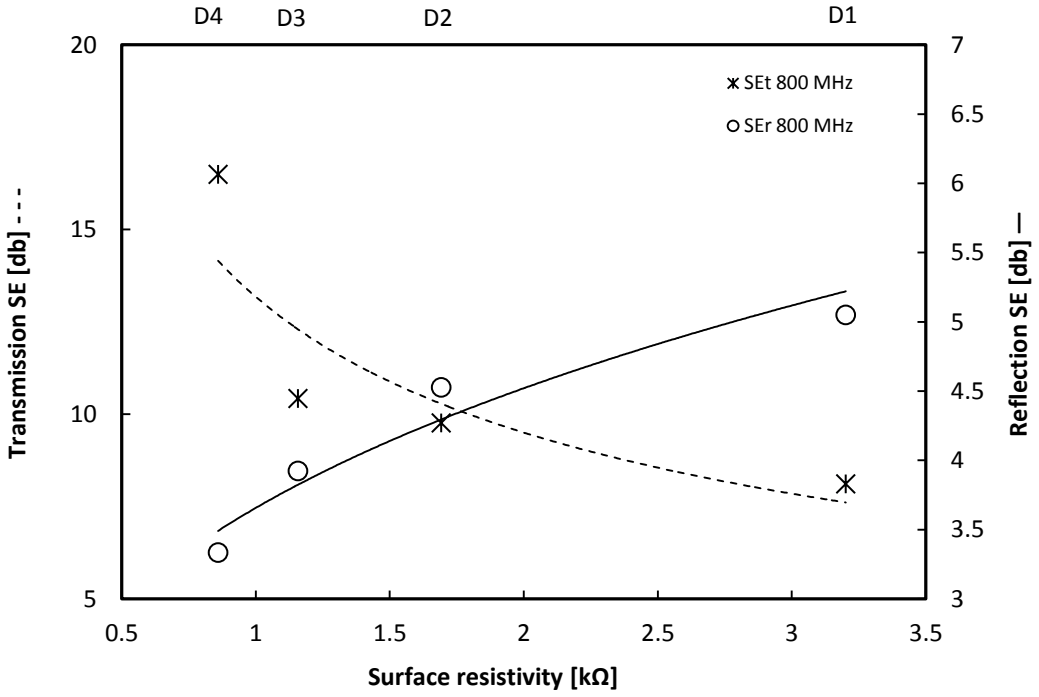

Figure 37: Dependence of SE_t and SE_r on surface resistivity of PPy coated glass fabric sample of structure 2

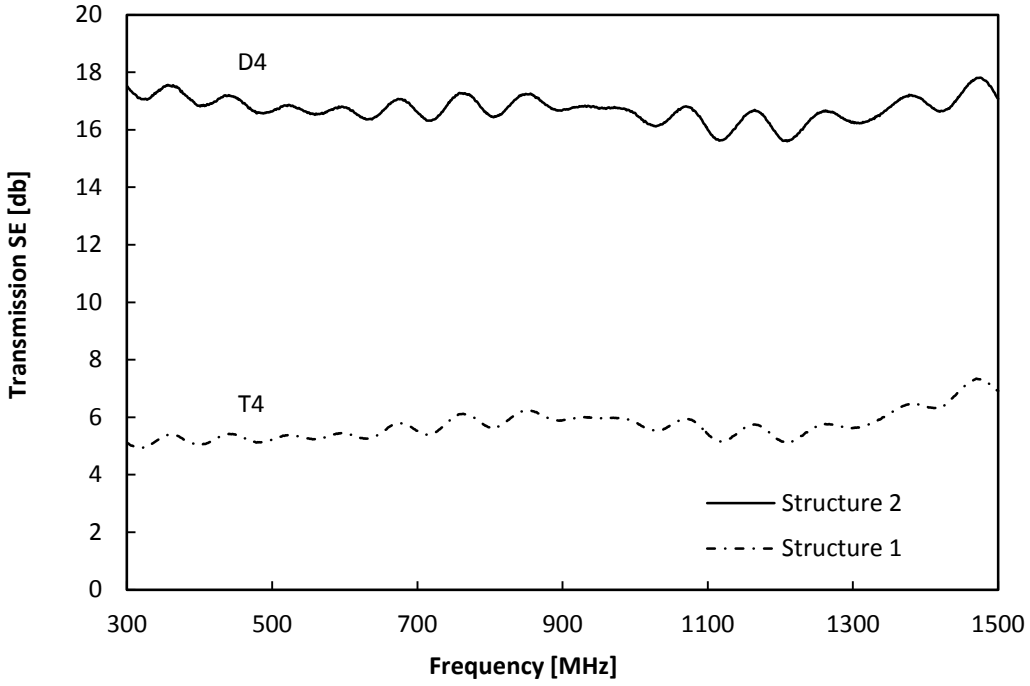

Figure 38: Dependence of SE_t on density of the glass fabric coated with PPy

The power type model with intercept equal to infinity for EMSE for transmission and reflection against surface resistivity of structure 2 was used because EMSE at very high level of resistivity is too poor. By the least squares regression for this model the relations written as Equation 33 and 34 with R^2=0.79 and 0.93 respectively.

$$SE_t = 13.18 \cdot \rho_s^{-0.472} \tag{33}$$

$$SE_r = 3.66 \cdot \rho_s^{0.306} \tag{34}$$

For the evaluation of dependence of EMSE on density of the fabric two samples T4 from structure 1 and D4 from structure 2 have been compared in Figure 38. It can easily be perceived that fabric of structure 2, which has higher density than structure 1, has more than twice EMSE than structure 1 throughout the whole frequency range and can be used as grade 3 (good) for general use or grade 1 (fair) for professional use [148].

5.3. Conclusion

Comparatively thin fabric structure allows higher adsorption in the core of the yarns follows linear dependence of electrical conductivity as well as EMSE on the concentration of the oxidant. Meanwhile PPy is polymerized on the more exposed

areas only in case of highly dense structure and thus the conductivity and EMSE follow power function of concentration of oxidant and dopant. Nevertheless, EMSE of PPy coated higher density fabric structure outperformed the lower density fabric structure by using the same concentration of oxidant and dopant.

The characterization of the interaction of electromagnetic radiations with PPy coated fabric samples is important because accurate determination and evaluation of the shielding effectiveness is an incentive for further research and subsequent implementation of the conducting textiles in appropriate applications, which may include space materials, shielding of special rooms and chambers and frequency selective protection from electronic surveillance.

Chapter 6

Heat Generated by PPy Coated Glass Fabric

The conversion of electricity to heat has always attracted a great attention because of applications in heaters, coolers and thermoelectric power generators. In terms of electrical heating devices, the parameter measuring the suitability of a material for these applications is Joule heating effect. This chapter mainly focuses on the Joule heating effect in the PPy coated glass fabric under applied electric field as well as the heat transfer to the air by convection.

6.1. Joule heating in PPy coated glass fabric

For the purpose of evaluating heat generation by PPy coated glass fabric, samples were taken out from D4 and different DC voltage 5V, 10V, 15V and 20V were supplied. The rise in temperature was determined by thermo couples in connection with data acquisition module. Sharp increase in temperature was observed in first 3 min with the applied voltage which was then stabilized after reaching a plateau as shown in Figure 39 and it shows the ease with which heat could be generated by employing a reasonable dc voltage.

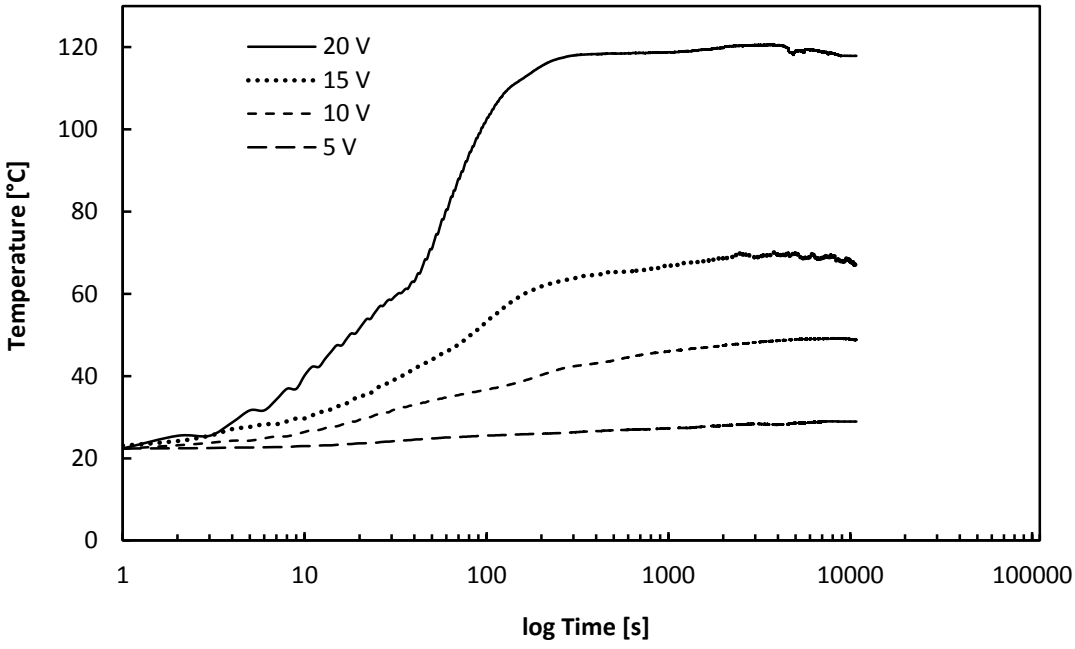

Figure 39: Escalation of temperature of PPy coated glass fabric specimen D4 with increase in time and different DC voltage *V*

Power density P_D (volume specific power) is the amount of power (time rate of energy transfer) per unit volume. It is then also called volume power density which is expressed as [W/m^3]. Volume power density is sometimes an important consideration where space is constrained. In this study power density P_D is extremely linear function of voltage supplied to the PPy coated glass fabric as illustrated in Figure 40. By the least squares regression of line model the relation was obtained which can be expressed as Equation 35.

As per the discussion in section 2.4,

$$\dot{e}_{gen} = \dot{E}_{gen} \Big/ v_{element} = P_D = 82.58V - 245.83 \tag{35}$$

However, temperature rise in fabric sample at equilibrium (after 3 min of supplied voltage) follow exponential function of voltage. By the least squares regression for this model the relation can be written as Equation 36 having coefficient of determination R^2= 0.9717.

$$T = T_0 e^{0.0795V} \tag{36}$$

Here, T is the temperature in [°C] measured at equilibrium at applied DC V and T_o is the temperature of fabric at ambient conditions, which in this study was 22.3°C.

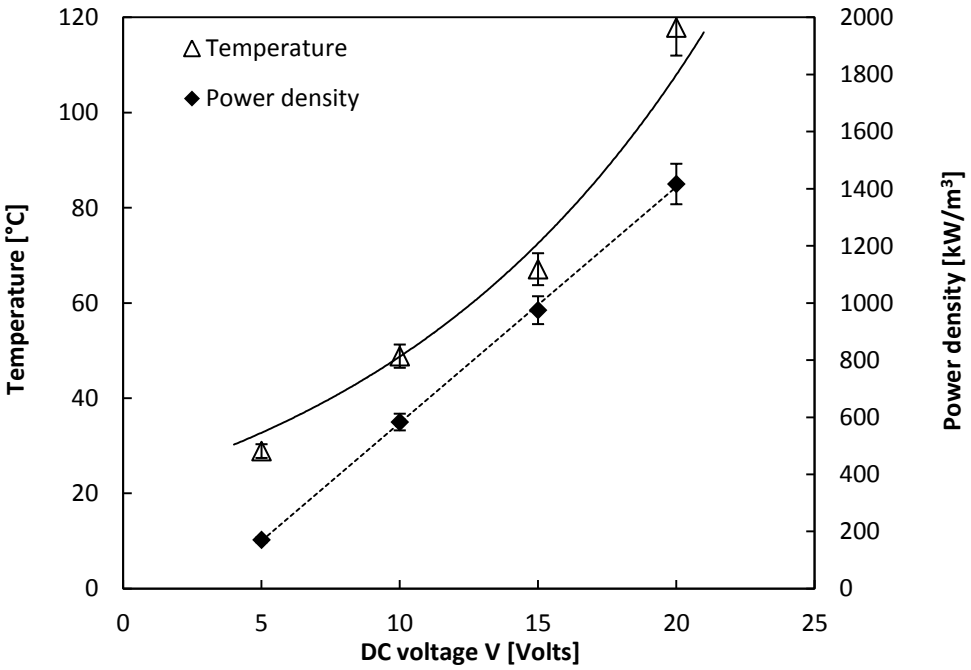

Figure 40: Rise in power density and temperature of sample D4 as a function of DC voltage.

6.2. Flow profile over a fabric specimen by convection

Heat energy transfers between a solid and a fluid when there is a temperature difference between them. This is known as "convection heat transfer". The temperature of the solid due to an external field such as fluid buoyancy can induce a fluid motion. This is known as "natural convection" and it is a strong function of the temperature difference between the solid and the fluid. Blowing air over the solid by using external devices such as fans, pumps and even heat generation within the object can also generate a fluid motion which is known as "forced convection". Fluid mechanics plays a major role in determining convection heat transfer.

6.2.1. Reynolds Number (Re)

Two-dimensional flow analysis over a flat object serves well to illustrate several key concepts in forced convection heat transfer. The viscosity of the fluid μ requires that the fluid of density ρ, have zero velocity at the surface of the object. As a result a boundary layer exists where the fluid velocity changes from u_∞ in the free stream (far from the object) to zero at the object. Within this boundary layer, the flow is initially laminar but can proceed to turbulence once the Reynolds Number *Re* of the flow is sufficiently high. The transition from laminar to turbulent for flow over a flat object of length *L*, occurs in the range,

$$3\cdot10^5 < \mathrm{Re} < 3\cdot10^6, \qquad \mathrm{Re} = \frac{\rho u_\infty L}{\mu} \tag{37}$$

For the current study it has been assumed that the fabric specimen maintains its temperature at constant position T_w, making this problem isothermal. Laminar flow takes the interest in this study, so it is assumed that the specimen length *L* is sufficiently short such that turbulent flow is never triggered (i.e. $\mathrm{Re} < 3\cdot10^5$).

6.2.2. Nusselt Number (Nu)

In heat transfer at a surface within a fluid, the Nusselt number (*Nu*) is the ratio of convective to conductive heat transfer across the boundary. In this context, convection includes both advection and conduction and it is a dimensionless number. The

conductive component is measured under the same conditions as the heat convection but with a (hypothetically) stagnant fluid. It is defined by the equation;

$$Nu_L = \frac{hL}{k} \tag{38}$$

where, L=characteristic length of the object, k=thermal conductivity of the fluid and h=convective heat transfer coefficient

6.2.3. Prandtl Number (Pr)

The Prandtl Number *Pr* is a non-dimensional ratio of the viscous boundary layer thickness to the thermal boundary layer thickness. It is defined by the equation,

$$\mathrm{Pr} = \frac{\nu}{\alpha} = \frac{c_p \mu}{k} \tag{39}$$

where, ν=kinematic viscosity $=\mu/\rho$, α=thermal diffusivity $=k/(\rho c_p)$, c_p= specific heat

If the object (of length L) is uniformly heated over its entirety, then the average Nusselt Number is found to be,

$$Nu_L = 0.664 \cdot (\mathrm{Pr})^{1/3} \sqrt{\mathrm{Re}_L} \tag{40}$$

The Equation 38 can be used to calculate the heat transfer coefficient h of fabric specimen via,

$$h = \frac{k}{L} Nu_L \tag{41}$$

which can then be used to calculate the heat transfer by convection from the specimen by the fluid via Newton's Law of cooling,

$$\dot{Q} = h \cdot A(T_w - T_\infty) \tag{42}$$

By using Equation 41 in Equation 42, we get,

$$\dot{Q} = 0.664 \cdot (\mathrm{Pr})^{1/3} \sqrt{\mathrm{Re}_L} \frac{kA}{L} \Delta T \tag{43}$$

Since fluid properties (such as viscosity, diffusivity, etc.) can vary significantly with temperature, there can be some ambiguity as to which temperature one should use to select property values. The recommended approach is the use the average of the object and free-stream temperatures, defined as the film temperature T_f,

$$T_f = \frac{(T_w + T_\infty)}{2} \tag{44}$$

In this study T_w has been taken when the temperature of the fabric specimen reaches to maximum followed by a levelling-off to plateau after 300 to 400s of supplied voltage. Following parameter and their respective values were taken into account in order to calculate heat transfer rate to the air by the PPy coated glass fabric specimen.

The length of the specimen	L = 6 cm
Area of the specimen	A = 12 cm^2
Air free-stream velocity	u_∞ = 2 $m.s^{-1}$
Air free-stream temperature	T_∞ = 22°C
Air viscosity	μ = 0.017 cP
Air density	ρ = 1.29 $kg.m^{-2}.K^{-1}$
Air specific heat	c_p = 1.005 $kJ.kg^{-1}.K^{-1}$
Thermal conductivity of air	k = 0.025 $W.m^{-1}.K^{-1}$

On the basis of this data following parameters have been calculated along with heat transfer rate to air $\dot{Q}$ as plotted against heat energy generated $\dot{E}_{gen}$ inside the specimen in Figure 41.

Reynolds Number	$Re = 9.1 \cdot 10^3$
Prandtl Number	Pr = 0.683
Nusselt Number	Nu = 55.8
Heat Transfer Coefficient	h = 23.3 $W.m^{-2}K^{-1}$

This relationship can be written mathematically as;

$$\dot{Q} = 0.8559 \cdot \left(\dot{E}_{gen,element}\right)^{0.8638} \tag{45}$$

That shows heat generated at low voltages is transferred approximately all to the air through convection but thermal energy generated due to comparatively high voltage transfer partial energy to the air.

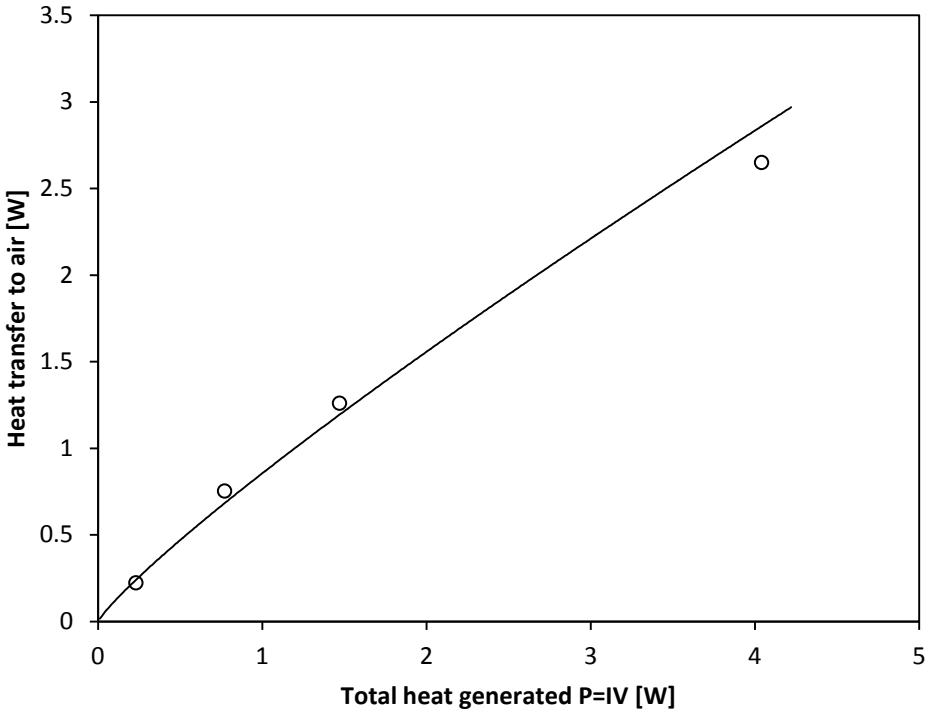

Figure 41: Relationship between heat transfer to air and total heat generated in fabric specimen

By recalling Equation 8 and rearranging,

$$\left[\begin{array}{c}\textit{Net heat}\\ \textit{conducted out}\end{array}\right] = \left[\begin{array}{c}\textit{Heat generated}\\ \textit{in the object}\end{array}\right] - \left[\begin{array}{c}\textit{Change in energy}\\ \textit{stored within}\end{array}\right]$$

$$\dot{Q} = \dot{E}_{gen,element} - \frac{de}{dt}$$

The change in internal energy *e* is related to the body's ability to store heat by raising its temperature, given by,

$$\frac{de}{dt} = \rho c_p \frac{dT}{dt} \tag{46}$$

6.3. Conclusion

Conducting polymer was coated on glass fabric by vapour deposition technique and rise in temperature by applying electrical field was analysed. For the specimen the

rate of change of temperature has two distinct phases; an initial sharp rise during the first 100 s or so, followed by a levelling-off to plateau at approximately 300 to 400 s. During the first phase, the electrical energy input to the samples exceeds the combined thermal energy losses in the forms of convection, radiation and conduction and hence, the temperature rises. As the temperature rises the heat losses increase until they are balanced with the heat generated and the temperature of the fabric stops rising. This is the stable temperature of the fabric under the applied voltage.

The electrical power supplied to the specimen that ultimately converts into thermal power follow linear dependence on the DC voltage supplied whereas rise in temperature of the specimen is a power function of supplied voltage. From analysing the heat flow profile through convection it was found that rate of heat transfer to air follows power function of rate of energy being produced during the supply of electrical field.

The estimated cost to produce PPy coated glass fabric at laboratory scale was roughly calculated as less than Kč 30 per m^2 and this kind of heat generating industrial textile can find its practical application as heating systems for small and medium spaces as well as for the drying of wet cement in civil works.

Chapter 7

Dependence of Resistance on Temperature

Unlike metals, more pronounced intrinsic conduction in conducting polymers occurs when electrons are promoted across the band gap into the conduction band by some means. Then both this electron and the hole in the valence band can contribute to net charge flow. This promotional energy can be obtained by raising the temperature of the conducting polymer. Some work has already been done in order to investigate the effect of temperature on the conductivity of PPy films in the temperature range from absolute zero to the room temperature. This chapter focuses on the thermal dependence of resistance of the PPy coated glass fabric, in the temperature range near Tg of PPy.

7.1. Electrothermal effect in PPy coated sample

To determine the electrothermal effect in PPy coated glass fabric, sample T4 was subjected to thermal heating and response in terms of change in electrical resistance was monitored with the passage of time.

With the help of thermo couple it was found that sample attains the temperature of preheated oven in 180s therefore data were collected after each second from **180s to 12600s**. By using surface response method of analysis, a model is proposed to estimate the approximate change in resistance due to change in temperature at different time intervals; the coefficients of regression are tabulated in Table 10 and surface plot is presented in Figure 42.

It is clear from the Figure 42 that resistance of PPy coated fabric sample decreases with the increase in temperature till 80°C beyond which slight increase in resistance can be observed. The Tg of PPy was found to be 76.1°C by DSC analysis shown in Figure 23 that is very near to this temperature. Above Tg significant increase in resistance was recorded which increases continuously with the passage of time.

As the loss in conductivity of PPy is permanent above Tg, Kaynak [139] explained the fact in terms of permanent degradation or damage of polymer structure upon

heating and this degradation becomes more pronounced with the increase in temperature.

Table 10: Estimates of the regression coefficients

Effect	Coefficient	Standard Error	t-value	p-value
CONSTANT	0.841	0.169	4.971	0.000
T	2.010	0.150	13.388	0.000
t	1.170	0.140	8.353	0.000
*T*T*	1.908	0.223	8.544	0.000
*t*t*	0.385	0.266	1.446	0.150
*T*t*	2.605	0.214	12.162	0.000

Coefficient of multiple determinations R^2: 0.858

Squared Multiple R: 0.737

Adjusted Squared Multiple R: 0.728

Residual Standard Deviation: 1.117

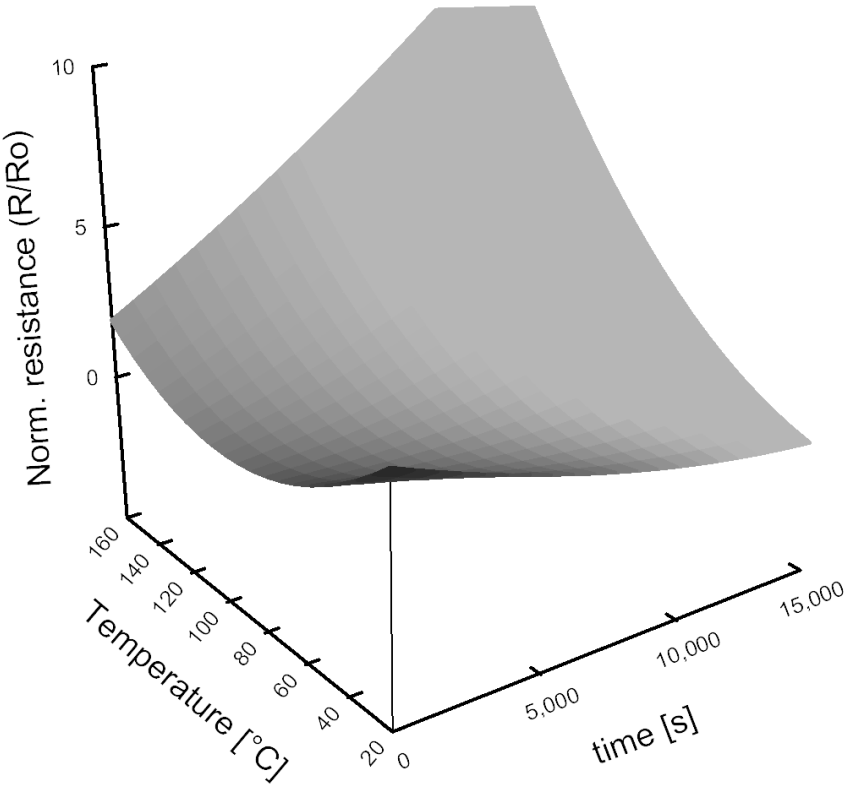

Figure 42: Surface plot of thermal influence of temperature and time on resistance of sample (T4)

The electrical resistivity ρ of most materials changes with temperature T. If the temperature T does not vary too much, a linear approximation is typically used:

$$\rho = \rho_0 \left[1 + \alpha (T - T_0)\right] \tag{47}$$

Here, α is called the temperature coefficient of resistivity in [K^{-1}], T_o is a fixed reference temperature in [K] (usually room temperature) and ρ_o is the resistivity at temperature T_o. The parameter α in Equation 47 is an empirical parameter fitted from measured data. Because the linear approximation is only an approximation therefore α is different for different reference temperatures and in this study it changes with the change in temperature as shown in Figure 43. Negative values of α show the typical behaviour of semiconductors whereas the positive temperature coefficient (PTC) after crossing Tg refers to the material that experiences an increase in electrical resistance with increase in their temperature such as conductors [149].

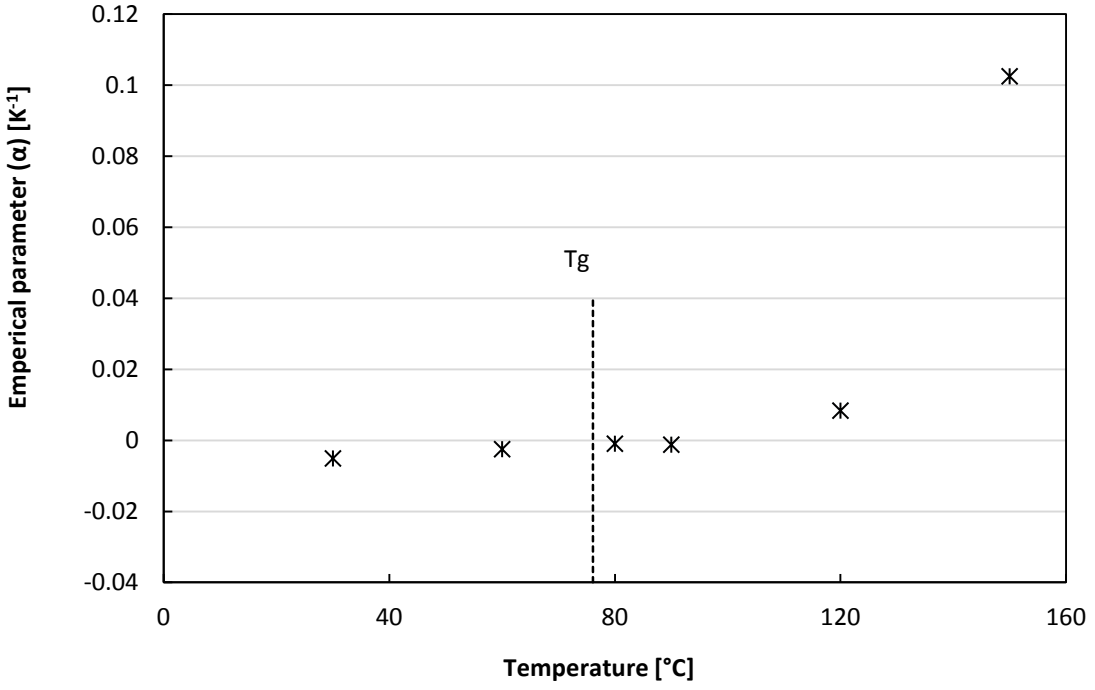

Figure 43: The dependence of empirical parameter α on the temperature of sample (T4)

7.1.1. Fitting the data into theory of conduction

As discussed in section 2.5 Mott (1968) was the first to realise that, as the range of the hop increases, the greater is the probability of the electron finding a site with a small energy barrier, and that such long-range hops depend on the extent of the tails of the

electron wave-functions. This leads to characteristic temperature dependence for variable range hopping, which differs from the Arrhenius law normally anticipated for a thermally activated process. By taking this fact into account, it was tried to find the temperature dependence of the exponent to take the form T^{n} rather than $T^{1/4}$ in Mott's model, where *n* was taken as 1, 1/2 and 1/4. The distinct temperature dependence $T^{1/2}$ and $T^{1/4}$ is a signature of hopping conduction and distinguishes it from conduction due to the thermal excitation of carriers across an energy gap.

Therefore, the natural logarithmic (*ln*) function of normalized conductivity was plotted against reciprocal temperature [K^{-n}] as discussed above and shown in Figure 44. It was observed that the curve is constant with all three exponents, suggesting that hopping conduction and band conduction, both are dominant mechanisms of conduction in PPy coated glass fabric in the temperature range near Tg of PPy.

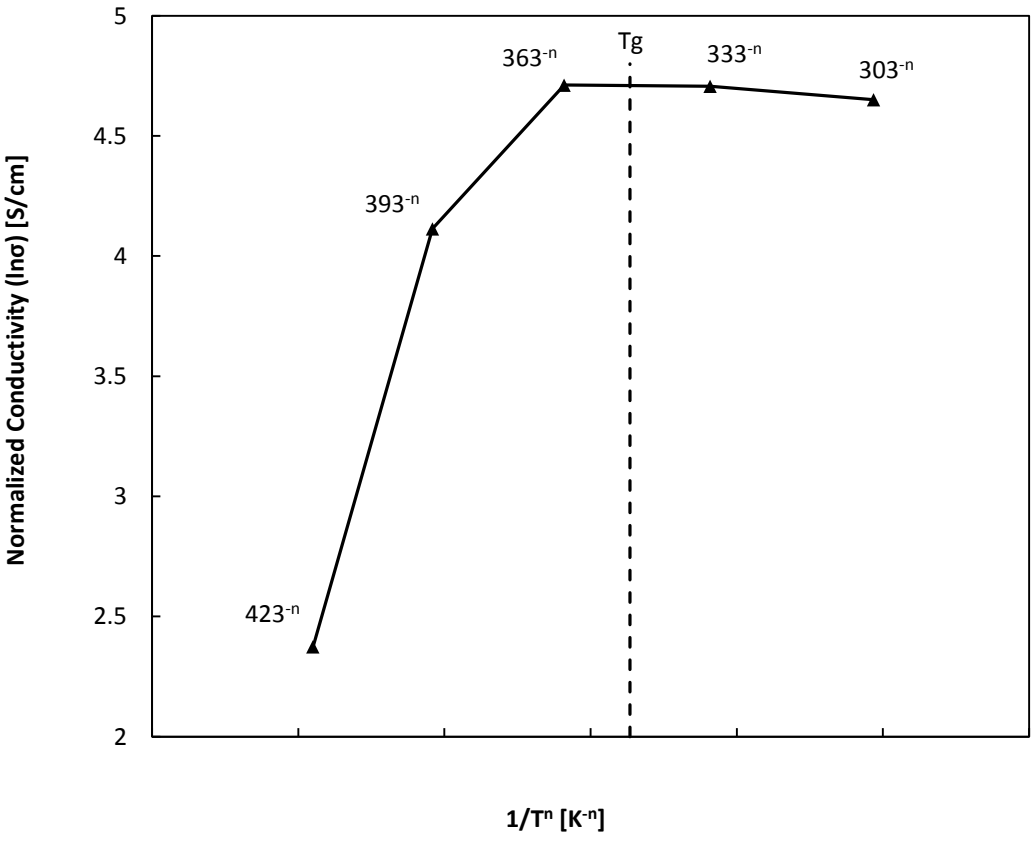

Figure 44: Mott's plot of conductivity with different exponents - PPy coated glass fabric (T4)

Conductivity of a material is determined by two factors: the concentration of free carriers available to conduct current and their mobility (or freedom to move). In a semiconductor, both mobility and carrier concentration are temperature dependent.

The mobility of the carriers in a semiconductor is influenced by the presence of charged impurities. Impurity scattering is caused by crystal defects such as ionized impurities. At lower temperatures, carriers move more slowly, so there is more time for them to interact with charged impurities. As a result, as the temperature decreases, impurity scattering increases and the mobility decreases.

7.2. Conclusion

Carriers can be generated thermally by excitation of electrons across the band gap, from the valence band to acceptor states or from donors to the conduction band, similarly it is also possible to more charge between localised states by thermal excitation. From the series of experiment conducted in this dissertation, it might be assumed that, at temperatures below Tg there is less interaction between charge carriers and ionized impurities and mobility of carrier follows general behaviour of semiconductors while at temperatures near and above Tg vibrations in lattice structure of PPy starts which decreases the charge mobility in it, hence resistance increases.

Chapter 8

Characterization of PPy Coated Latex/PA6 yarn

This chapter emphasises on the characterization of properties of strain sensor prepared by PPy coated Latex/PA6 stretchable yarn. The dependence of the change in resistance upon deformation of stretchable yarn and the uniformity of this response are the key topics in this chapter. The dependence of resistance on humidity and temperature, influence of laundering cycles and decay of conductivity are also discussed in the later part of the chapter.

8.1. Confirmatory tests

8.1.1. SEM micrographs

The SEM micrographs were taken from TESCAN® VEGA and corresponding to sample SY3 is depicted in Figure 45. It can be perceived from the figure that by vapour deposition technique, each individual fibre is covered by PPy thoroughly, even though the structure of Latex/PA6 stretchable yarn is very compact as shown in Figure 10 in section 3.1.2.

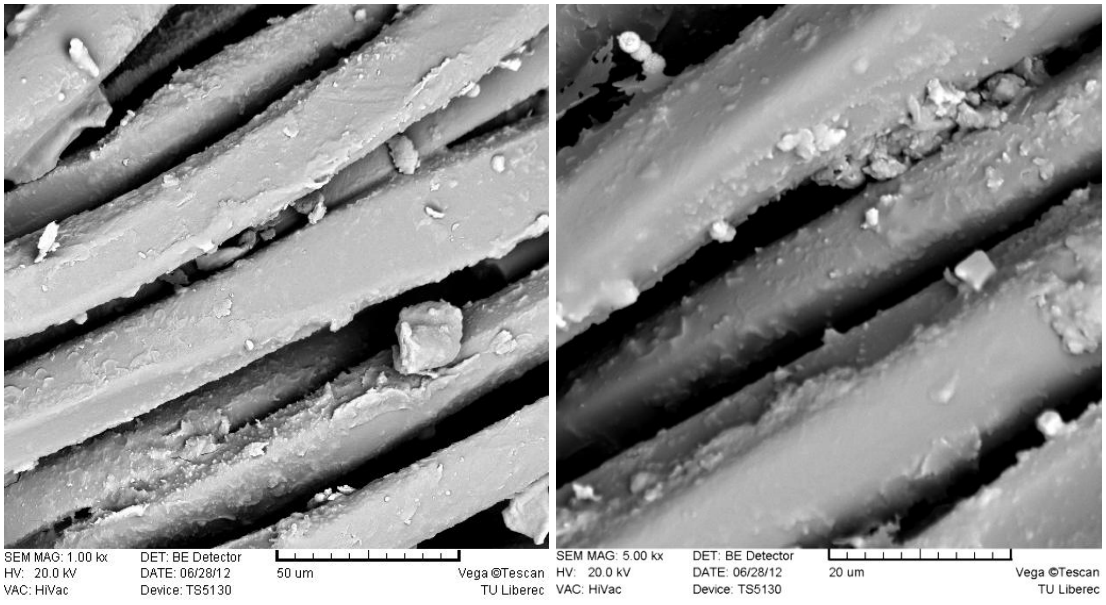

(a) (b)

Figure 45: SEM micrographs of PPy coated Latex/PA6 yarn sample SY3 (a) low magnification (b) high magnification

8.1.2. FTIR analysis

The presence of PPy on the Latex/PA6 specimens was characterized by Fourier transform infrared spectroscopy (FTIR) as shown in Figure 46.

The absorption at 1535 and 1448 cm^{-1} assigned to ring vibration of C=C and C=N in-plane as well as at 1168 cm^{-1} for N-C vibration confirms the presence of pyrrole ring of PPy. Absorptions at 1290 and 1029 cm^{-1} confirms in-plane vibration of =C-H whereas absorption at 779 cm^{-1} shows out plane vibration of =C-H. The most important peak at 3301 cm^{-1} represents amide group in PA6 which is vanished with the increase in concentration of PPy, shows that PA6 reacts with PPy and must have better adhesion.

The absorbance peaks are not so significant in SY3 because the amount of PPy on the substrate is very minute and hence beyond the limit of detection of FTIR.

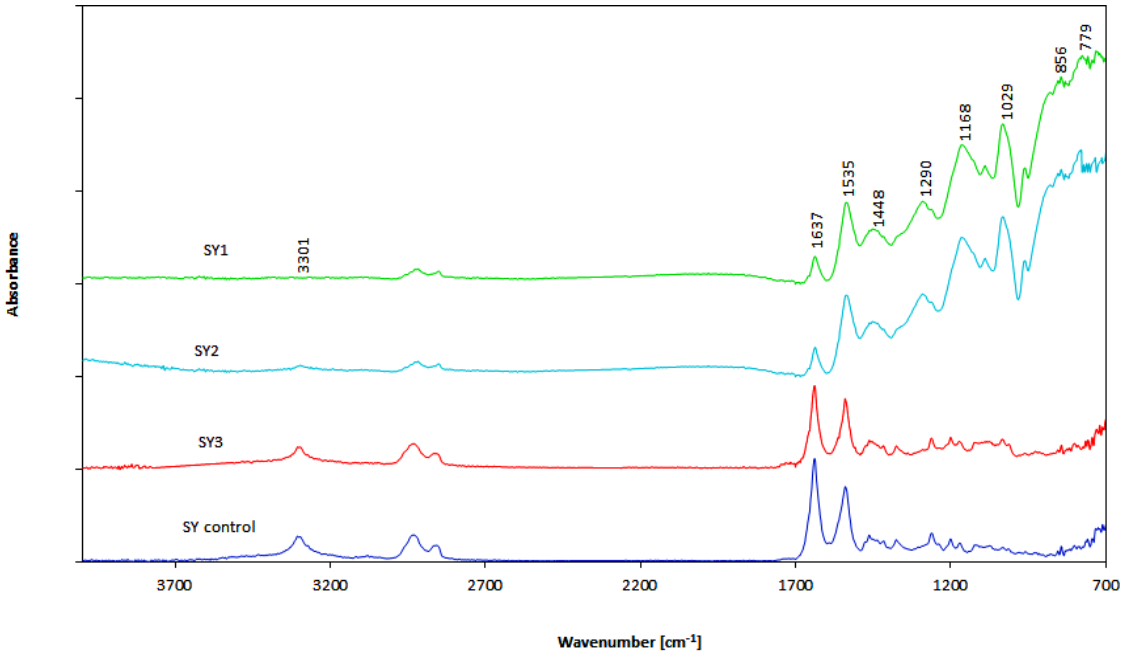

Figure 46: FTIR absorbance curves of Latex/PA6 stretchable yarn control and PPy coated samples SY1, SY2 and SY3.

8.1.3. Weight gain by Latex/PA6 yarn after coating with PPy

The influence of concentration of $FeCl_3$ and TsO^- on the total mass of the Latex/PA6 yarn was studied. Figure 47 describes the dependence of mass gain on the concentration of $FeCl_3$ and TsO^- while the molar ratio between $FeCl_3$ and TsO^- was kept 2:1.

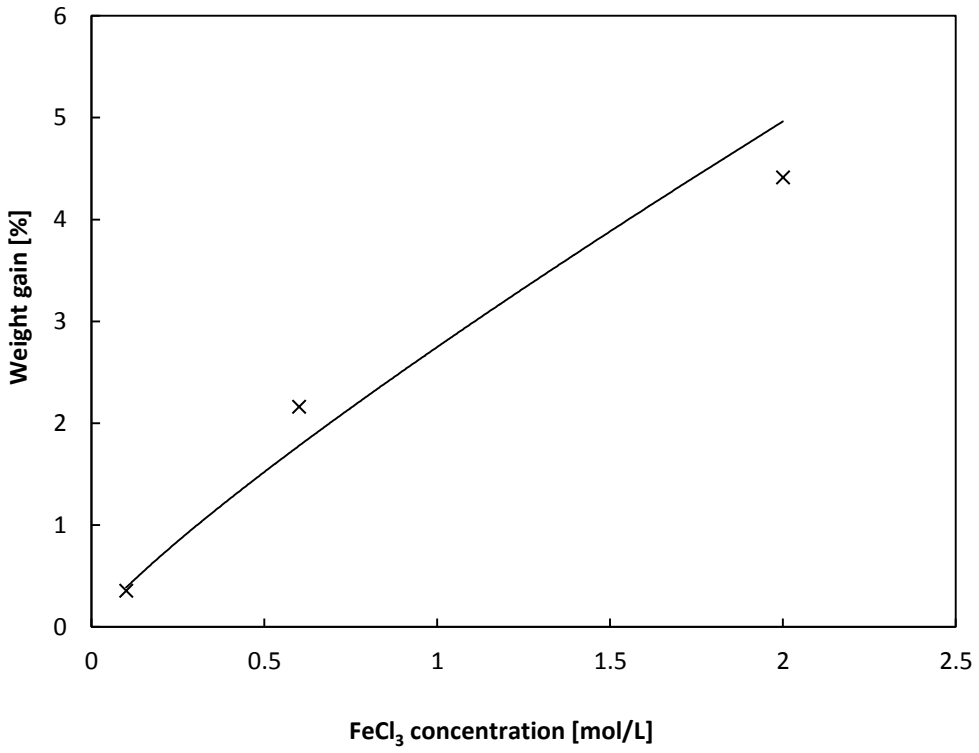

Figure 47: Weight gain [%] by Latex/PA6 yarn samples after PPy deposition

It can be perceived from this figure that weight gain by the yarn follow a power function to the concentration of the oxidant. This relation can be written as the line passing through the origin. By the least squares regression for this model the expression can be written as Equation 48.

$$W = 2.7486 \cdot C^{0.8526} \tag{48}$$

Here, W is the weight gain [%] by Latex/PA6 yarn and C is the concentration of $FeCl_3$ [mol/L]. The coefficient of determination R^2 is calculated as 0.9827

This power function is due to the fact that Latex is purely hydrophobic and does not allow pyrrole to polymerize even on its surface therefore, total polymerization occurs in PA6 fibrous structure as shown in Figure 48.

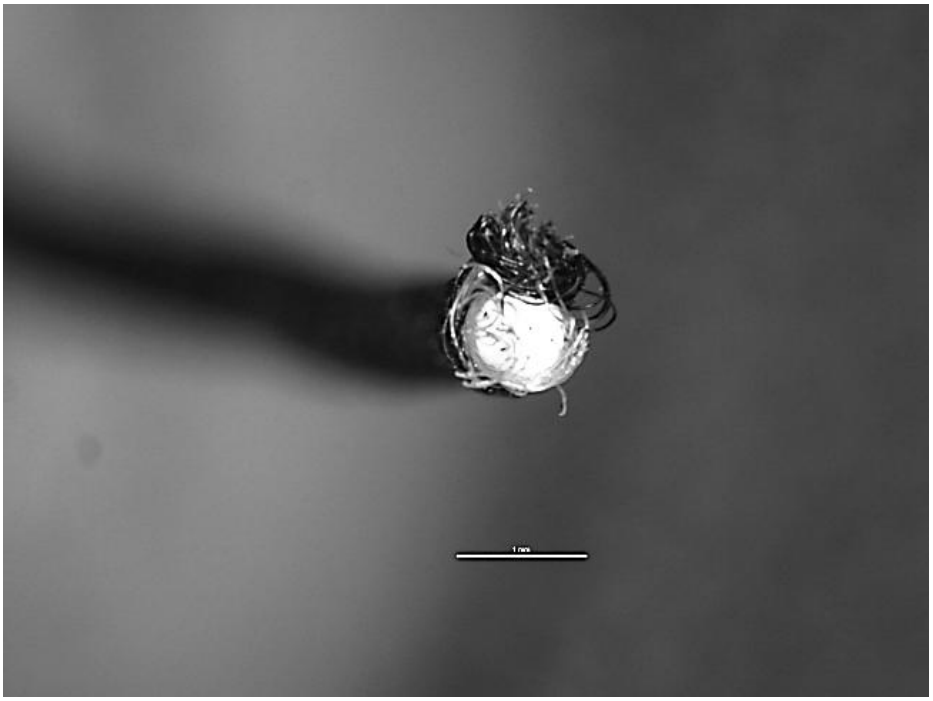

Figure 48: Cross-sectional view of PPy coated Latex/PA6 (SY1) from optical microscope

8.2. Linear dependence of resistance on length

In order to determine the dependence of resistance on the length of PPy coated Latex/PA6 yarn, sample was clamped between two stainless steel clamp type electrode and resistance was measured by varying the distance between them as described in section 3.3.2. It was found that resistance of PPy coated Latex/PA6 stretchable yarn is a linearly increasing function of the distance between the electrodes holding the yarn as shown in Figure 49. By the least squares regression for this model this relationship can be expressed as;

$$R = ZD + r \tag{49}$$

where, R is the resistance [kΩ] of PPy coated Latex/PA6 yarn sample, D the distance between measuring electrodes and r the resistance of the electrodes found to be 0.0001kΩ approx. in this work. However the slope Z is the directly proportional to the resistivity ρ in [kΩ.cm] of the PPy coated Latex/PA6 yarn samples as shown in the Figure 50 for this experiment and can be calculated as;

$$Z = 275.63 \cdot \rho - 0.0769 \tag{50}$$

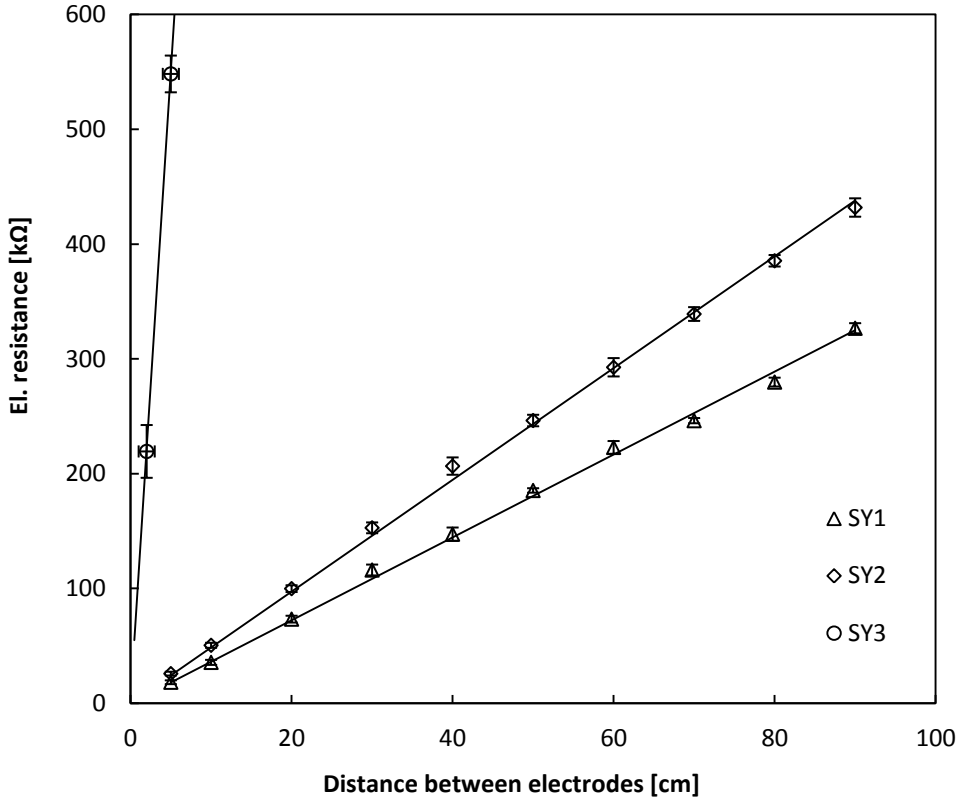

Figure 49: Dependence of electrical resistance of PPy coated Latex/PA6 yarn samples on length

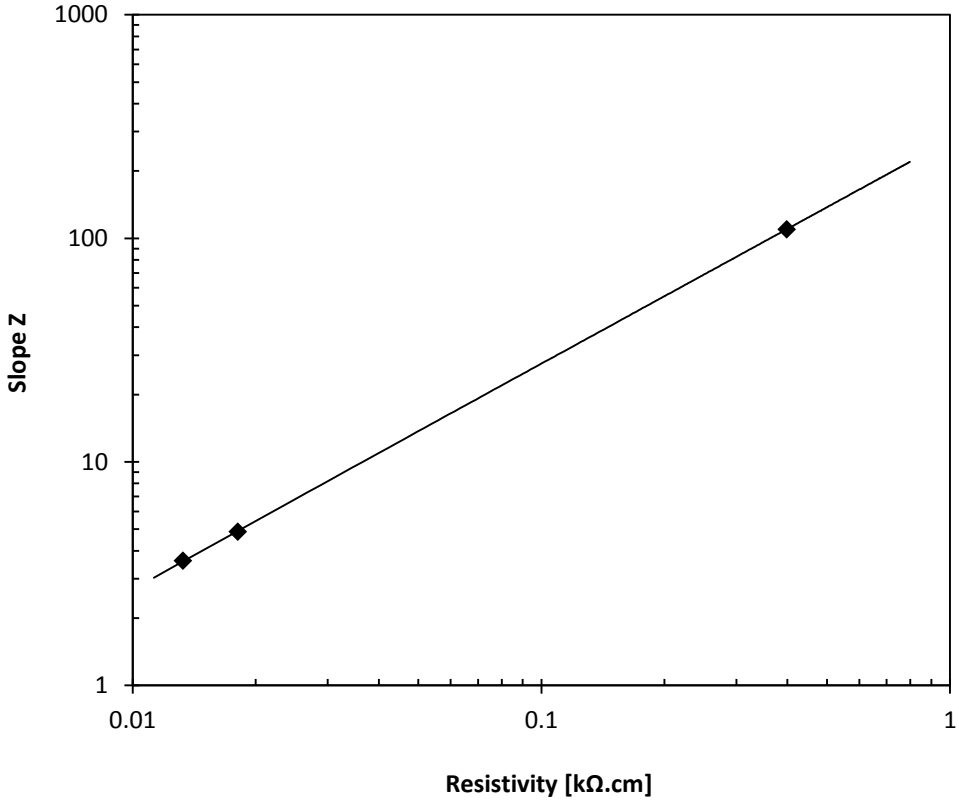

Figure 50: Relationship between slope Z and resistivity of the samples

8.3. Sensitivity of strain sensor against cyclic loading

The Latex/PA6 stretchable yarn samples were coated by PPy through vapour deposition technique and each PPy coated sample was subjected to cyclic loading for 40 cycles. The response of resistance of the samples on 2% deformation and relaxation during 40 cycles are plotted in Figure 51.

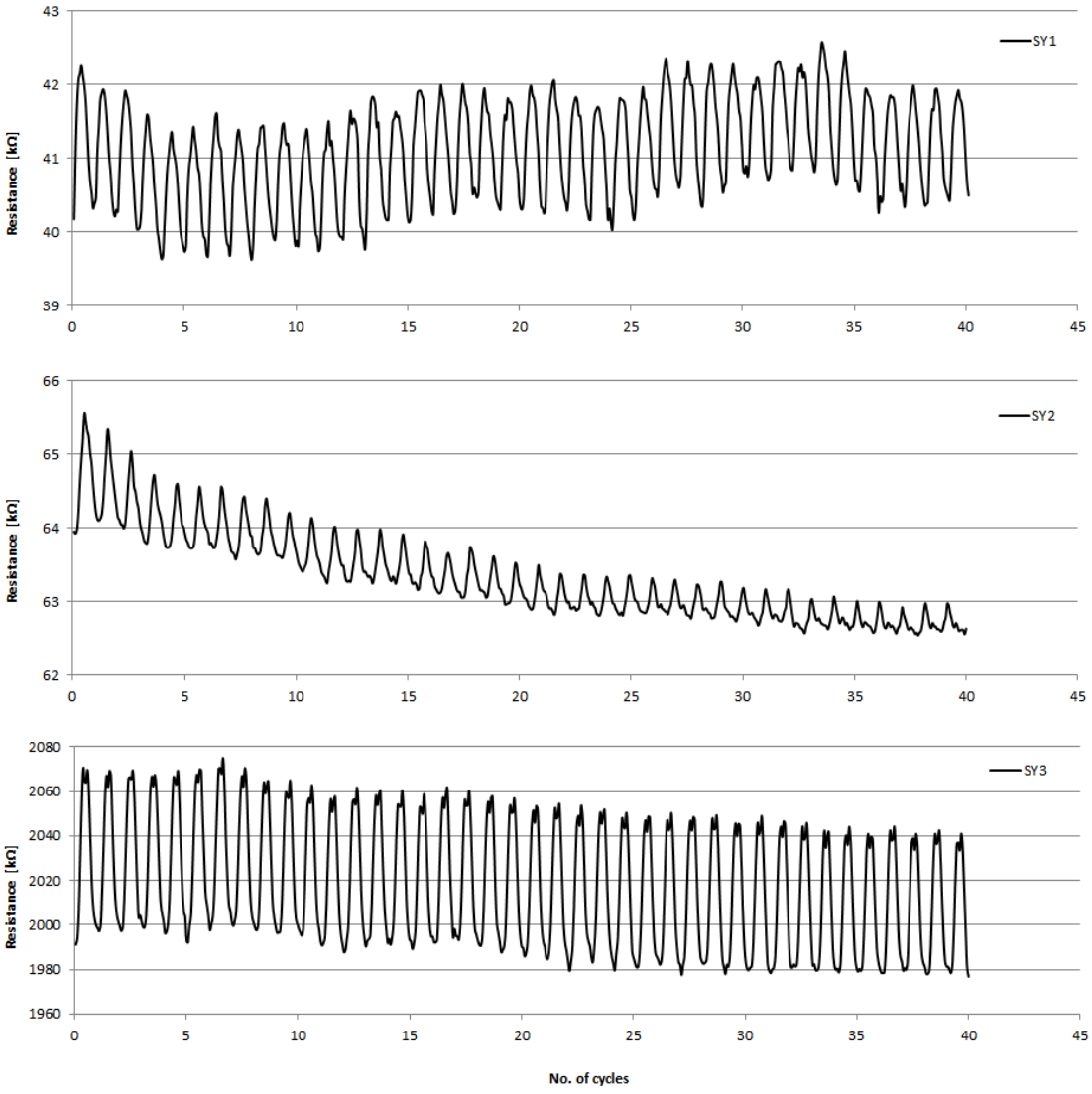

Figure 51: Response of PPy coated Latex/PA6 samples at 2% deformation for 40 cycles

From the Figure 51 it can be observed that SY1 gives almost equal response dR against deformation in terms of magnitude but this response is not consistent with the number of cycles. The SY2 gives neither an equal response against deformation (decreases with number of cycles) nor the consistency of the response. Whereas SY3

is the best among all the samples and it gives not only an equal response upon deformation but also the level of consistency of the response after each cycle is outstanding. The average response in terms of change in resistance against deformation has been calculated from 40 cycles and named as sensitivity $\left(dR/d\varepsilon\right)$ of each sample. The sensitivity levels of all PPy coated Latex/PA6 samples are shown in Figure 52.

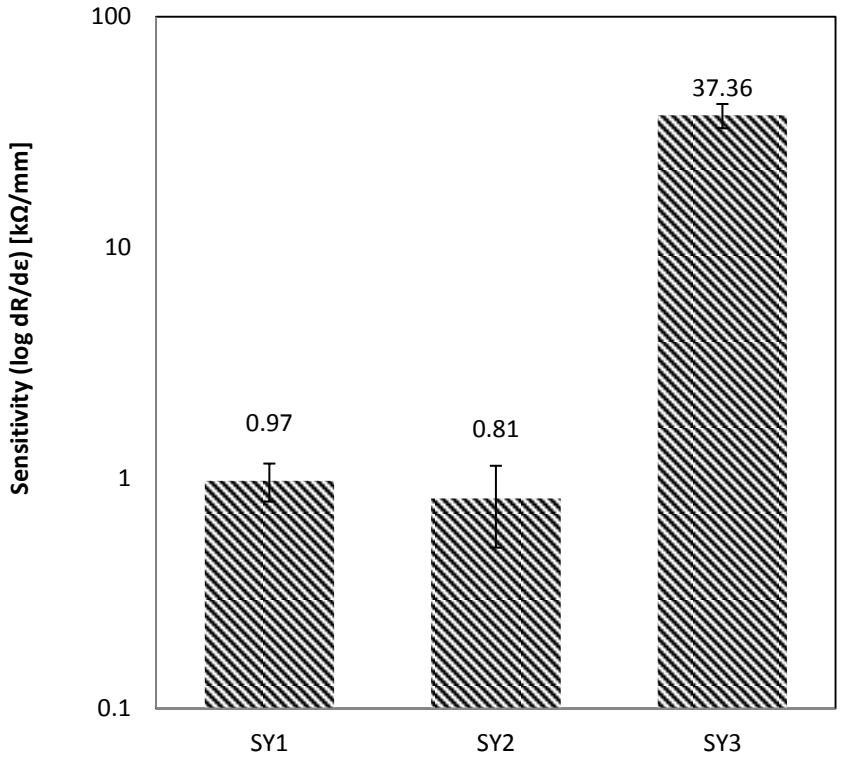

Figure 52: Dependence of sensitivity of the strain sensor on longitudinal deformation

Although SY3 has the highest resistivity among all three samples under study, however it outperformed SY1 and SY2 in terms of response against small extension. The sample SY2 has been found as the worst in terms of sensitivity and its deviation in the results. The standard deviations of the specimens were calculated as 0.182, 0.315 and 4.49 [kΩ.cm] for SY1, SY2 and SY3 respectively.

In addition to the high sensitivity, uniformity or the stability of the response on multiple loading is also important factor for practical applications. The uniformity can be analysed qualitatively from the plotted graphs of strain-resistance relationship such as shown in Figure 53.

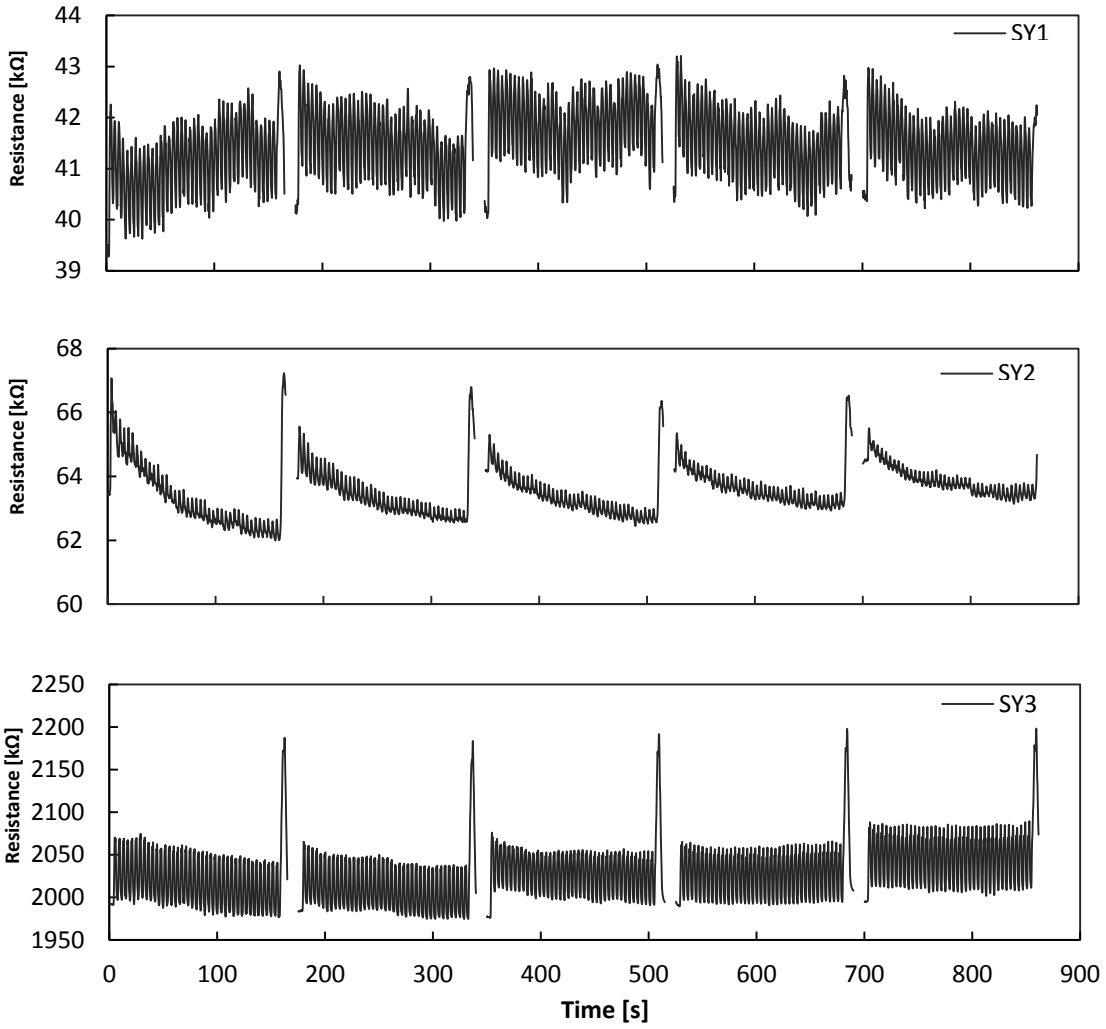

Figure 53: Responses of resistance of different samples at 2% elongation with multiple sets of 40 cycles

When the PPy coated Latex/PA6 yarn sample is elongated, the force is provided by an external motor of the testing rig that separates adjacent PPy grains which lead to the increase in electrical resistance due to the reduction in the available paths for the charge carriers. During the retraction stage the motor releases strain and the retraction force is provided by the Latex itself. Changes in the electrical resistance rely on the resilience property of the Latex to store the applied strain and utilise the stored energy to mirror the elongation stage. There is random shift in the electrical resistance observed in case of SY1 and downward shift in case of SY2 whereas deviation of amplitude from the mean on cyclic loading is not so huge in terms of SY3 and gradient remains constant.

8.4. Mechanical properties

During cyclic loading of PPy coated Latex/PA6 yarn samples, change in mechanical behaviour was also studied and average force-elongation curve, during 40 cycles of elongation and relaxation is plotted as shown in the Figure 54.

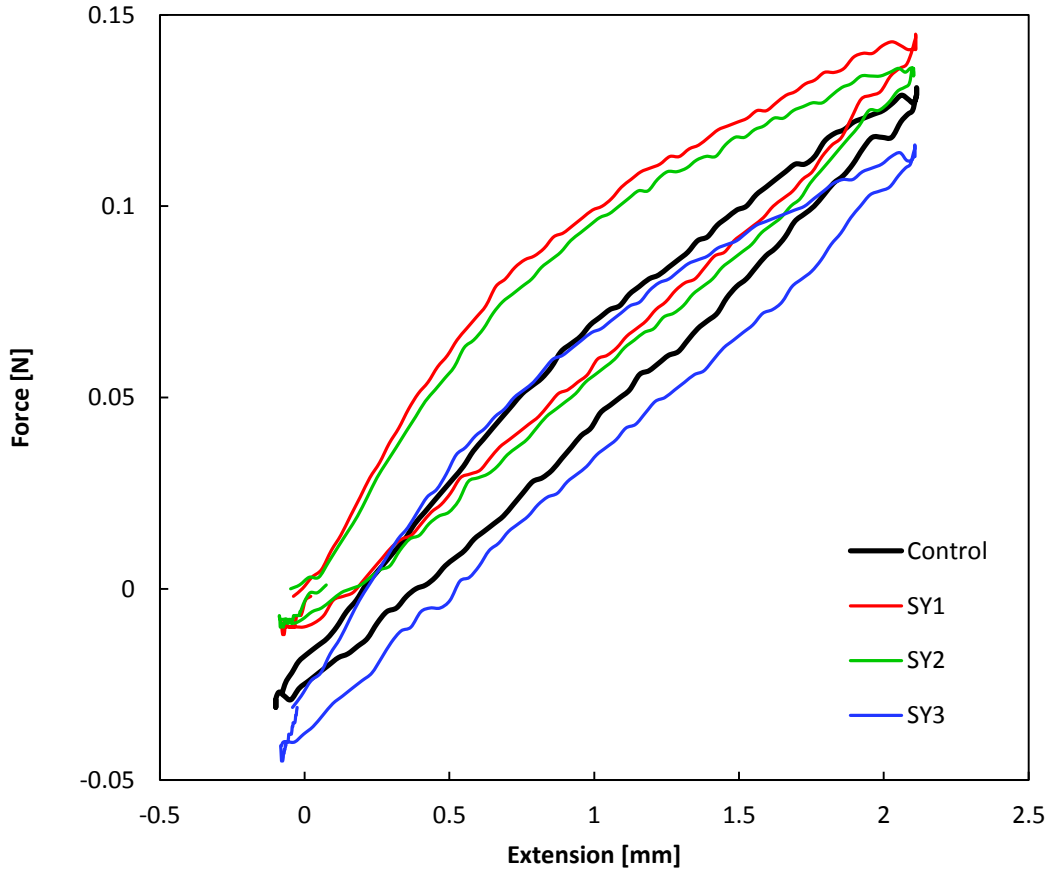

Figure 54: Average Force-elongation curve of control and PPy coated Latex/PA6 samples

It can be observed that SY1 and SY2 were affected most due to the presence of more quantity of PPy on the surface of each individual fibre. Whereas SY3 was found to be least affected and hence kept the resilience of original yarn. A tangent was drawn on the initial linear portion of the average curves and initial modulus was calculated as shown in Figure 55.

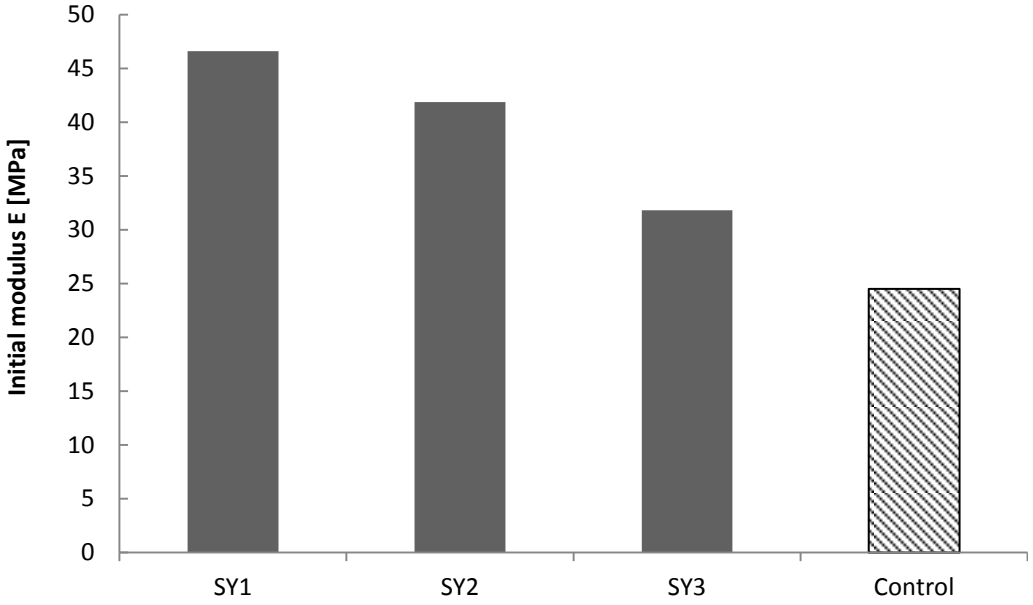

Figure 55: Initial modulus of control and PPy coated Latex/PA6 samples

Major changes occurred in the case of SY1 and SY2 which is practically undesirable on the basis of application point of view. The modulus of sample SY3 was found to be 30% increased only compared to 70% and 90% in case of SY2 and SY1 respectively.

8.5. Decay of conductivity with time

Although PPy has excellent conductive nature but being as a chemical conductor, the major drawback is the decay in conductivity with the passage of time. In order to monitor this decay, PPy coated Latex/PA6 yarn samples was kept under temperature of 20±2°C and relative humidity for 40±2% for 21 weeks. Figure 56 illustrates the change in resistivity ρ of each sample after every four weeks during storage. It is worth noting that the resistivity increases significantly in the first week and this rise is more pronounced in the case of SY2 and SY3 whereas there is a continuous rise found in case of SY1 being as most conductive sample. The change in resistivity continues even after first week in SY2 but rise has been found to be less significant compared to first week and resistivity increases to 8% of the initial resistivity. In the case of SY3, the change in resistivity can be observed in first week more momentously which is then stabilized after reaching to plateau in 17 weeks with the increase of 1.7% of the initial.

The surface morphology of the PPy film on the substrate plays an important role for oxygen access and thus changes resistivity [150,6]. The higher magnification of surface morphological study shown in Figure 40b of PPy coated Latex/PA6 substrate reveal that PPy covers each individual PA6 fibre very well and that the coating is smooth thus the increase in resistivity found to be not as sharp as observed by Patil [151] and Kaynaf [152].

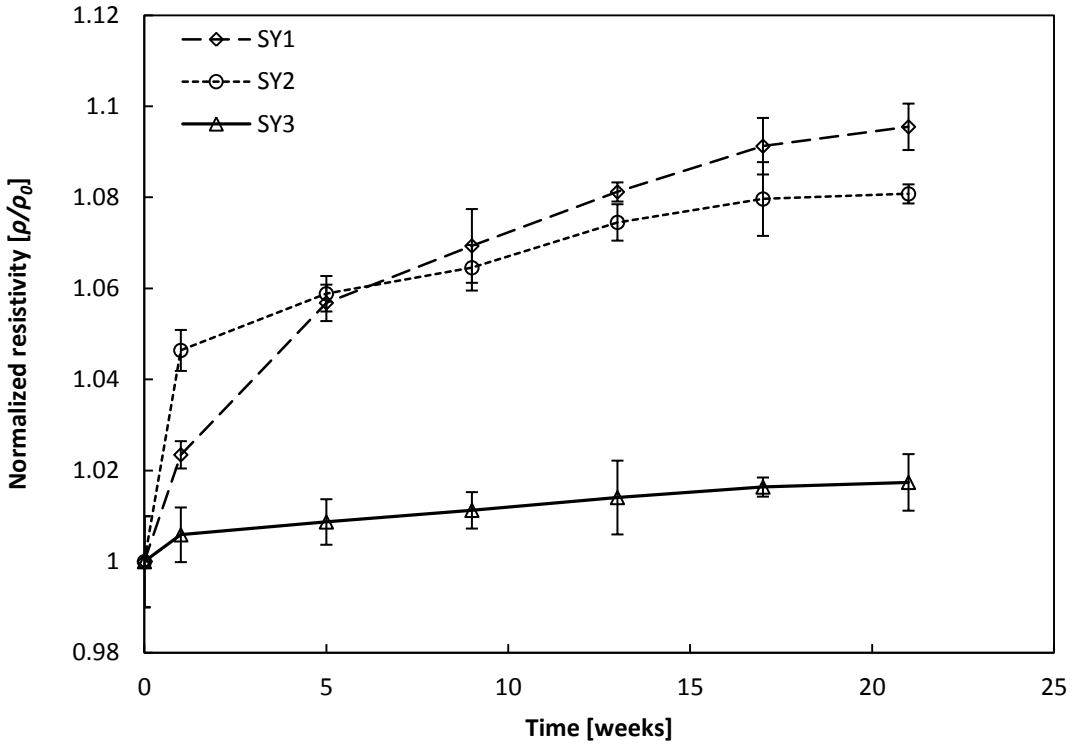

Figure 56: Aging behaviour of PPy coated Latex/PA6 samples at ambient conditions

8.6. Effect of washing on resistance

As the conducting polymers adhere to the surface of the fibre substrate only during polymerization and they are not absorbed in the fibre structure therefore smaller amount can be detached during washing cycle. When the samples of PPy coated Latex/PA6 were washed according to ISO 105-C06:2010, it was observed that resistivity increases significantly in all the samples as expected that can be seen from Figure 57. Only the first wash increases resistivity up to 70 % in SY1, 65% in SY2 and 20% in SY3. The change in resistivity continues in subsequent washing cycles and becomes manifold after five washing cycles. It can be perceived easily that the change in resistivity happens more drastically in samples SY1 and SY2 whereas SY3

is the least affected. From this observation, it can inferred that substrates containing more amount of PPy on them loose their conductivity more pronouncedly than compared to that with less amount.

In the literature it has been found that the loss in the conductivity of PPy film on multiple rinsing with water alone causes degradation of hydroxyl groups of PPy and consequently loss in conductivity [153].

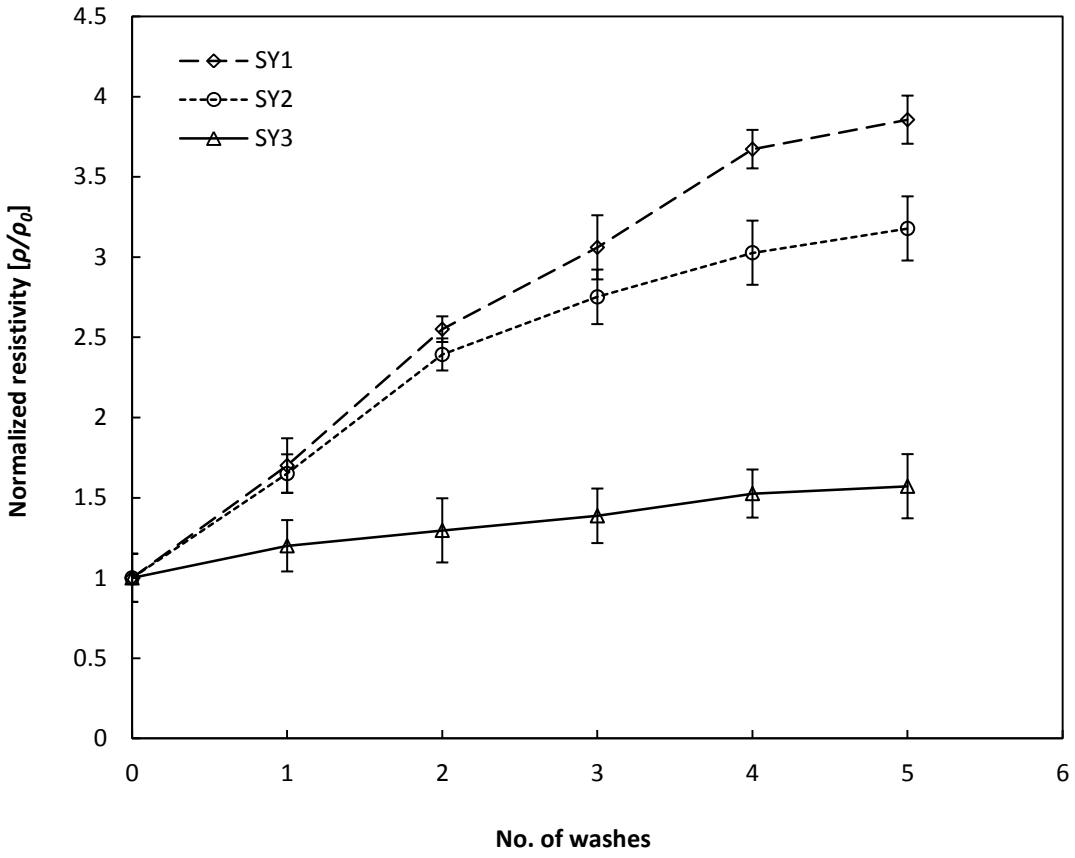

Figure 57: Dependence of resistance on commercial washing cycles

8.7. Effect of humidity and temperature

PPy coated Latex/PA6 samples can find their practical application as body movement or a strain sensor, however it is very essential to determine the effect of humidity and temperature of the working environment on the conductivity. In this context, these samples were monitored under different temperatures and humidity levels and response of resistance was examined. Figure 58 illustrates the effects of temperature and humidity on the resistivity of PPy coated Latex/PA6 samples. It is commonly known that the resistivities of semiconductors decrease with increase in temperature

as the number of charge carriers increases with temperature rise. On the other hand, for metals, resistivity increases with temperature due to phonon-induced scattering. As it can be seen, in all samples resistivity decreases as the temperature rises from 10°C to 50°C keeping the humidity constant. The change is more significant in samples SY1 and SY2 compared to SY3.

Aside from temperature, humidity also has an effect on the resistivity of PPy, and thus PPy is capable of responding rapidly to humidity change, and does so in a reversible manner. Cassignol et al [154] reported that the resistivity of PPy samples those are chemically doped with TsO^- and hydrogen sulphate decrease with relative humidity and plateau around their equilibrium values. From the experimental data conducted in this dissertation, PPy behaves differently. Figure 58 illustrates that, as the humidity increases from 30% to 70% resistivity of samples SY1 and SY2 increases but in the case of SY3 it remains almost unchanged.

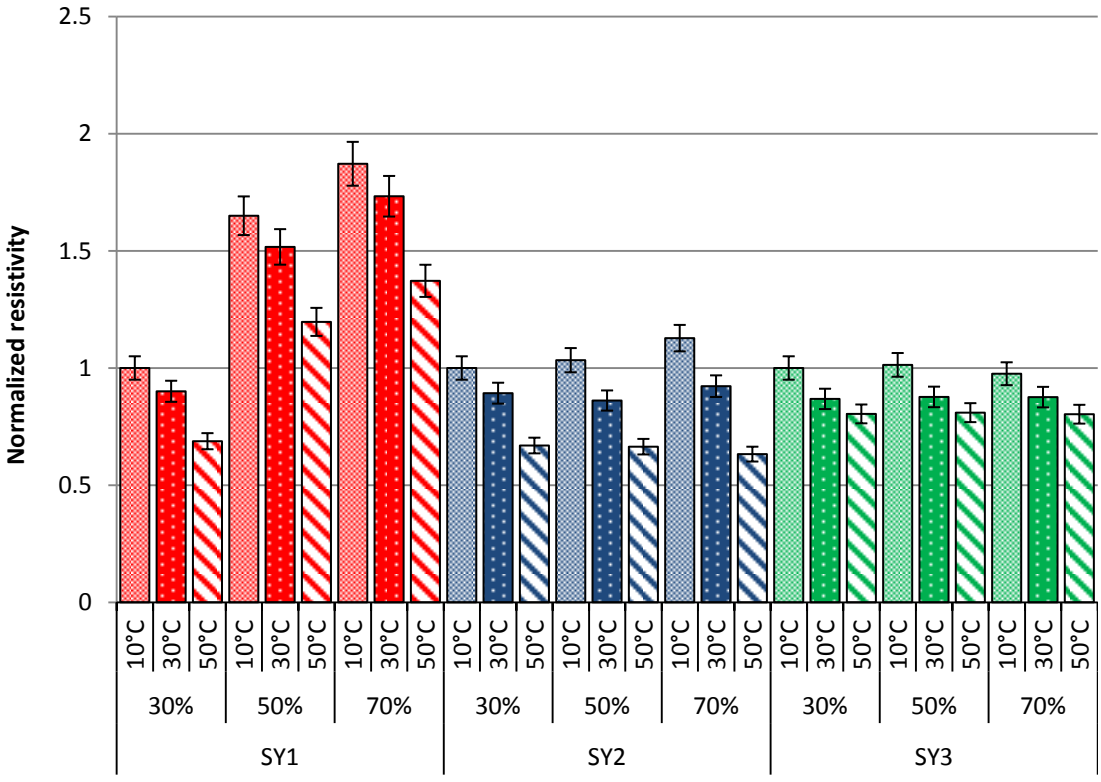

Figure 58: The effect of temperature and humidity on resistivity of PPy coated Latex/PA6 samples

8.8. Conclusion

PPy was coated on PA6 wrapped Latex yarn samples through vapour phase polymerization by varying concentration of oxidant and dopant thus samples were varied in resistivity levels. It was found that resistance of all the samples follow exactly a linear function of length and hence follow Ohm's law.

The sensitivity or the change in resistance per unit deformation is a useful tool to figure the suitability of the strain sensor out. The high resistive sample gives best sensitivity as well as uniformity or the consistency of the response against small cyclic deformation (2%) whereas low resistive samples fail to give the equal and uniform response.

The amount of PPy deposited on the fibre surface changes its mechanical properties. It is observed that samples with more concentration of PPy on its surface have more tangent modulus than that with less concentration. At the same time, the increase in resistivity depending on the time of storage of samples and commercial washing cycles has been observed.

It is noted that the presented strain sensor is sensitive to environmental conditions such as humidity and temperature. Resistivity increases with rise in humidity whereas decreases with the increase in temperature. The sample of high resistivity found to be least affected by the humidity and temperature.

Chapter 9

Summary

9.1. Conclusions drawn from the work

The main aim of this research work is to study few different applications of PPy coated textile substrates. In this context pyrrole was polymerized on two kinds of glass fabric and a stretchable yarn (Latex wrapped with PA6) by vapour deposition technique. Anhydrous Iron(III) Chloride as an oxidizing agent and tetraethyl ammonium p-toluene sulfonate as a doping agent were used in the polymerization. The concentration of polypyrrole was controlled by varying the concentration of oxidizing and doping agents whereas the rest of the process parameters such as time, temperature, pressure etc. were kept constant.

SEM and LSCM micrographs show that during vapour phase polymerization PPy is deposited on the surface of the fibres and covers them very well. The average thickness of the PPy produced on glass fibre by using 0.6mol/L Iron(III) Chloride and 0.3mol/L p-toluene sulfonate is calculated as 1.165±0.502μm from SEM image analysis and 1.372±0.223μm from LSCM analysis. Meanwhile FTIR analysis of PPy coated substrates also confirms the completion of polymerization of pyrrole through characteristic absorbance peaks.

Weight gain by glass fabric substrate after PPy deposition was found to be linear increasing function of concentration of Iron(III) Chloride (which is responsible for the oxidation of pyrrole monomer and hence regulate the yield). The electrical resistivity and EMI shielding effectiveness of PPy coated glass fabric having areal density of 410g.m^{-2} was found to be decreased linearly depending on the concentration of Iron(III) Chloride whereas the fabric having 900g.m^{-2} follows a power function. It can be inferred from the cross-sectional view of the coated fabric specimens that PPy develops on each individual fibre of the fabric structure mentioned former while later structure does not allow pyrrole vapours to access fibres in the core of yarn and hence PPy is not formed there. Due to this circumstance PPy is deposited on the fibres which are well exposed. It was also resolved that density of the fabric also makes a

great influence on EMI shielding effectiveness and found to be significantly increased for higher density fabric.

The tensile strength of PPy coated glass fabric considerably decreases with the increase in concentration of PPy on fabric substrate regardless of the density of the fabric whereas elongation at break increases in terms of high density and decreases in low density fabric structure. The reason might be the presence of friction between more numbers of PPy coated fibres in the denser fabric structure.

When DC voltage is supplied to PPy coated glass fabric, it produces heat instantly mainly depending upon the time and potential of voltage being supplied. The temperature rises very sharply within 300 to 400s and level off after reaching to plateau. The thermal power density produced in the fabric follows a linear function of the voltage supplied whereas temperature follows a power function. With the help of dimensionless numbers and equation of heat transfer by convection, it was calculated that the amount of heat transferred to air follows a positive power function to the heat being converted from electrical energy. This interprets that ratio between heat conducted to air by convection and heat produced does not remain constant at different levels and that the remaining amount of heat conducted within fabric itself more than conducted out at higher voltage.

Thermal treatment at elevated temperatures affects the electrical conductivity and electroactivity of PPy. The rate of thermal degradation of conductivity is also very much dependent on temperature and duration of heating. During the series of experiments conducted in this dissertation it was observed that conductivity of PPy coated glass fabric increases as the temperature increases till it reaches to Tg of PPy which determines the common behaviour of semiconductors. While thermal treatment above Tg cause a loss in conductivity and this loss is permanent. The reason for this fact could be the lattice vibrations in the amorphous regions which do not allow charge to flow easily.

The strain sensor was developed by deposition of PPy on Latex wrapped with PA6 fibres through a vapour deposition technique. With the aim of studying dependence of resistance on the length of the conductor, extensive experimental analysis was carried out and concluded that resistance follows an extremely linear function of length and a

model has been proposed to calculate the resistance at a particular length. The slope of this said function can be calculated from resistivity of the sample.

PPy coated Latex/PA6 samples were subjected to cyclic deformation of 2% and corresponding change in resistance was analysed. It was found that samples with more amount of PPy coating on them perform worse than sample with least amount of PPy. It means that high resistive sample gives higher level of sensitivity and consistency of response against small deformations.

PPy being as a brittle polymer changes the mechanical properties of the textile substrate on which it has been coated. In case of Latex/PA6 samples, PPy increases the friction between the PA6 fibres and consequently tangent modulus increases. More amount of PPy on the fibres make a larger change in the modulus that is utterly undesirable compared to fewer amount.

Conductivity of conducting polymers is highly dependent on the time of storage in a particular environment. Latex/PA6 samples coated with PPy were kept under ambient conditions for several weeks. All the samples drop conductivity within couple of weeks more pronouncedly which continues to be dropped in case of relatively high conductive sample whereas the drop is not so significant in the case of least conductive sample.

Commercial and domestic laundering plays an important role if the characteristic component of the garment loses its property such as colour, softness and conductivity etc. PPy coated Latex/PA6 samples were tested under standard commercial laundering procedure for few times and found to lose conductivity constantly on every cycle. Similarly, in the case of time decay property, more conductive samples lose conductivity more drastically than the one with least conductivity.

The effect of humidity and temperature of environment on resistivity of PPy coated Latex/PA6 samples was also found to be imperative. The resistivity decreases with the increase in temperature from 10°C to 50°C, clearly reflects the general behaviour of semiconductors. However, humidity causes an increment in resistivity which is a typical phenomenon in intrinsically conducting polymers only.

In the context of sensitivity, uniformity of the response, effect of environmental conditions and decay properties, among all three samples of PPy coated Latex/PA6,

highly resistive sample is considered to be a best suitable for the practical application of strain sensing. While the total cost of manufacturing of this strain sensor is less than 1Kč per meter.

9.2. Recommendations for future work

In the light of the results obtained from the present study, author makes the following recommendations for the future work.

The major part of the present work mainly focused on electrical resistivity and EMI shielding effectiveness of PPy coated glass fabric of two different densities only. Similar study can be carried out by taking different structures of glass fabric and influence of fabric density parameter on EMI shielding effectiveness can be analysed more deeply.

Similarly, instead of measuring EMI shielding effectiveness only in the frequency range of 300MHz to 1500MHz, it can be measured in a wide range of frequency in order to propose the presented fabric as shield for RADAR barrier applications.

Only limited tensile properties of PPy coated glass fabric were studied in this work. Other properties of the fabric such as tear strength, surface roughness and bending strength can also be analysed to understand the fabric serviceability.

For the Joule heating effect in PPy coated glass fabric, only one kind of sample was taken into consideration. However, it is important to know the influence of different levels of conductivity on the temperature rise during the supply of particular DC voltage. In this regard, one kind of glass fabric with different concentration of PPy can be taken to analyse this effect.

As far as strain sensor is concerned, response of resistance was monitored against small deformation by using a force loading machine but response in a practical application was not analysed therefore, it can be implanted in the textile garment together with small electronic circuit to monitor the body movements of human being.

References

[1]. Vladimir, A. and Alexander, C. US Patent No. 5968854, 1999.

[2]. Lin, J. C. Safety standards for human exposure to radio frequency radiation and their biological rationale, *IEEE Microwave Magazine,* **4,** 2003, pp. 22-26.

[3]. Kuhn, H. H. and Child, A. D. in Hand book of conductive textiles, 1998, Marcel Dekker, INC., New York.

[4]. MacDiarmid, A. G. and Epstein, A. J. 'Synthetic Metals': A novel role for organic polymers, *Macromolecular Chemistry Symposium*, **51,** 1991, pp. 11-28.

[5]. Kuhn, H.H. AATCC's International Conference & Exhibition, Atlanta, U.S.A., 28-September-1 October, *Book of Papers,* 1997, p.114.

[6]. Kuhn, H. H., Child, A. D. and Kimbrell, W. C. Toward real applications of conductive. polymers, *Synthetic Metals,* **71,** 1995, pp. 2139-2142.

[7]. Kincal, D., Kumar, A., Reynolds, J. R. and Child, A. D. Conductivity switching in polypyrrole-coated textile fabrics as gas sensors, *Synthetic Metals,* **92,** 1998, pp. 53-55.

[8]. de Lacy Costello, B. P. J., Evans, P. and Ratcliffe, N. M. Preparation of polypyrrole composites and the effect of volatile amines on their electrical properties, *Analyst,* **121,** 1996, pp. 793-797.

[9]. Boutrois, J. P., Jolly, R. and Petrescu, C. Process of polypyrrole deposit on textile - product characteristics and applications, *Synthetic Metals,* **85,** 1997, pp. 1405-1406.

[10]. Heisey, C. L., Wightman, J. P., Pittman, E. H. and Kuhn, H. H. Surface and adhesion properties of polypyrrole-coated textiles, *Textile Research Journal,* **63,** 1993, pp. 247-256.

[11]. Kuhn, H. H., Kimbrell, W. C., Fowler, J. E. and Barry, C. N. Properties and applications of conductive textiles, *Synthetic Metals,* **57,** 1993, pp. 3707-3712.

[12]. Child, A. D. and Kuhn, H. H. Enhancement of the thermal stability of chemically synthesized polypyrrole, *Synthetic Metals,* **84,** 1997, pp. 141-142.

[13]. Baik, D. H., Kim, H. S. and Park, Y. H. Effect of physical structure of matrix copolyester on the conductivity of polypyrrole/copolyester composite films, *Molecular Crystals and Liquid Crystals,* **377,** 2002, pp. 377-380.

[14]. Kim, H. K., Byun, S. W., Jeong, S. H., Hong, Y. K., Joo, J. S., Song, K., Park, Y. H. and Lee, J. Y. Environmental stability of EMI shielding PET fabric/polypyrrole composite *Molecular Crystals and Liquid Crystals,* **377,** 2002, pp. 369-372.

[15]. Gregory, R. V., Kimbrell, W. C. and Kuhn, H. H. Conductive textiles, *Synthetic Metals,* **28,** 1989, pp. 823-835.

[16]. Gregory, R. V., Kimbrell, W. C. and Kuhn, H. H. Electrically Conductive Non-Metallic Textile Coatings, *Journal of Coated Fabrics,* **20,** 1991, pp. 167-175.

[17]. Kaynak, A., Najar, S. S. and Foitzik, R. C. Conducting nylon, cotton and wool yarns by continuous vapor polymerization of pyrrole, *Synthetic Metals,* **158,** 2008, pp. 1-5.

[18]. Kim, J. Y., Lee, J. H. and Kwon, S. J. The manufacture and properties of polyaniline nano-films prepared through vapor-phase polymerization, *Synthetic Metals,* **157,** 2007, pp. 336-342.

[19]. Bhadani, S. N., Sen Gupta, S. K. and Gupta, M.K. Electrically conducting natural fibers, *Indian Journal of Fibre & Textile Research,* **18,** 1993, pp. 46.

[20]. Dhawan Bull, S. K. and Trivedi, D. C. Thin conducting polypyrrole films on insulating surfaces and its applications, *Material Science,* **16,** 1993, pp. 371-380.

[21]. Kaynak, A., Wang, L., Hurren, C. and Wang, X. Characterization of Conductive Polypyrrole Coated Wool Yarns, *Fibres and Polymers,* **3,** 2002, pp. 24-30.

[22]. Hao, L., Yi, Z., Li, C., Li, X., Yuxiu, W. and Yan G. Development and characterization of flexible heating fabric based on conductive filaments, *Measurement,* **45,** 2012, pp. 1855-1865.

[23]. Hamdani, S. T. A., Potluri, P. and Fernando, A. Thermo-mechanical behavior of textile heating fabric based on silver coated polymeric yarn, *Materials,* **6,** 2013, pp. 1072-1089.

[24]. Oh, K. W., Kim, D. J. and Kim, S. H. Adhesion improvement of electroless copper plated layer on PET film - effect of pretreatment conditions, *Polymer (Korea),* **25,** 2001, pp. 302-310.

[25]. Joo, J. and Epstein, A. J. Electromagnetic radiation shielding by intrinsically conducting polymers, *Applied Physics Letters,* **65,** 1994, pp. 2278-2280.

[26]. Kuhn, H. H., Child, A. D. and Kimbrell, W. C. Toward real applications of conductive polymers, *Synthetic Metals*, **71,** 1995, pp. 2139-2142.

[27]. Wang, L. X., Li, X. G. and Yang, Y. L. Preparation, properties and applications of polypyrroles, *Reactive & Functional Polymers*, **47,** 2001, pp. 125-139.

[28]. Li, H. H., Shi, C. Q., Ye, W., Li, C. and Liang Y. Q. Polypyrrole carbon fiber composite film prepared by chemical oxidative polymerization of pyrrole, *Journal of Applied Polymer Science*, **64,** 1997, pp. 2149-2154.

[29]. Kim, S. H., Jang, S. H., Byun, S. W., Lee, J. Y., Joo, J. S., Jeong, S. H. and Park, M.-J. Electrical properties and EMI shielding characteristics of polypyrrole–nylon 6 composite fabrics, *Journal of Applied Polymer Science*, **87,** 2003, pp. 1969-1974.

[30]. Oh, K. W., Kim, S. H. and Kim, E. A. Improved surface characteristic and the conductivity of polyaniline nylon fabrics by plasma treatment, *Journal of Applied Polymer Science*, **81,** 2001, pp. 684-694.

[31]. Oh, K. W., Hong, K. H. and Kim, S. H. Electrically conductive textiles by in situ polymerization of aniline, *Journal of Applied Polymer Science*, **74,** 1999, pp. 2094-2101.

[32]. Im, S. S. and Byun, S. W. Preparation and properties of transparent nylon6-based composite films, *Journal of Applied Polymer Science*, **51,** 1994, pp. 1221-1229.

[33]. Lee, C. Y., Lee, D. E., Joo, J., Kim, M. S., Lee, J. Y., Jeong, S. H. and Byun, S.W. Conductivity and EMI shielding efficiency of polypyrrole and metal compounds coated on (non) woven fabrics, *Synthetic Metals*, **119,** 2001, pp. 429-430.

[34]. Lee, Y. K. and Cho, J. C. Preparation and Physical Properties of Conductive Poly(acrylonitrile) Fabrics Containing Polypyrrole, *Polymer (Korea)*, **24,** 2000, pp. 276-280.

[35]. Heisey, C. L., Wightman, J. P., Pittman, E. H. and Kuhn, H. H. Surface and adhesion properties of polypyrrole-coated textiles, *Textile Research Journal*, **63,** 1993, pp. 247-256.

[36]. Murray, P., Spinks, G. M., Wallace, G. G. and Burford, R. P. Electrochemical induced ductile–brittle transition in tosylate-doped (pTS) polypyrrole, *Synthetic Metals*, **97,** 1998, pp. 117-121.

[37]. Li, Y., Cheng, X. Y., Leung, M. Y., Tsang, J., Tao, X. M. and Yuen, M. C. W. A flexible strain sensor from polypyrrole-coated fabrics, *Synthetic Metals,* **151**, 2005, pp. 89-94.

[38]. Xue, P., Tao, X. M. and Tsang, H. Y. In situ SEM studies on strain sensing mechanisms of PPy-coated electrically conducting fabrics, *Applied Surface Science,* **53,** 2007, pp. 3387-3392.

[39]. Wu, J., Zhou, D., Too, C. O. and Wallace, G. G. Conductive polymer coated lycra, *Synthetic Metals,* **155**, 2005, pp. 698-701.

[40]. Molina, J., del Río, A. I., Bonastre, J. and Cases, F. Chemical and electrochemical polymerisation of pyrrole on polyester textiles in presence of phosphotungstic acid, *European Polymer Journal,* **44**, 2008, pp. 2087-2098.

[41]. Bunsomsit, K., Magaraphan, R., O'Rear, E. A. and Grady, B. P. Polypyrrole-coated natural rubber latex by admicellar polymerisation, *Colloid and Polymer Science,* **280,** 2002, pp. 509-516.

[42]. Anand, J., Palaniappan, S. and Sathyanarayana, D. N. Conducting polyaniline blends and composites, *Progress in Polymer Science,* **23,** 1998, pp.993-1018.

[43]. MacDiarmid, A. G. Synthetic metals: a novel role for organic polymers, *Synthetic metals,* **69,** 2002, pp.11-22.

[44]. Shirakawa, H., Louis, E. J., MacDiarmid, A. G., Chiang, C. K. and Heeger, A. J. Synthesis of electrically conducting organic polymers: halogen derivatives of polyacetylene (CH)x, *Journal of the Chemical Society, Chemical Communications,* **16,** 1977, pp. 578-580.

[45]. Skorobogatov, V. M. and Krivoshei, I. V. *Usp. Khim.* **57,** 1988, pp. 832-850 [The structure and properties of highly conducting polyacetylene complexes, *Russian Chemical Reviews,* **57(**5), 1988, pp. 461].

[46]. Shirakawa, H. Anisotropic electrical conductivity of partially oriented polyacetylene, *Journal of Polymer Science Part B,* **17,** 1979, pp. 195-201.

[47]. Nigrey, P. J., MacDiarmid, A. G. and Heeger, A. J. Electrochemistry of polyacetylene, (CH)x: electrochemical doping of (CH)x films to the metallic state, *Journal of the Chemical Society, Chemical Communications,* **14,** 1979, pp. 594-595.

[48]. Ivory, D. M., Miller, G. G., Sowa, J. M., Shacklette, L. W., Chance, R. R. and Baughman, R. H. highly conducting charge-transfer complexes of poly(p-phenylene), *Journal of Chemical Physics,* **71,** 1979, pp. 1506-1507.

[49]. Kanazawa, K. K., Diaz, A. F., Geiss, R. H., Gill, W. D., Kwak, J. F., Logan, J. A., Rabolt, J. F. and Street, G. B. 'Organic metals': polypyrrole, a stable synthetic 'metallic' polymer, *Journal of the Chemical Society, Chemical Communications*, **19,** 1979, pp. 854-855.

[50]. Hernandez, R., Diaz, A. F., Waltman, R. and Bargon, J. Surface characteristics of thin films prepared by plasma and electrochemical polymerizations, *Journal of Chemical Physics*, **88,** 1984, pp. 3333-3337.

[51]. Bryce, M. R., Chisse, A., Kathirgamanathan, P., Parker, D. and Smith, N. R. M. Soluble, conducting polymers from 3-substituted thiophenes and pyrroles, *Journal of the Chemical Society, Chemical Communications*, **6,** 1987, pp. 466-467.

[52]. Chiang, J. C. and MacDiarmid, A. G. 'Polyaniline': Protonic acid doping of the emeraldine form to the metallic regime, *Synthetic Metals*, **13,** 1986, pp. 193-205

[53]. Kumar, D. and Sharma, R. C. Advances in conductive polymers, *European Polymer Journal*, **34,** 1998, pp. 1053-1060.

[54]. Naarmann, H. "Polymers, Electrically Conducting" in *Ullmann's Encyclopedia of Industrial Chemistry*, 2002, Wiley-VCH, Weinheim.

[55]. Naarman, H., Electronic properties of conjugated polymers, *Springer series in Solid State Science*, **76,** 1987, p.12.

[56]. Kulszewicz-Bajer, I., Sobczak, J., Hasik, M. and Pretula, J. Spectroscopic Studies of polyaniline protonation with poly(akylene phosphates), *Polymer*, **37,** 1996, pp. 25-30.

[57]. Erdem, E., Sacak, M. and Karakisla, M. Synthesis and properties of oxalic acid-doped polyaniline, *Polymer International*, **39,** 1996, pp. 153-159.

[58]. Chen, S. A. and Tsai, C. C. Structure/properties of conjugated conductive polymers. 2. 3-Ether-substituted polythiophenes and poly(4-methylthiophenes), *Macromolecules*, **26,** 1993, pp. 2234-2239.

[59]. Wei, Y., Tian, J., MacDiarmid, A. G., Masters, J. G., Smith, A. L. and Li, D. Preparation and Conductivities of Fullerene-doped Polyanilines, *Journal of the Chemical Society, Chemical Communications*, **7,** 1993, pp. 603-604.

[60]. Beadle, P., Armes, S. P., Gottesfeld, S., Mombourquetts, C., Houlton, R., Andrews, W. D. and Agnew, S. F. Electrically conductive polyaniline-copolymer latex composites *Macromolecules*, **25,** 1992, pp. 2526-2530.

[61]. Somanathan, N. and Wegner, G. Studies on Poly (3-cyclohexylthiophene). *Indian Journal of Chemistry,* **33a,** 1994, pp. 572-579.

[62]. Vadera, S. R., Kumar, N. and Fuchem, H. Room Temperature Magnetic Ordering in $FeC1_4^-$ Doped Copolymers: A New Observation in *1st Int. Conf. on frontiers of polymer Research,* New Delhi 1991, pp.443-448.

[63]. Annapoorni, S., Sundaresan, N. S., Pandey, S. S. and Malhotra, B. D. Photocarrier mobility in processable Polyaniline, *Journal of Applied Physics,* **74,** 1993, pp. 2109-2111.

[64]. Yagüe, J. L. and Borrós, S. Conducting plasma polymerized polypyrrole thin films as carbon dioxide gas sensors, *Plasma Processes and Polymers,* **9,** 2012, pp. 485–490.

[65]. Swager, T. M. Precursor routes to conducting polymers from the ring-opening metathesis polymerization of cyclic olefins, *Dissertation (Ph.D.),* California Institute of Technology 1988, accessed from http://resolver.caltech.edu/CaltechETD:etd-08152005-160834

[66]. McNeill, R., Siudak, R. Wardlaw, J. H., Weiss, D. E. Electronic Conduction in Polymers: The Chemical Structure of Polypyrrole, *Australian Journal of Chemistry*, **16,** 1963, pp. 1056-1075.

[67]. Shirakawa, H. and Ikeda, S. Infrared spectra of polyacetylene, *Polymer Journal,* **2,** 1971, pp. 231-244.

[68]. Ohtani, A and Shimidzu, T. Effective Doping of Polymer Anion during Chemical Polymerization of Pyrrole Using $Fe(OH)_3$ Oxidant, *Bulletin of the Chemical Society of Japan*, **62,** 1989, pp. 234-238.

[69]. Angeli, A. Sopra i neri di pirrolo, *Gazzetta Chimica Italiana,* **46,** 1916, pp. 279.

[70]. Armes, S. P. Optimum reaction conditions for the polymerization of pyrrole by iron (III) chloride in aqueous solution, *Synthetic Metals,* **20,** 1987, pp. 365-371.

[71]. Duchet, J., Legras, R. and Demoustier-Champagne, S. Chemical synthesis of polypyrrole: structure-properties relationship, *Synthetic Metals,* **98,** 1998, 113-122.

[72]. Kumar, D. and Sharma, R. C. Advances in conductive polymers, *European Polymer Journal,* **34,** 1998, pp. 1053-1060.

[73]. Inzelt, G., Pineri, M., Schultze, J. W. and Vorotyntsev, M. A. Electron and proton conducting polymers: recent developments and prospects, *Electrochimica Acta,* **45,** 2000, pp. 2403-2421.

[74]. Genies, E. M., Bidan, G. and Diaz, A. F. Spectroelectrochemical study of polypyrrole films, *Journal of Electroanalytical Chemistry,* **149**, 1983, pp. 101-113.

[75]. Asavapiriyanont, S., Chandler, G. K. Gunawardena, G. A. and Pletcher, D. The electrodeposition of polypyrrole films from aqueous solutions, *Journal of Electroanalytical Chemistry,* **177,** 1984, pp. 229-244.

[76]. Kim, B. S., Kim, W. H., Hoier, S. N. and Park, S.-M. Electrochemistry of conductive polymers XVI. Growth mechanism of polypyrrole studied by kinetic and spectroelectrochemical measurements, *Synthetic Metals,* **69**, 1995, pp. 455-458.

[77]. Waltman, R. J. and Bargon, J. Reactivity/structure correlations for the electropolymerization of pyrrole: An INDO/CNDO study of the reactive sites of oligomeric radical cations, *Tetrahedron,* **40**, 1984, pp. 3963-3970.

[78]. Lowen, S. V. and Van Dyke, J. D. Mechanistic studies of the electrochemical polymerization of pyrrole: Deuterium isotope effects and radical trapping studies, *Journal of Polymer Science: Part A,* **28,** 1990, pp. 451-464.

[79]. Raymond, D. E. and Harrison, D. J. Observation of soluble electroactive intermediates during the anodic formation of conducting polypyrrole films, *Journal of Electroanalytical Chemistry,* **296,** 1990, pp. 269-273.

[80]. Raymond, D. E. and Harrison, D. J. Observation of pyrrole radical cations as transient intermediates during anodic formation of conducting polypyrrole films, *Journal of Electroanalytical Chemistry,* **361,** 1993, pp. 65-76.

[81]. Audebert, P. and Hapiot, P. Fast electrochemical studies of the polymerization mechanisms of pyrroles and thiophenes. Identification of the first steps. Existence of p-dimers in solution. *Synthetic Metals,* **75**, 1995, pp. 95-102.

[82]. Diaz, A. F. and Bargon, J. in Handbook of Conducting Polymers Vol. 1 , 1986, Marcel Dekker, INC., New York, pp. 81

[83]. Imanishi, K., Satoh, M., Yasuda, Y., Tsushima, R. and Aoki, S. The effects of electrolyte on electrical conductivity of electrochemically prepared polypyrrole and polythiophene films, *Journal of Electroanalytical Chemistry,* **260,** 1989, pp. 469-473.

[84]. Beck, F., Braun, P. and Oberst, M. Organic electrochemistry in the solid state: over-oxidation of polypyrrole, *Physical Chemistry,* **91,** 1987, pp. 967-974.

[85]. Walker, J. A., Warren, L. F. and Witucki, E. F. New chemically prepared conducting "pyrrole blacks", *Journal of Polymer Science: Part A,* **26,** 1988, pp. 1285-1294.

[86]. van den Schoor, R. C. G. M., van de Leur, R. H. M. and de Wit, J. H. W. Synthesis of a polypyrrole film on a non-conducting substrate: the influence of the acid concentration on the Fe^{3+} equilibria, *Synthetic Metals,* **102,** 1999, pp. 1404-1405.

[87]. Audebert, P. and Bidan, G. Comparison of carbon paste electrochemistry of polypyrroles prepared by chemical and electrochemical oxidation paths. Some characteristics of the chemically prepared polyhalopyrroles, *Synthetic Metals,* **14,** 1986, pp.71-80.

[88]. Machida, S. and Miyata, S. Chemical synthesis of highly electrically conductive polymer, *Synthetic Metals,* **31,** 1989, pp. 311-318.

[89]. Whang, Y. E., Han, J. H., Nalwa, H. S., Watanabe, T. and Miyata, S. Chemical synthesis of highly electrically conductive polymers by control of oxidation potential, *Synthetic Metals,* **41-43,** 1991, pp. 3043-3048.

[90]. Druy, M. A. The role of the counterion in the reactivity of conducting polymers, *Synthetic Metals,* **15,** 1986, pp. 243-248.

[91]. Stejskal, J., Omastová, M., Fedorova, S., Prokeš, J. and Trchová, M. Polyaniline and polypyrrole prepared in the presence of surfactants: a comparative conductivity study. *Polymer,* **44,** 2003, pp. 1353-1358.

[92]. Qi, Z. and Pickup, P. G. Size control of polypyrrole particles, *Chemistry of Materials,* **9,** 1997, pp. 2934-2939.

[93]. Zotti, G. Zecchin, S. Schiavon, G. and Groenendaal, L. B. Conductive and magnetic properties of 3,4-dimethoxy- and 3,4-ethylenedioxy-capped polypyrrole and polythiophene, *Chemistry of Materials,* **12,** 2000, pp. 2996-3005.

[94]. Gassner, F., Graf, S. and Merz, A. On the physical properties of conducting poly(3,4-dimethoxypyrrole) films, *Synthetic Metals,* **87,** 1997, pp. 75-79.

[95]. Zong, K. and Reynolds, J. R. 3,4-Alkylenedioxypyrroles: functionalized derivatives as monomers for new electron-rich conducting and electroactive polymers, *The Journal of Organic Chemistry.* **66,** 2001, pp. 6873-6882.

[96]. Sonmez, G., Schottland, P., Zong, K. and Reynolds, J. R. Highly transmissive and conductive poly(3,4-alkylenedioxypyrrole) (pxdop) films prepared by air or transition metal catalyzed chemical oxidation, *Journal of Materials Chemistry*, **11,** 2001, pp. 289-294.

[97]. Forsyth, M. and Smith, M. E. Solid state NMR characterization of polypyrrole: The nature of the dopant in PF_6^- doped films, *Synthetic Metals,* **55,** 1993, pp.714-719.

[98]. Blythe, T. in Electrical properties of polymers, 2nd Edition, 2005, Cambridge University Press.

[99]. Little, W. A. Possibility of Synthesizing an Organic Superconductor, *Physical Review*, **134,** 1964, pp. A1416–A1424.

[100]. Bredas, J. L. in Handbook of Conducting Polymers Vol. 2 , 1986, Marcel Dekker, INC., New York, pp. 859.

[101]. Bredas, J. L., Chance, R. R. and Silbey, R. Comparative theoretical study of the doping of conjugated polymers: Polarons in polyacetylene and polyparaphenylene, *Physical Review: B,* **26**, 1982, pp. 5843-5854.

[102]. Themans, B., Andre, J. M., Chance, R. R. and Silbey, R. The role of mobile organic radicals and ions (solitons, polarons and bipolarons) in the transport properties of doped conjugated polymers, *Synthetic Metals,* **9,** 1984, pp. 265-274.

[103]. Pratt, C. Essay on conducting polymers, 1996, accessed from homepage.ntlworld.com/colin.pratt/cpoly.pdf

[104]. Bredas, J. L. and Street, G. B. Polarons, bipolarons, and solitons in conducting polymers, *Accounts of Chemical Research,* **18,** 1985, pp. 309-315.

[105]. Chance, R. R., Bredas, J. L. and Silbey, R. Bipolaron transport in doped conjugated polymers, *Physical Review: B,* **29**, 1984, pp. 4491-4495.

[106]. Bredas, J. L. Bipolarons in doped conjugated polymers: a critical comparison between theoretical results and experimental data, *Molecular Crystals and Liquid Crystals*, **118,** 1985, pp. 49-56.

[107]. Bjorklund, R. B. and Lundstrom, I. Some Properties of Polypyrrole-Paper Composites, *Journal of Electronic Materials,* **13,** 1984, pp. 211-229.

[108]. Miyata, S. and Ozio, T. US Patent 4699804, 1987.

[109]. Maus, L., Witucki, E. F. and Warren, L. F. US Patent 4696835, 1987.

[110]. Newman, P., Warren, L. and Witucki, E. US Patent 4617228, 1986.

[111]. Mizuki, T. and Watanabe, K. Japan Patent 01,266,280. 1989.

[112]. Lee, G. J., Lee, S. H., Ahn, K. S. and Kim, K. H. Synthesis and characterization of soluble polypyrrole with improved electrical conductivity, *Journal of Applied Polymer Science,* **84,** 2002, pp. 2583-2590.

[113]. Genies, E. M., Petrescu, C. and Olmedo, L. Conducting materials from polyaniline on glass textile, *Synthetic Metals,* **41,** 1991, pp. 665-668.

[114]. Gregory, R. V., Kimbrell, W. C. and Kuhn, H. H. Conductive textiles, *Synthetic Metals,* **28,** 1989, pp. 823-835.

[115]. Bartholomew, G. W., Jongchul, K., Volpe, R. A. and Wenzel, D. J. US Patent 5211810, 1993.

[116]. Kuhn, H. H.; Child, A. D. Electrically Conducting Textiles. In Handbook of Conducting Polymers, 1998, Marcel Dekker, INC., New York, pp. 993.

[117]. Kuhn, H. H., US Patent 5108829. 1992.

[118]. Mithra, L. M. M., Cao, Y., Cho, S., Sutar, D., Lee, K., Menon, R. and Subramanyam, S. V. Electrical transport and reflectance studies on polypyrrole - $CF_3SO_3^-$ in the vicinity of metal-insulator transition, *Synthetic Metals,* **119,** 2001, pp. 437-438.

[119]. Bhadani, S. N., Kumari, M., Gupta, S. K. S. and Sahu, G. C. Preparation of conducting fibers via the electrochemical polymerization of pyrrole, *Journal of Applied Polymer Science,* **64,**1997, pp. 1073-1077.

[120]. Šafářová, V. and Militký, J. Electromagnetic shielding of hybrid fabrics, in Selected topics of textile and material science, 2011, House of WBU, Pilsen, pp. 376.

[121]. Nurmi, S., Hammi, T. and Demoulin, B. Protection against electrostatic and electromagnetic phenomena, in Multifunctional Barriers for Flexible Structure, 2000, Springer-Verlag Berlin Heidelberg.

[122]. Simon, R. M. Conductive plastics for EMI shielding, in *Thirty-Eighth Annual Technical Conference,* 1980, p. 207.

[123]. Shinagawa, S., Kumagai, Y. and Urabe, K. Conductive Papers Containing Metallized Polyester Fibers for Electromagnetic Interference Shielding, *Journal of Porous Materials,* **6,** 1999, pp. 185-190.

[124]. White D. R. J. A. in Handbook Series on Electromagnetic Interference and Compatibility, Vol. 5, 1971, Don White Consultants, Germantown, MD.

[125]. Colaneri, N. F. and Shacklette, L. W. EMI shielding measurements of conductive polymer blends, *IEEE Transaction Instrumentation and Measurement*, **41,** 1992, pp. 291-297.

[126]. Mott, N. F. and Davis, E. A. in Electronic process in non-crystalline materials, 1979, Clarendon Press, Oxford.

[127]. Kaynak, A. DC Conduction in electrochemically synthesized polypyrrole films, *Turkish Journal of Chemistry*, **22,** 1998, pp. 81-85.

[128]. Militký, J., Vik, M., Viková M. and Křemenáková, D. Influence of fabric construction on their porosity and air permeability, *2nd SIENTEX Conference "International Symposium of Textile Engineering,"* Natal, Brazil, September 2004. pp. 1-18.

[129]. Hassan, H. M., Ali, M. M., Bayomi, S. M. and Yousif, M. M. Reactions of 2-amino-1-benzyl-3-t-butoxycarbonyl- 4,5- dimethylpyrrole and its derivatives with some aldehydes and dienophiles, *Mansoora Science Bulletin*, **15**, 1988, pp. 347-353.

[130]. Data extracted from Hazardous Substances Data Bank, accessed from http://toxnet.nlm.nih.gov/cgi-bin/sis/htmlgen?HSDB

[131]. Rao, S. R. Resource recovery and recycling from metallurgical wastes, in Waste Management Series 7, 2006, Elsevier B. V. UK.

[132]. Yavuz, M. S. Conducting polymers from processable precursors and their applications to gold surfaces, *Dissertation (PhD)*, 2007, pp. 47, accessed from http://digitalcommons.uconn.edu/dissertations/AAI3300647/

[133]. Sun, B., Jones, J., Burford, R. and Skyllas-Kazacos, M. Stability and mechanical properties of electrochemically prepared conducting polypyrrole films, *Journal of Materials Science*, **24,** 1989, pp. 4024-4029.

[134]. Zinger, B. Catalytic electrosynthesis of conducting polymers, *Journal of Electroanalytical Chemistry*, **244,** 1988, pp. 115-121.

[135]. Jiang, M. and Wang, J. Recognition and detection of oligonucleotides in the presence of chromosomal DNA based on entrapment within conducting-polymer networks, *Journal of Electroanalytical Chemistry*, **500,** 2001, pp. 584-589.

[136]. Misoska, V., Price, W. E., Ralph, S. F., Ogata, N. and Wallace, G. G. Synthesis, characterisation and ion transport studies on

polypyrrole/deoxyribonucleic acid conducting polymer membranes, *Synthetic Metals,* **123,** 2001, pp. 279-286.

[137]. Kiani, M. S. and Mitchell, G. R. The role of the counter-ion in the preparation of polypyrrole films with enhanced properties using a pulsed electrochemical potential, *Synthetic Metals,* **48,** 1992, pp. 203-218.

[138]. Kiani, M. S., Bhatt, N. V., Davies, F. J. and Mitchell, G. R. Highly anisotropic electrically conducting films based on poly- pyrrole, *Polymer,* **33,** 1992, pp. 4113-4120.

[139]. Lin, T., Wang, L., Wang, X. and Kaynak, A. Polymerising pyrrole on polyester textiles and controlling the conductivity through coating thickness, *Thin Solid Films,* **479,** 2005, pp. 77-82.

[140]. Cremer, C. and Cremer, T. Considerations on a laser-scanning-microscope with high resolution and depth of field, *Microscopica Acta,* **81,** 1978, pp. 31-44.

[141]. Sandu, T., Sarbu, A. Contantin, F., Spataru, C. I., Gabor, R. A., Samoghi, R. and Iovu, H. Characterization of functionalized polypyrrole, *Revue Roumaine de Chimie*, **57,** 2012, pp. 177-185.

[142]. Mavinakuli, P., Wei, S., Wang, Q., Karki, A. B., Dhage, S., Wang, Z., Young, D. P. and Guo, Z. Polypyrrole/silicon carbide nanocomposites with tunable electrical conductivity, *Journal of Physical Chemistry,* **114,** 2010, pp. 3874-3882.

[143]. Vishnuvardhan, T. K., Kulkarni, V. R., Basavaraja, C. and Raghavendra, S. C. Synthesis, characterization and a.c. conductivity of polypyrrole/Y2O3 composites, *Bulletin of Material Science,* **29,** 2006, pp. 77-83.

[144]. Patil, A. J. and Pandey, A. K. A novel approach for in situ polymerization of polypyrrole on cotton substrates, *Indian Journal of Fibre & Textile Research,* **37,** 2012, pp. 107-113.

[145]. Kaynak, A., Wang, L., Hurren, C. and Wang, X. Characterization of conductive polypyrrole coated wool yarns, *Fibers and Polymers,* **3,** 2002, pp. 24-30.

[146]. Yildiz, Z., Usta, I. and Gungor, A. Electrical properties and electromagnetic shielding effectiveness of polyester yarns with polypyrrole deposition, *Textile Research Journal,* **82,** 2012, pp. 2137-2148.

[147]. Kim, S. H., Jamg, S. H., Byun, S. W., Lee, J. Y., Joo, J. S., Jeong, S. H. and Park, M. J. Electrical properties and emi shielding characteristics of polypyrrole–nylon 6 composite fabrics, *Journal of Applied Polymer Science,* **87,** 2003, pp. 1969-1974.

[148]. Committee for conformity assessment on accreditation and certification of functional and technical textiles, Sep 2003, Specified Requirements of Electromagnetic Shielding Textiles, accessed from http://www.ftts.org.tw/images/fa003E.pdf

[149]. Alenitsyn, A. G., Butikov, E. I. and Kondratyev, A. S. Concise Handbook of Mathematics and Physics, 1997, CRC Press, pp. 331-332.

[150]. Moss, B. K. and Burford, R. P. A kinetic study of polypyrrole degradation, *Polymer*, **33,** 1992, pp. 190-198.

[151]. Patil, A. J. and Deogaonkar, S. C. Conductivity and atmospheric aging studies of polypyrrole-coated cotton fabrics, *Journal of Applied Polymer Science,* **125,** 2012, pp. 844-851.

[152]. Kaynak, A. Aging studies on conducting polypyrrole, *Fibers and Polymers*, **2,** 2001, pp. 171-177.

[153]. Carlsson, D. O., Sjödin, M., Nyholm, L. and Strömme, M. A comparative study of the effects of rinsing and aging of polypyrrole/ nanocellulose composites on their electrochemical properties, *Journal of Physical Chemistry B*, **117,** 2013, pp. 3900-3910.

[154]. Cassignol, C., Olivier, P. and Ricard, A. Influence of the dopant on the polypyrrole moisture content: effects on conductivity and thermal stability, *Journal of Applied Polymer Science,* **70,** 1998, pp. 1567-77.